Sołowski, Wojciech Tomasz; Tran, Quoc; Seyedan, Seyedmohammadjavad

AN OVERVIEW OF THE MATERIAL POINT METHOD

ECCOMAS

EUROPEAN COMMUNITY ON COMPUTATIONAL METHODS IN APPLIED SCIENCES

ECCOMAS NEWSLETTER

JUNE 2018

EUROPEAN COMMUNITY ON COMPUTATIONAL METHODS IN APPLIED SCIENCES
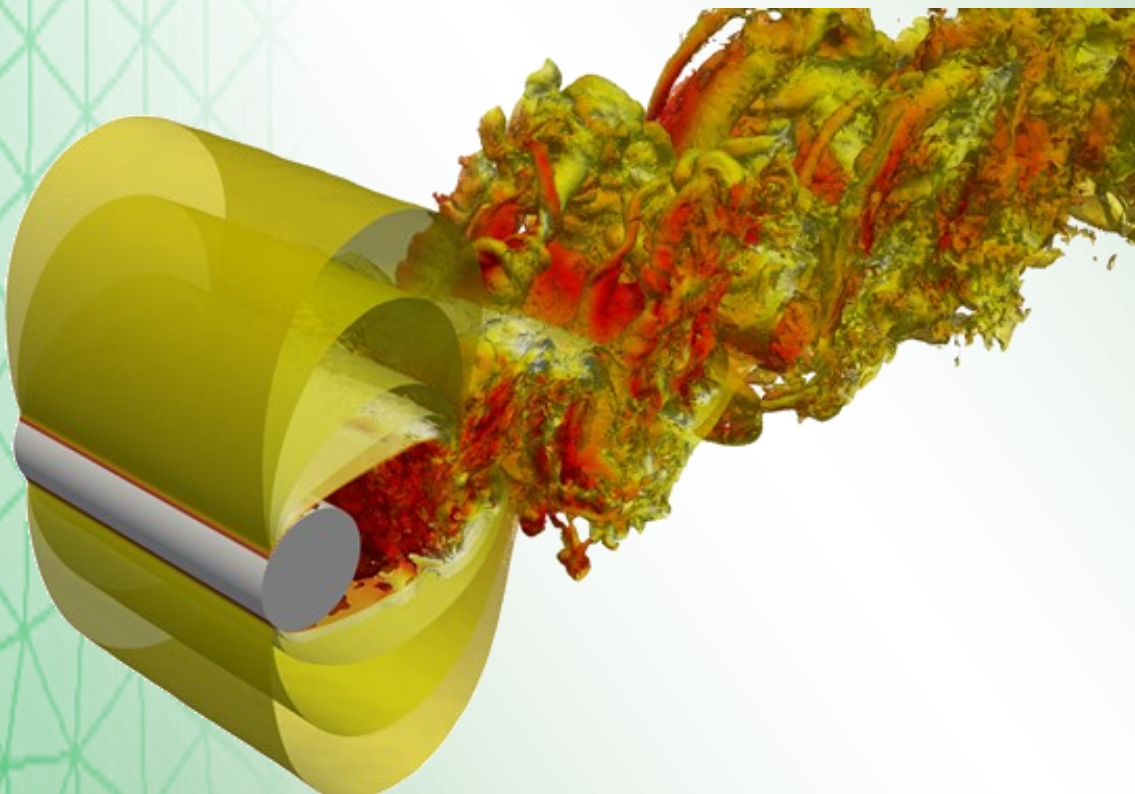
CONTENTS

MESSAGE OF THE PRESIDENT

The European Community on Computational Methods in Applied Sciences enters the year of 2018 with a strong commitment to continue its wide-ranging activities of the past years and to further perfect its engagements in supporting the European computational science community by giving it a solid background for exchange of novel ideas and promoting collaboration.

ECCOMAS was founded in 1993 so that in the coming year we shall celebrate its 25th anniversary – not by having jubilee parties but by trying hard to be as helpful to our community as possible. We shall make every effort to fulfill in an optimal way our mission of promoting joint efforts in research and innovative industrial applications of European universities, research institutes and industry active in the broadly understood field of numerical methods and computer simulations in engineering and applied sciences. Our goal is to assist researchers and institutions to effectively address critical technological and social problems in the above broad field of science and modern technology with particular emphasis on multidisciplinary applications. As a newly elected ECCOMAS president I declare on behalf of the whole organization to make every effort in our reach to work towards the effective realization of this policy. To this aim we shall continue to organize large-scale congresses, actively support regional and thematic conferences, endorse smaller workshops, promote young investigator meetings and courses as well as encourage organization of open industrial days in different areas of our common interest.

The ECCOMAS calendar is arranged according to even and odd years. The odd years feature the ECCOMAS Thematic Conferences. The steady increase in the number of Thematic Conferences clearly exhibits the potential of computer simulations in a growing number of application areas, as well as the vitality of our community. More than 30 Thematic Conferences were organized in 2017. The even years feature the main ECCOMAS congresses: the European Congress on Computational Methods in Applied Sciences and Engineering, and the ECCM and ECFD conferences. The key event this year is the joint 6th European Conference on Computational Mechanics (Solid, Structures and Coupled Problems) and the 7th European Conference on Computational Fluid Dynamics, ECCM-ECFD 2018, which will be held June 11-15, 2018 in Glasgow, UK. The ECCM-ECFD 2018 conference will also be the occasion to celebrate the 25th anniversary of ECCOMAS together.

The main event organized by ECCOMAS has been the large European Congress on Computational Methods in Applied Sciences and Engineering taking place every four years with participation of researchers and engineers from Europe and beyond. The previous most successful Congresses were held in Brussels, Belgium (1992), Paris, France (1996), Barcelona, Spain (2000), Jyvaskyla, Finland (2004), Venice, Italy (2008) in conjunction with the World Congress on Computational Mechanics of IACM, Vienna, Austria (2012) and Crete, Greece (2016). The next, VIII European Congress will be organized jointly with the 14th WCCM and it will be held in Paris, France on July 19-24, 2020.

As every organization aspiring to play an important role in an active and diversified community we face a number of challenges which have to be addressed during our four-year term. As the most important among them I would consider establishing a stronger connection with the individual researchers in the ECCOMAS community. ECCOMAS is at present an "organization of organizations". This setup makes perfect sense from a historical perspective, but it requires reconsideration in the context of present societal developments.

In trying to effectively solve these and many other problems I am confident that the collaboration of all our colleagues elected to the governing bodies of ECCOMAS will be smooth and effective. I am looking forward to the exchange of ideas as to the ways we can best serve the European community of researchers and engineers in the key area of modern science and technology in which we all professionally engaged. The needs of industry in this respect are enormous. I know it from a hands-on experience in one of the most promising and fast developing areas of modern technology. Having been for a decade the President of the European Materials Forum – a Strasbourg-based umbrella-type organization aiming at a coordination of material R&D activities in Europe and beyond – I have convincingly learned that the techniques of computer simulations are a key factor determining the pace of progress in this area. And we know that in other areas the situation is similar.

I look forward to seeing you all in Glasgow!

MICHAŁ KLEIBER
PRESIDENT OF ECCOMAS

MKLEIBER@IPPT.PAN.PL

MESSAGE OF THE GUEST EDITOR

When I was asked in 2017, if I would act as Guest Editor for the Newsletter you hold in your hands (or gaze at on a screen) it was a "distant elephant"; something significant but a long way off. I am glad to say that around a year later, while the elephant was indeed large, the task of editing was not unpleasant or time-consuming. This is a function of the actions of the contributors to the Newsletter, who came up with material on time and of high quality, and of the Technical Editor, Panagiota Kouniaki.

Here, in this "bumper" edition, you will find journal-paper level articles, general introductions to numerical methods such as the Material Point Method and Discontinuity Layout Optimisation, an opinion article taking a new look at mechanics, and a survey of

Charles Augarde (centre) with Associate Professor Will Coombs and PhD student Lei Fan, in Durham

activity in a country currently without a national association for computational mechanics. I am particularly pleased that a significant part of the Newsletter is devoted to the activities of the Young Investigators Committee (YIC) who are becoming more active in ECCOMAS (see the "Science Slam" at the Glasgow conference for instance). I consider the development of the next generation of computational mechanicians to be perhaps the most important job for senior people like myself (see photo!) so the rise in activity of the YIC is welcome.

So, I hope you enjoy reading this Newsletter, and perhaps you are doing this at the conference below …

CHARLES AUGARDE
DURHAM UNIVERSITY,
UNITED KINGDOM
CHARLES.AUGARDE@DURHAM.AC.UK

ECCM-ECFD 2018

ECCM-ECFD 2018 is being held in Glasgow, Scotland, 11-15 June 2018. This brings together two of the ECCOMAS major conferences in a joint event to celebrate the 25th anniversary of ECCOMAS:

- 6th European Conference on Computational Mechanics (Solids, Structures and Coupled Problems) - ECCM 6
- 7th European Conference on Computational Fluid Dynamics - ECFD 7.

The City of Glasgow is proud to be the venue for this event, with the University of Glasgow, the University of Edinburgh and the UK Association of Computational Mechanics as the host organisations. The conference is taking place at the Scottish Events Campus on the banks of the River Clyde, just to the west of Glasgow's city centre. Scotland and Glasgow have a rich history in Science, Mathematics and Engineering. One of

its most famous sons is the mathematical physicist and engineer, Lord Kelvin, who was Professor of Natural Philosophy at the University of Glasgow for over 50 years. James Watt was working at the University when he invented the separate condenser as a design enhancement for steam engines, that radically improved their power, efficiency, and cost-effectiveness. Another scientific giant, James Clark Maxwell, was born in Edinburgh, and studied at the University of Edinburgh.

Scotland is home to four of the UK's six ancient universities, including the University of Glasgow and the

University of Edinburgh. The Regius Chair of Civil Engineering and Mechanics was established at the University of Glasgow in 1840 by Queen Victoria. It was the first Chair in Engineering in the English-speaking world. The first incumbent was Lewis Gordon, brother-in-law to Sir Charles William Siemens. The second incumbent was William Rankine, famous engineer, mathematician and physicist. These were followed by many notable engineers, including in the field of Computational Mechanics, namely Nenad Bićanić and René de Borst. The Regius Chair of Engineering at the University of Edinburgh was established in 1868 and Jason Reese is the ninth and current incumbent.

CHRIS PEARCE
GENERAL SECRETARY
FOR ECCM-ECFD 2018
CHRIS.PEARCE@GLASGOW.AC.UK

HIGH-ORDER COMPUTATIONAL FLUID DYNAMICS ON MANY-CORE HARDWARE

INTRODUCTION

There is an increasing desire amongst industrial practitioners of computational fluid dynamics (CFD) to undertake high-fidelity scale-resolving simulations of unsteady flows within the vicinity of complex geometries. For example, to improve the design of next generation unmanned aerial vehicles (UAVs), there exists a need to perform simulations at Reynolds numbers 10^4-10^7 and Mach numbers 0.1-1.0 of highly separated flow over deployed spoilers/air-brakes; separated flow within serpentine intake ducts; acoustic loading in weapons bays; and flow over entire UAV configurations at off-design conditions. Unfortunately, current generation industry-standard CFD software based on first- or second-order accurate Reynolds Averaged Navier-Stokes (RANS) approaches is not well suited to performing such simulations. Henceforth, there has been significant interest in the potential of high-order accurate methods for unstructured mixed grids, and whether they can offer an efficient route to performing scale-resolving simulations within the vicinity of complex geometries. Popular examples of high-order schemes for unstructured mixed grids include the discontinuous Galerkin (DG) method, first introduced by Reed et al. [1], and

the spectral difference (SD) methods originally proposed under the moniker a staggered-gird Chebyshev multi-domain methods by Kopriva et al. [2] and later popularised by Sun et al. [3]. In 2007 Huynh [4] proposed the flux reconstruction (FR) approach; a unifying framework for high-order schemes on unstructured grids that incorporates a nodal DG scheme of the variety described by Hesthaven and Warburton [5] and, at least for a linear flux function, any SD scheme. In addition to offering high-order accuracy on unstructured mixed grids, FR schemes are also compact in space, and thus when combined with explicit time marching offer a significant degree of element locality. As such, explicit high-order FR schemes are characterised by a large degree of structured computation, even on unstructured grids. This makes them particularly well suited to modern 'many-core' hardware platforms, which are characterised by an abundance of FLOPs relative to memory bandwidth, and significant levels of parallelism.

PyFR

PyFR is an open-source Python based framework for solving advection-diffusion type problems on many-core hardware platforms using the FR approach [6]. It is

designed to solve a range of governing systems on mixed unstructured grids containing various element types. It is also designed to target a range of hardware platforms via use of a Mako-derived domain specific language. The current release of PyFR is able to solve the incompressible and compressible Euler and Navier-Stokes equations on unstructured grids of quadrilateral and triangular elements in 2D, and unstructured grids of hexahedral, tetrahedral, and prismatic elements in elements in 3D, targeting clusters of CPUs, Nvidia GPUs, AMD GPUs. If required, PyFR can also target heterogeneous systems, with a mix of CPUs and GPUs.

The Python programming language was selected on account of it combining a clean syntax with a rich repository of packages. Garbage collection and exception handling serve to greatly reduce the amount of boiler-plate code required in order to interact with complicated libraries, such as OpenCL and HDF5, compared with C++ and Fortran. Further, high-quality wrappers are available for many libraries of scientific interest. The majority of these packages also provide out-of-the-box support for runtime code generation, which is a paradigm PyFR employs extensively to achieve platform portability.
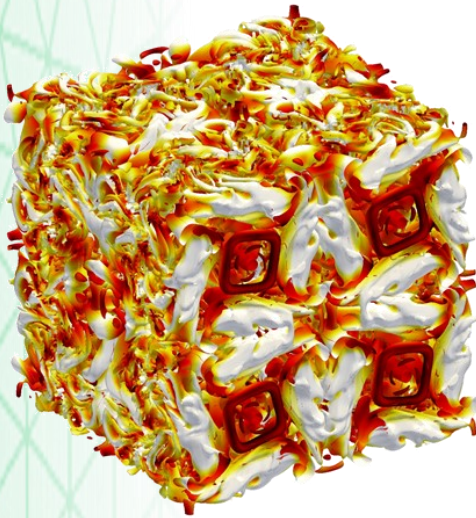
Figure 1. Taylor Green vortex breakdown [7] (copyright Vermeire et al. reused with permission).
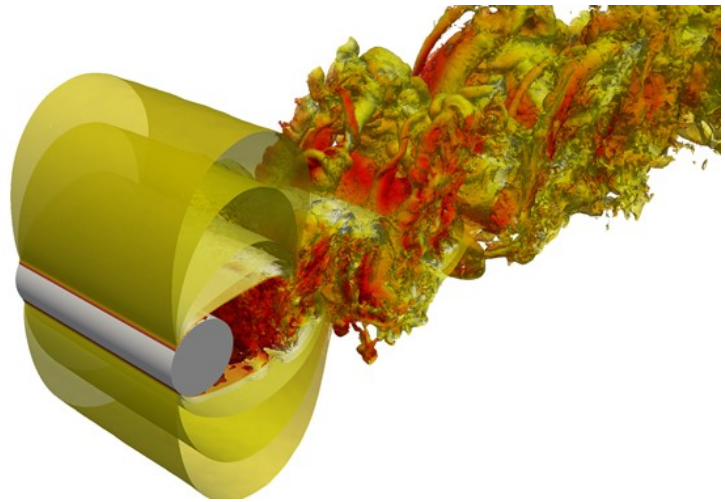
Figure 2. Flow over a cylinder [8] (copyright Vermeire et al. reused with permission).

The PyFR project adopts sustainable and open software development paradigms. Version control is achieved using Git and Github, and a Gitflow `fork-and-pull' collaborative development model is employed. Formatting follows PEP8. An in-house framework based on BASH scripts automates feature testing across all target platforms (feature parity across all target platforms is strictly enforced). Finally, PyFR is released on a rolling basis under an open-source 3-Clause New-Style BSD license, which promotes sharing, testing and utilisation across academia and industry.

APPLICATIONS

PyFR has been used to undertake a range of simulations, including Taylor-Green vortex breakdown [7] (see Fig. 1), flow over cylinders [8] (see Fig. 2), flow over an SD7003 aerofoil [9] (see Fig. 3), flow over a NACA0021 aerofoil in deep stall at a 60 degree angle of attack [10], and flow over a T106D low-pressure turbine linear cascade [11] (see Fig. 4). The latter achieved up to 13.7 double precision PFLOPs on 18,000 K20X GPUS of Titan at Oak Ridge National Laboratory, and were shortlisted for the Gordon Bell Prize in 2016 [11].

FUTURE WORK

We are currently looking to develop insight extraction tools for petascale, and eventually exascale, high-fidelity time-accurate simulations of turbulent flow. Given the amount of data such simulations could potentially generate, classical paradigms of writing to magnetic disk for a posteriori 'off-line' processing are no longer fit for purpose. Instead, visualisation and analysis must be undertaken on-the-fly as the simulation progresses. We are also exploring how machine-learning techniques can leverage large DNS datasets, generated with PyFR, to train turbulence models.
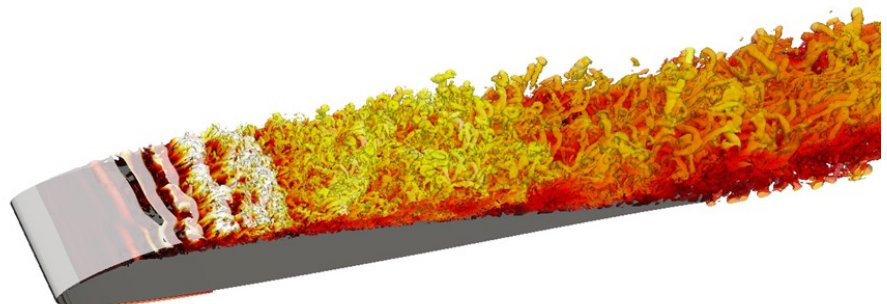
Figure 3. Flow over an SD7003 aerofoil [9] (copyright Vermeire et al. reused with permission).

Figure 4. Flow over a T106D low-pressure turbine linear cascade [11] (copyright Vincent et al. reused with permission).

REFERENCES

[1] W H Reed and T R Hill. Triangular mesh methods for the neutron transport equation. Technical Report LA-UR-73-479, Los Alamos National Laboratory, New Mexico, USA, 1973.

[2] D A Kopriva and J H Kolias. A conservative staggered-grid Chebyshev multidomain method for compressible flows. Journal of Computational Physics, 1996.

[3] Y Sun, Z J Wang, and Y Liu. High-order multidomain spectral difference method for the Navier Stokes equations on unstructured hexahedral grids. Communications in Computational Physics, 2007.

[4] H T Huynh. A flux reconstruction approach to high-order schemes including discontinuous Galerkin methods. AIAA Paper 2007-4079, 2007.

[5] J S Hesthaven and T Warburton. Nodal discontinuous Galerkin methods - algorithms, analysis, and applications. Springer, 2008.

[6] F D Witherden, A M Farrington, and P E Vincent. PyFR: An open source framework for solving advection-diffusion type problems on streaming architectures using the flux reconstruction approach. Computer Physics Communications, 2014.

[7] B C Vermeire, F D Witherden, P E Vincent. On the utility of GPU accelerated high-order methods for unsteady flow simulations: a comparison with industry-standard tools. Journal of Computational Physics, 2017.

[8] F D Witherden, B C Vermeire, P E Vincent. Heterogeneous computing on mixed unstructured grids with PyFR. Computers and Fluids, 2015.

[9] B C Vermeire, P E Vincent. On the properties of energy stable flux reconstruction schemes for implicit large eddy simulation. Journal of Computational Physics, 2016.

[10] J S Park, F D Witherden, P E Vincent. High-order implicit large-eddy simulations of flow over a NACA0021 aerofoil. AIAA Journal, 2017.

[11] P E Vincent, F D Witherden, B C Vermeire, J S Park, A Iyer. Towards green aviation with Python at petascale. ACM Gordon Bell Finalist and Best Paper Finalist. Article 1. SC16 Proceedings of the International Conference for High Performance Computing, Networking, Storage and Analysis, 2016.

PETER VINCENT
IMPERIAL COLLEGE LONDON,
UNITED KINGDOM

P.VINCENT@IMPERIAL.AC.UK

COMPUTATIONAL LAYOUT OPTIMIZATION: RECENT DEVELOPMENTS AND APPLICATIONS

1 INTRODUCTION

Layout optimization (LO) and Discontinuity layout optimization (DLO) are powerful analysis and design procedures that utilize numerical optimization to determine the optimal layout of a connected system of lines, bars, shells or discontinuities to satisfy given criteria. Applications range from the derivation of minimal volume truss and frame structures to the derivation of critical slip or yield line plastic collapse mechanisms.

A key advantage of the approach is that by formulating such problems in terms of *discontinuities* rather than *solid elements*, the solution is not constrained by an initial mesh layout as encountered when element based methods are employed and mathematical singularities are handled inherently.

While in principle the approach may be regarded as a meshless method, the approach is very different to conventionally defined meshless methods. In LO and DLO, it is conditions along lines (or other entities) connecting nodes that are computed, rather than conditions within a domain surrounding a node.

The aim of this paper is to give a brief overview of the technique, example solutions, and to comment briefly on recent developments and future work. While in-depth derivations of the formulations described are beyond the scope of this contribution, references to key works will be given.

2 LAYOUT OPTIMIZATION

Layout optimization is most often used to determine the minimum volume 2D or 3D truss for a given design domain and set of loads and supports.

Consider a potential planar design domain which is discretized using n nodes and m potential nodal connections (truss bars), which interconnect each pair of nodes to form a fully connected 'ground structure'. In simple terms the aim is to find the minimum volume arrangement of truss bars that can carry the defined load.

In mathematical terms, the classical 'equilibrium' plastic truss layout optimization formulation for a single load case is defined as follows (after Dorn et al. 1964):

$$\min V = \mathbf{c}^{\mathrm{T}} \mathbf{q} \qquad (1)$$

subject to:
$$\mathbf{Bq} = \mathbf{f} \qquad (2)$$

and
$$\mathbf{q} \geq 0 \qquad (3)$$

where V is the total volume of the structure, $\mathbf{q}^{\mathrm{T}} = \{q_1^+, q_1^-, q_2^+, q_2^- ... q_m^-\}$, and q_i^+, q_i^- are the tensile and compressive forces in bar i; $\mathbf{c}^{\mathrm{T}} = \{l_1/\sigma_1^+, l_1/\sigma_1^-, l_2/\sigma_2^+, l_2/\sigma_2^- ... l_m/\sigma_m^-\}$, and where l_i/σ_i^+ and σ_i^- are respectively the length and tensile and compressive yield stress of bar i. $\mathbf{B}$ is a suitable ($2n \times 2m$) equilibrium matrix containing direction cosines and $\mathbf{f}^{\mathrm{T}} = \{f_1^x, f_1^y, f_2^x, f_2^y, ... f_n^y\}$ where f_j^x and f_j^y are the x and y components of the external load applied to node j ($j = 1...n$). The presence of supports at nodes can be accounted for by omitting the relevant terms from $\mathbf{f}$, together with the corresponding rows from $\mathbf{B}$.

This problem is in a form which can be solved using linear optimization, with the bar forces in $\mathbf{q}$ being the optimization variables. Use of modern interior point optimizers allows large problems to be solved and the linear, convex, nature of the problem ensures that a globally optimum solution will be found.

Equation 1 is the optimization objective function, which specifies that the minimum volume is being sought. Equation 2 enforces force
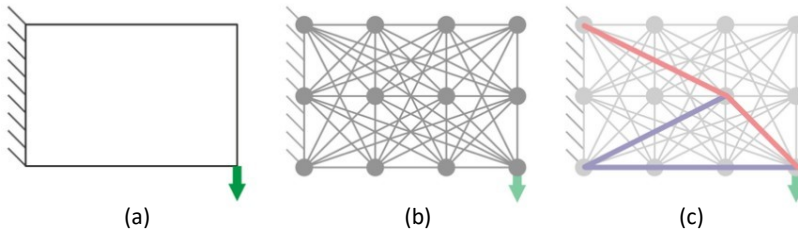
Figure 1. Simple truss layout optimization problem: (a) design domain (b) initial 'ground structure' comprising nodes and interconnecting potential bar con- nections (c) optimal solution (tension bars shown in red, compression bars in blue).
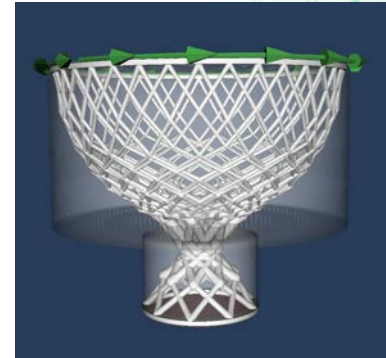

Figure 2. Three-dimensional truss layout optimization problems showing applied loading (green arrows) and design domain space (lighter coloured cylinders).

equilibrium at nodes and equation 3 ensures that only positive values of q are allowed, ensuring that a positive volume is always computed. The minimization process ensures that one of any pair of force values, q^+ and q^-, will always be zero.

Figure 1(a) shows a simple 2D truss layout optimization problem. This is discretized using 4 × 3 nodes, Figure 1(b), with every node inter-connected to every other node to create a fully connected 'ground structure'. Linear optimization is then used to identify the least volume subset of truss bars forming the optimal solution, as shown in Figure 1(c).

The approach is easily extended to 3D and can also be formulated to seek the optimal structure satisfying multiple load cases (e.g. Hemp 1973, Sokół 2014). Figure 2 shows a more complex 3D optimized form designed to carry an applied torque. It is evident that elegant forms be generated using the layout optimization procedure.

An iterative adaptive 'member adding' approach (Gilbert & Tyas 2003) can be used to solve problems involving 100s of nodes and >10^5 potential members in seconds. Problems involving over 15000 nodes and 10^8 potential members can be solved in 10s of minutes on a modern PC.

3 DISCONTINUITY LAYOUT OPTIMIZATION

The same basic LO procedure can be modified to determine the optimal layout of discon- tinuities for upper bound plastic collapse mechanisms (DLO, Smith and Gilbert 2007) and there is a direct mathematical analogy between parameters in a DLO problem and those in an LO problem.

Stages in a typical 2D planar DLO analysis are outlined in Figure 3, with the plastic limit analysis problem couched in terms of the potential discontinuities which inter-link the nodes used to discretize the region under consideration. In the kinematic formulation compatibility

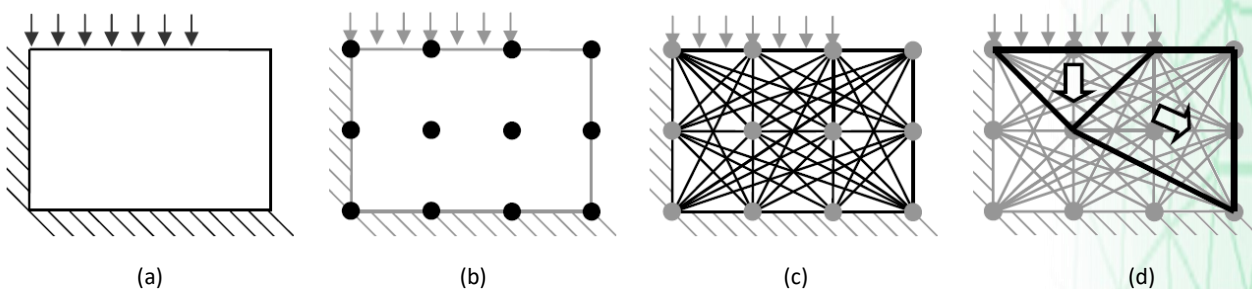Figure 3. Stages in the DLO procedure (after Gilbert et al. 2010): (a) starting problem (surcharge applied to block of soil close to a vertical cut); (b) discretization of soil using nodes; (c) interconnection of nodes with potential discontinuities; (d) identification of critical subset of potential discontinuities using optimization (giving the layout of slip-lines in the critical failure mechanism).

(a) $V/V_0 = 0.50$, $M/M_0 = 0.98$.
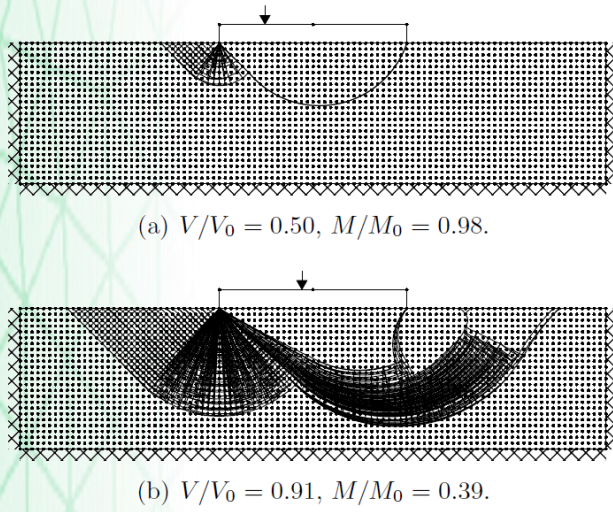
(b) $V/V_0 = 0.91$, $M/M_0 = 0.39$.

Figure 4. Application to geotechnical engineering problems: evolution of plane strain footing collapse mechanism on cohesive soil, with combined vertical V and moment M loading, where V0 and M0 are the failure loads for vertical or moment only loading respectively. (Anti-clockwise applied moment.)

(a)

(b)

Figure 5. Application to mechanical engineering problems: (a) plastic failure of notched beam subjected to pure bending; (b) plastic failure mechanism in metal cutting.

at nodes is explicitly enforced and implicitly enforced at points where discontinuities crossover one another (as each node is typically connected to every other node).

The general kinematic formulation for 2D and 3D problems can be stated as follows for a discretization using m discontinuities (Smith and Gilbert 2007, Hawksbee et al.

2013, Smith and Gilbert 2013, Gilbert et al. 2014):

$$\min \lambda \mathbf{f}_L^T \mathbf{d} = -\mathbf{f}_D^T \mathbf{d} + \mathbf{g}^T \mathbf{p} \quad (4)$$

subject to: $\quad \mathbf{B}\mathbf{d} = 0 \quad (5)$

$$\mathbf{N}\mathbf{p} - \mathbf{d} = 0 \quad (6)$$

$$\mathbf{f}_L^T \mathbf{d} = 1 \quad (7)$$

$$\mathbf{p}_i \geq f_i(\mathbf{d}_i) \quad \forall i \in \{1, \dots, m\} \ (8)$$

where λ is an unknown load factor at collapse, $\mathbf{f}_D$ and $\mathbf{f}_L$ are vectors containing respectively specified dead and live loads applied at discontinuities, $\mathbf{d}$ contains displacements along the discontinuities, $\mathbf{p}$ is a vector of

plastic multipliers and $\mathbf{g}$ contains the corresponding dissipation coefficients. $\mathbf{B}$ is a suitable compatibility matrix containing direction cosines and $\mathbf{N}$ is a suitable flow matrix. $f_i(\mathbf{d}_i)$ is function limiting the plastic multiplier(s) corresponding to a particular discontinuity i.

The specific definition of the above parameters depends on the problem type and will differ for planar and 3D problems, and for translational vs. rotational problems (where sliplines/slip surfaces may be curved). The key features of the formulation are that compatibility is explicitly enforced at nodes/ discontinuity junctions by equation 5 and that the flow rule is imposed by equation 6. Since a solution complying with the formal theorems of plastic limit analysis is usually sought, the flow rule must be associative. A simple 100 line MATLAB implementation of the

basic DLO kinematic formulation is available; for details see Appendix A.

There also exists a dual (equilibrium) version of this formulation which can alternatively be solved via optimization, yielding an identical solution.

Example solutions for problems relevant to the fields of geotechnical, mechanical and structural engineering are provided in Figures 4, 5, and 6 respectively.

While inherently an upper bound method, with a reasonable number of nodes (in the 2D formulation), the optimization process means it is possible to achieve highly accurate solutions well within 1% of the true solution. It is also noteworthy that the DLO analysis procedure can directly identify single isolated sliplines, such as that shown in Figure 4 (a), and can also inherently model singularities, which are challenges that typically require special
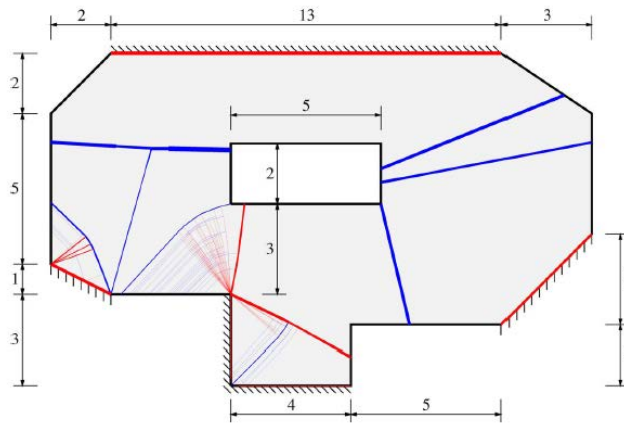
Figure 6. Application to a structural engineering problem: critical yield-line pattern for an irregular reinforced concrete slab subject to uniformly distributed load.

in (2010), Leshchinsky (2014) and Al-Defae and Knappett (2015).

While the main application originally envisaged for truss layout optimization was to conventionally fabricated structural frameworks, the recent advent of additive manufacturing has opened up opportunities for the design of strong and light mechanical components, for application in e.g. the aerospace, automotive and space industries; see for example Figure 8.

attention in element based methods. Since the original development of DLO, work has been undertaken to more fully realize its potential; for example, contributions by Clarke et al. (2013) addressing soil reinforcement, Hawksbee et al. (2013) addressing 3D analysis as illustrated in Figure 7, and Babiker (2013) addressing non-associative analysis.

4 APPLICATION IN INDUSTRY

University of Sheffield spinout company LimitState Ltd has actively developed the LO and DLO procedures described, embedding it

software packages suitable for use by industry. A key attraction is the speed at which solutions can be found, the general nature of the solution methodology and the easy to interpret output, in the form of slip or yield-line patterns or truss layouts. This allows highly interactive use by the engineer, a trend which is likely to also apply to other techniques as computers and algorithms get faster.

LimitState software is also available free of charge for educational use (www.limitstate.com/education) providing useful tools for teaching limit analysis and for undertaking design, analysis and parametric studies, e.g. Merifield and Smith

5 FUTURE DEVELOPMENTS

DLO is a comparatively recently developed numerical limit analysis procedure. While it has already been demonstrated that the procedure has significant capabilities, there remains scope to extend its range of application, and to also improve the computational efficiency of the method (particularly when solving three-dimensional problems, currently computationally expensive). Recent efforts in this regard include works by Crumpton et al. (2014) and Zhang (2017). Ongoing development work includes modelling rotational failure modes in general cohesive-
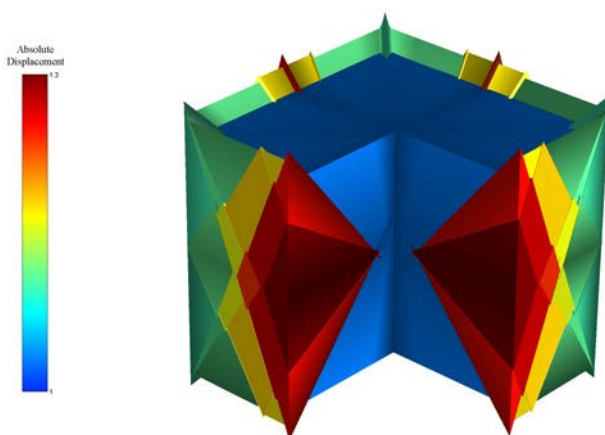

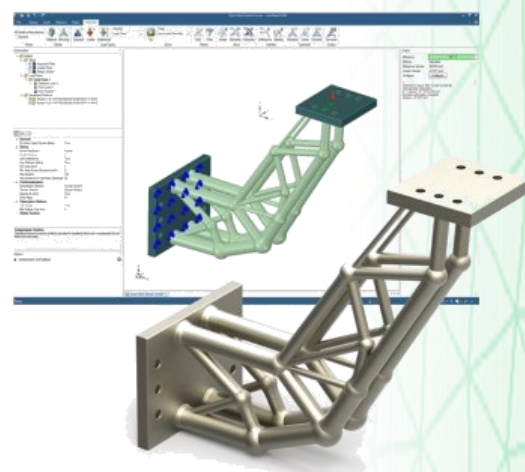*Figure 7. 3D failure mechanism for a square footing (after Hawksbee et al. (2013))*

Figure 8. An additively manufactured satellite mount component designed using inter- active design optimization software (LimitState:FORM).

frictional materials, identification of lower bound solutions, and application of decomposition and nodal adaptivity techniques.

Combining convex optimization with non-linear optimization is also providing significant benefits. The former has the advantage that it can identify global optima, but the problem must be couched in specific terms, while the latter provides significant flexibility and is a powerful tool for refining a solution, e.g. He and Gilbert (2015).

Finally, while LO involves design optimization and DLO involves analysis via optimization, it is possible to combine the two. For example, recent work has led to the development of an approach for the optimal design of soil reinforcement layouts in earthwork structures, to be published shortly.

6 CONCLUSIONS

Layout optimization (LO) and discontinuity layout optimization (DLO) are computationally efficient procedures for a range of problem types, which circumvent some of the disadvantages associated with traditional solid element based approaches.

Current applications include design optimization of structures and components and plastic analysis of problems involving geotechnical, metallic and concrete materials. Considering DLO, as a comparatively recently developed numerical procedure, there exists considerable scope to both further develop its theoretical underpinnings and to extend its range of application.

7 AKNOWLEDGEMENTS

8 APPENDIX A - MATLAB SCRIPT

Gilbert et al. (2010) described an implementation of the basic translational DLO procedure in a relatively short (<150 line) MATLAB script. This script can be used to analyse cohesive-frictional plane strain problems involving rectangular domains with multiple boundary conditions and soil self weight. The full script can be viewed or downloaded from http://cmd.shef.ac.uk/dlo).

REFERENCES

[1] Al-Defae, A. & J. Knappett (2015). Newmark sliding block model for pile-reinforced slopes under earthquake loading. Soil Dynamics and Earthquake Engineering 75, 265–278.

[2] Babiker, A. (2013). Limit Analy- sis Using a Non-Associative Flow Rule. Ph. D. thesis, University of Sheffield.

[3] Clarke, S., M. Gilbert, & C. Smith (2013, 5). Modelling discrete soil reinforcement in numerical limit analysis. Canadian Geotechnical Journal 50, 705–715. Accessed on 2018/03/28.

[4] Crumpton, M., A. Abbo, & S. Sloan (2014). Discontinuity layout optimization with adaptive node refinement. In Computer Methods and Recent Advances in Geomechanics, pp. 141–146. CRC Press.

[5] Dorn, W., R. Gomory, & H. Greenberg (1964). Automatic design of optimal structures. J. de

[6] Mechanique 3 (25-52).

[7] Gilbert, M., L. He, C. Smith, & C. Le (2014, 8). Automatic yield-line analysis of slabs using dis-continuity layout optimization.

[8] Gilbert, M., C. C. Smith, I. Haslam, & T. Pritchard (2010). Application of discontinuity layout optimization to geotechnical limit analysis problems. In Proc. 7th Eur. Conf. Numer. Methods Geotech. Eng. (NUMGE), Trondheim, Norway, pp. 169–174.

[9] Gilbert, M. & A. Tyas (2003). Layout optimization of large-scale pin-jointed frames. Engineering

[10] Computations 20 (8), 1044–1064.

[11] Hawksbee, S., C. C. Smith, & M. Gilbert (2013). Application of discontinuity layout optimization.

[12] Proc. R. Soc. A. 469, 20130009.

[13] He, L. & M. Gilbert (2015). Rationalization of trusses generated via layout optimization. Structural and Multidisciplinary Optimization 52, 677–694.

[14] Hemp, W. (1973). Optimum Structures. Clarendon Press, Oxford, UK.

[15] Leshchinsky, B. (2014). Limit analysis optimization of design factors for mechanically stabilized earth wall-supported footings. Transportation Infrastructure Geotechnology 1 (2), 111–128.

[16] Merifield, R. & C. Smith (2010). The ultimate uplift capacity of multi-plate strip anchors in undrained clay. Computers and Geotechnics 37 (4), 504–514.

[17] Smith, C. C. & M. Gilbert (2007). Application of discontinuity layout optimization to plane plasticity problems. Proc. R. Soc. A. 463 (2086), 2461–2484.

[18] Smith, C. C. & M. Gilbert (2013). Identification of rotational failure mechanisms in cohesive media using discontinuity layout optimization. Geotechnique 63 (14), 1194–1208. doi:10.1680/geot.12.P.082.

[19] Sokol, T. (2014). Multi-load truss topology optimization using the adaptive ground structure approach. In Recent Advances in Computational Mechanics, pp. 9. CRC Press.

[20] Zhang, Y. (2017). Multi-slicing strategy for the three-dimensional discontinuity layout optimization (3D DLO). International Journal for Numerical and Analytical Methods in Geomechanics 41 (4), 488–507.

COLIN SMITH
MATTHEW GILBERT

UNIVERSITY OF SHEFFIELD,
UNITED KINGDOM

C.C.SMITH@SHEFFIELD.AC.UK

"IT'S MOVING!! IT'S MOVING!!" IS DEAD, LONG LIVE "IT'S ALIVE!! IT'S ALIVE!!"

Computational Mechanics is a field aimed at leveraging computational methods to study mechanical problems, with an obvious focus on solids and fluids, but also electromagnetism or thermodynamics, among others. This field is relatively young, with the UK creating its own association, the UK Association for Computational Mechanics (UKACM), in 1992 under the guidance of celebrities of the field such as Prof. Zienkiewicz. On the other side of the Atlantic, the US counterpart, the USACM, was born a few years earlier, in 1988, again with some of the biggest names at its lead: Profs Bathe, Belytschko, Hughes to name but a few. This trend was mirrored worldwide through the creation of many similar associations.

As the field grew, it naturally developed two strong poles: Computational Fluid Dynamics (technically, only a subset of Computational Fluid Mechanics) and Computational Solid Mechanics. The interest was rather obvious, with early direct industrial applications in Aeronautics and Civil Engineering. The underlying methods of predilection quickly established themselves as the Finite Volume Method and the Finite Element Method (FEM), with the Finite Difference and Boundary Element Methods (BEM) being used to a lesser extent for specific problems or other physics (e.g., electromagnetism for the BEM). More recently the Spectral Methods have made their way into many of our solvers, and it is becoming quite clear that Machine Learning will have to be counted with in the years to come.

Solvers put aside, all these methods led the way to increasingly more complex evolutions, such as additional degrees of freedom or non-local constitutive models. In some cases, and as often in many fields, simultaneous efforts effectively ended up proposing similar methods, e.g., XFEM, Phantom Nodes approach, PUFEM, AFEM, GFEM, etc. Until recently, all of these evolutions clearly strengthened the leading roles of solids and fluids in the field.

Boris Karloff / Frankenstein / 1931 directed by James Whale [Universal Pictures]

However, having been a student not such a long time ago and an academic even less of a long time ago, it appears to me that the excitation of creating the FE model of an object, and watching it deform nicely on my monitor with a stress field colour map changing at each step does not have the same mesmerising effect nowadays as it used to have. As a matter of fact, a lot of these advanced methods are now part of commercial software and the "magic" of simulating fluid flow or material deformation is not necessarily the sole apanage of academia. As such, because of the very nature of academic research, what has found its place in everyday use in industry invariably diminishes the academic attractiveness among future PhD candidates.

One could argue that the FEM is clearly not just about a nice mesh being pulled around, and that constitutive models, solvers, etc. are equally as important as the visualisation of their effect, if not as observable. This is true, but, I will argue that the novelty of witnessing a solid deformation simulated from one's own hands is not as it used to be, and that what led me to bellow "It's moving!! It's moving!!" at my first simulation would nowadays at best be welcome with a blunt "it's finally working" for the same problem (or so I have witnessed in my Matlab FEM lectures).
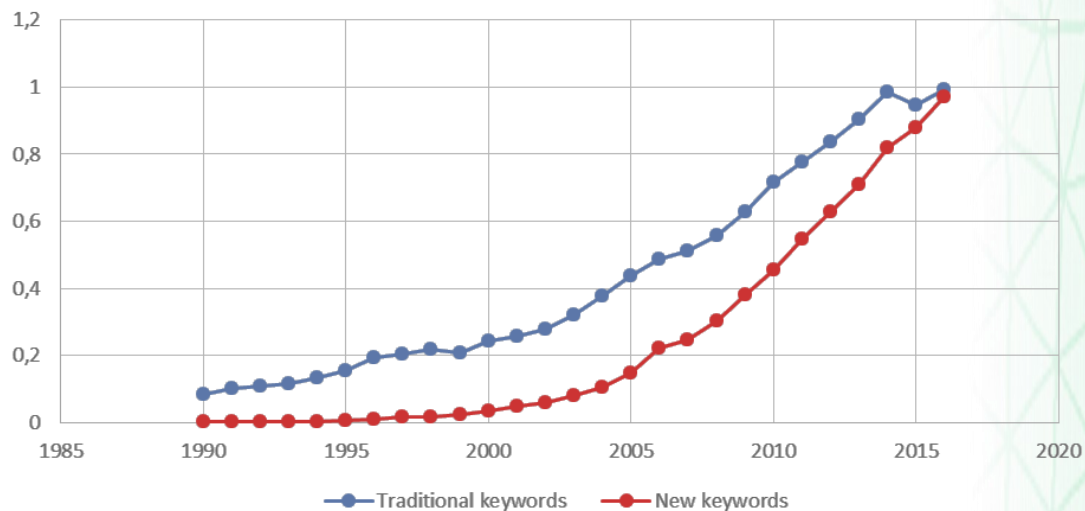
Figure 1. normalised keywords search occurrence in Scopus (Traditional: "computational mechanics", computational solid mechanics", "computational fluid dynamics", "finite element", "finite volume"; New: "multiphysics simulation", "multiphysics"+"simulation", "multiscale simulation", "multiscale"+"simulation").

For the sake of having a couple of figures in this opinion piece, I searched a few "traditional" keywords or expressions (namely, "computational mechanics", computational solid mechanics", "computational fluid dynamics", "finite element", "finite volume") on Scopus and plotted the normalised sum of their occurrence from 1990 to 2016 (I avoided 2017 in case some recent work are still not captured), see Figure 1. It is starting to plateau (note that it does too in 2017).

Now clearly, our field is not plateauing. If anything it is growing, and cunningly seeping through many other *a priori* orthogonal fields. Medical devices, MEMS, Microfluidics, to name a few are all heavily depending on complex multiphysics simulations. Many of the more "traditional" fields have now geared away towards multiscale analysis and computational scale up (especially in industrial applications). And of course, in some cases such as mine (Brain Mechanics), both multiphysics and multiscale aspects are simultaneously targeted.

I thus reopened Scopus and chose a new set of keywords to represent this shift. I also tried to take into account that the word "computational" has also been less used conjointly with words such as "multiphysics" or "multiscale" than the word "simulation" (a quick search on Scopus showed that the number of publications with the keyword "computational" grew by 39% from 1990 to 2016, vs. 50% for "simulation"). The final set ("multiphysics simulation", "multiphysics" + "simulation", "multiscale simulation", "multi-scale" + "simulation") is represented in Figure 1. Clearly those "newer" concepts are not plateauing.

This relatively trivial (and probably statistically dubious) study simply seems to confirm that the field is shifting. It is shifting from being a purely engineering application driven field to a widespread multiphysics multiscale analysis field. The last proof I needed to convince me of this fact (potentially obvious to the reader) was the email of a student working on cardiac mechanics a few years ago. He had just managed to couple mechanical deformation to cardiac electrophysiological behaviours in a cubic FE model. He was as excited as I had been when doing my first tensile simulation on a linear elastic dogbone sample. The video of the cube compressing and relaxing as electrical waves bounced back and forth in the geometry was accompanied by an excited quote from the 1931 classic horror movie "Frankenstein": "It's alive!! It's alive!!".

ANTOINE JERUSALEM
UNIVERSITY OF OXFORD,
UNITED KINGDOM

ANTOINE.JERUSALEM@ENG.OX.AC.UK

AN OVERVIEW OF THE MATERIAL POINT METHOD

The Material Point Method (MPM) is a versatile tool for the analysis of solid mechanics problems characterised by large or extreme displacements. The method is based on continuum mechanics, therefore it can use a large number of already developed and validated constitutive material models and modelling techniques. The Material Point Method can reliably provide solutions for large displacement problems which are difficult or impossible to solve with other numerical methods based on continuum mechanics, such as the Finite Element and Boundary Element Method. Currently, the term 'Material Point Method' typically encompasses the original method [1-2], as well as number of improved methods, including the Generalized Interpolation Material Point Method (GIMP) [3], the Convected Particle Domain Integration Material Point Method (CPDI) [4-5], the Dual Domain Material Point Method (DDMP) [6] and some developing implicit Material Point methods, e.g. [7-11].

In the Material Point Method, the material domain is discretised with material points, which are cast over a computational grid with nodes (Figure 1). The advantage of such a discretisation is that the information about the material and solution is carried by the material points, which are not fixed, unlike nodes in the Finite Element or Boundary Element Method. The computational grid is arbitrarily chosen and, in principle, any grid is allowed, with any number of material points in each grid cell.

However, there are numerical benefits of choosing a reasonable number of material points in each grid cell (e.g. 2-3 in each direction). Also, sometimes a special computational grid, e.g. one which is altered in line with the material point positions as in [12-13], may be beneficial. Nonetheless, the most usual choice currently is to have a regular and fixed computational grid.

The original Material Point Method [1-2] algorithm loop starts with the transfer of the information (momentum, internal force and possibly body forces) from the material points to the grid nodes with the help of the shape functions. The accelerations of the grid nodes are computed (based on unbalanced forces), as well as the new nodal velocities (after the time step). The computed updated nodal momenta are subsequently transferred to the material points, again using the same shape functions. Each material point velocity, position and stress are updated, and the algorithm loop is repeated in the next step.

The described Material Point Method algorithm could solve large displacement dynamic problems with advanced material models, but suffers from number of shortcomings. Those are mainly related to accuracy, as well as material continuity and contact. In particular, the material points lose contact when being separated by more than a single grid cell, leading to so called material separation. Even though the material separation may be also viewed as an advantage, because it allows for simple and qualitatively correct modelling of fractures, the results of simulations in which the separation of the material occurred may depend on the number of material points per grid cell and grid size itself, leading to difficulties in obtaining quantitatively correct results. Furthermore, simulations made with the original MPM formulation suffer from numerical noise associated with the points passing through the grid boundaries, leading to errors and oscillations in the results.

These shortcomings led to further development of the original Material Point Method. In 2004, Bardenhagen & Kober proposed the Generalized Interpolation Material Point Method (GIMP) [3], which introduced
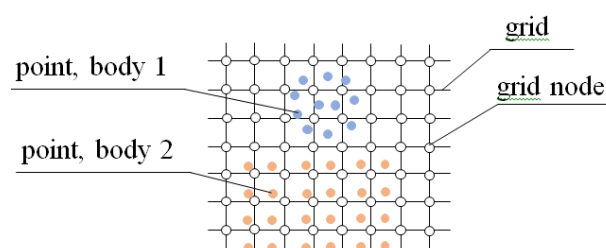

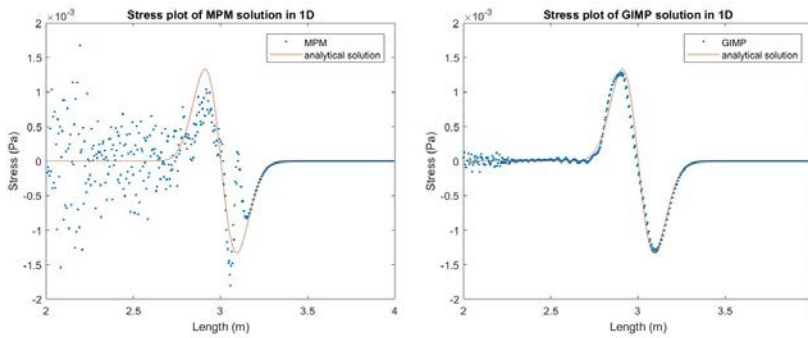*Figure 1. MPM discretisation – material points, grid and grid nodes*

Figure 2. The original MPM (left) and GIMP (right) solutions of an impulse travellling in a Neo-Hookean elastic beam vs analytical solution (continuous line)

particle domains. Physically, particle domains, defined by the non-zero particle characteristic functions, signify that the material is physically spread over space, improving on the original formulation where the material mass is concentrated in the points only. GIMP increases complexity of the computations somewhat, as the mapping of the data from and to particles becomes a bit more difficult. Nonetheless, GIMP does reduce the oscillation when particles are crossing the grid boundaries, as well as generally improve the method accuracy. For example, in Fig. 2, the solution obtained with the original MPM has clearly lost coherence after 500 steps, whereas GIMP replicates the correct analytical solution quite accurately for a much longer time. The Generalized Interpolation Material Point Method also gives a wider framework for the formulation in which the functions related to transfer of data from and to particles, as well as particle domains, can be chosen relatively freely. Formulations with novel functions are being constantly explored, e.g. [14].

Relatively quickly it has been noticed that the constant domains of the material points mean that those can overlap when the material points move. Also, during simulation with the Generalized Interpolation Material Point Method material separation can still occur at large

strains, breaking the notion of material continuity. Again, the possibility of material separation may help in simulation of discontinuities, but it leads to mesh dependency and difficulties with formal convergence proofs as the assumptions of continuum mechanics are not satisfied after material separation. This issue has been first addressed by a rather computationally expensive tracking of the domain of the material points, and later by the Convected Particle Domain Interpolation Material Point Method (CPDI) [4] where the shape functions are defined so that the material points are always linked to each other, ensuring continuity (see Fig. 3). However, the limitation, partially removed in CPDI2 [5], is that modelling of indentations or problems where material should separate is more difficult and may need special techniques.

The majority of Material Point Method implementations described in the literature to date are explicit, which means that they are suited for

simulation of rather quick dynamic problems, where elastic waves, shock waves and inertial forces are important. However, in many problems the final very large deformations build slowly over longer periods of time. In such cases, it is not necessary to monitor every elastic wave in the material and hence implicit versions of the MPM, which neglects dynamic effects, are preferable, e.g. [7-11]. Implicit Material Point Methods allow for much larger time steps, not being limited by the Courant condition related to the speed of sound in the material.

The Material Point Method is easy to couple with other numerical methods based on continuum mechanics, such as the Finite Element Method, e.g. [15]. Such coupling allows for combination of the best features of both methods in a simulation. Typically, the domain is divided into two parts, one which is solved with Finite Element Method or similar numerical method and the other part where the Material Point Method is used. The Material Point Method also allows for simultaneous simulation of different phases of the material. The coupling may be either done via defining two different domains, e.g. solids, solved with the Material Point Method and fluids, solved with another method. However, it is entirely possible to model all the material phases with the Material Point Method only, including the flow of fluid or gas in a deforming porous material e.g. [16].

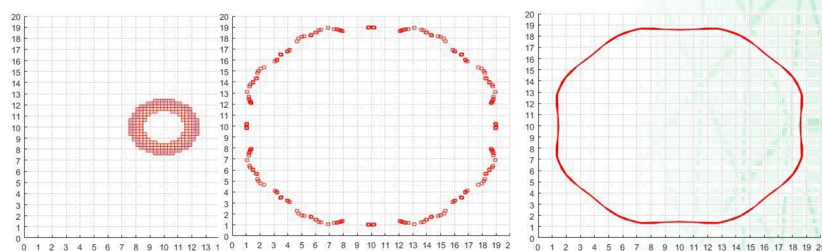Simulations with the Material Point

Figure 3. Expanding Neo-Hookean elastic ring: initial state (left), GIMP solution with material separation (middle) and continuous CPDI solution
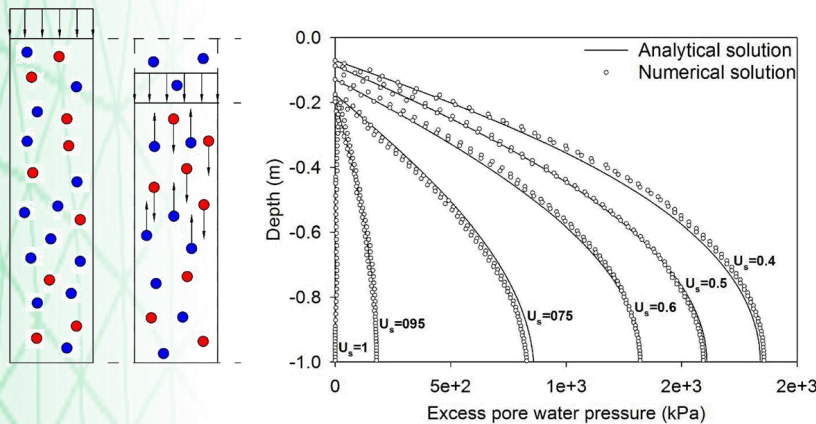
17

Figure 4. DDMP solution of large displacement 1D consolidation. Initial condition (left) show schematically porous material (red material points) saturated with water (blue points). During consolidtaion water flow out of the material (middle). Solution replicates well the analytical solution (right) [17]

Method can be rather demanding in terms of computer resources, as even simple problems (see Fig. 5), need hundreds of thousands of material points to obtain accurate solution in time. Currently, that issue can be partially mitigated by parallelisation of the code. The other alternative is to use implicit versions of the method, which allows for much larger time steps and thus quicker simulations.

The Material Point Method has to date been applied to a wide range of problems, including simulations for movies (e.g. the Disney film 'Snow' [19]), explosions and penetrations for military applications and many other problems in engineering. In general, Material Point Method simulations with extreme deformations, such as landslides, are now one of the most typical applications of MPM (e.g. [20]). There is strong interest from engineering companies, as in the future the Material Point Method may allow for realistic estimation not only of landslide flow, but also forces on obstacles and barriers during avalanches and landslides (see Fig. 6).

In conclusion, the Material Point Method seems to be a very promising tool for solving problems where large or extreme displacements are present. At the moment, the explicit version of the method is only competitive with other existing numerical methods for dynamic / short duration problems, whereas the implicit MPM, possibly better suitable for quasi-static problems, is still relatively scientifically unexplored. The research community working on the method has grown and is constantly improving the method and addressing its shortcomings. For example, much effort is spent on improving the MPM convergence rate (which would reduce the required number of material points in a simulation), increasing the method stability and accuracy, developing more accurate contact and boundary condition algorithms [22], as well as on development of

the implicit MPM. The end-user experience is also improving, with creation of not only better user interfaces but also improved parallelisation and optimised algorithms. To that end, well-known companies who offer advanced Finite Element software investigate the coupling of FEM and MPM as means to allow for simulations of very large displacements in their codes. Integrated MPM-FEM suite would use MPM in parts of the computational domain experiencing large deformations, while the parts of the domain with small displacements could be modelled very accurately with the well-proven existing FEM code.

REFERENCES

[1] Sulsky D, Chen Z, Schreyer HL. A particle method for history-dependent materials. *Comput Meth Appl Mech Eng* 1994; **118** (1):179–96.

[2] Sulsky D, Zhou S-J, Schreyer HL. Application of a particle-in-cell method to solid mechanics. *Comput Phys Commun* 1995; **87** (1):236–52.

[3] Bardenhagen S, Kober E. The generalized interpolation material point method. *Comput Model Eng Sci* 2004; **5**(6):477–96.

[4] Sadeghirad A, Brannon RM, Burghardt J. A convected particle domain interpolation technique to extend applicability of the material point method for problems involving massive deformations.
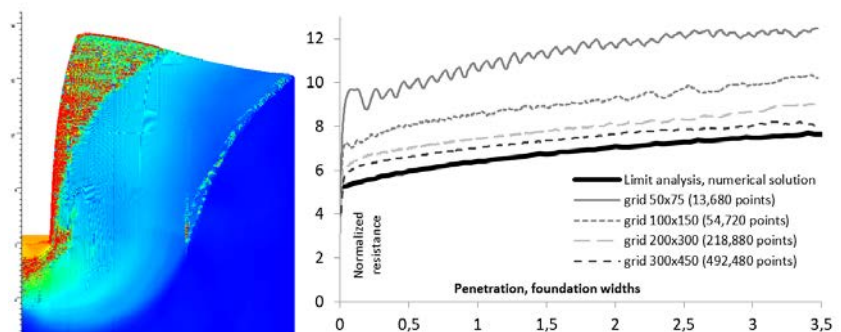
Figure 5. Foundation penetrating perfectly plastic soil solved with GIMP. Simulated penetration (left) and convergence to the expected result with increase in number of material points (right) [18]
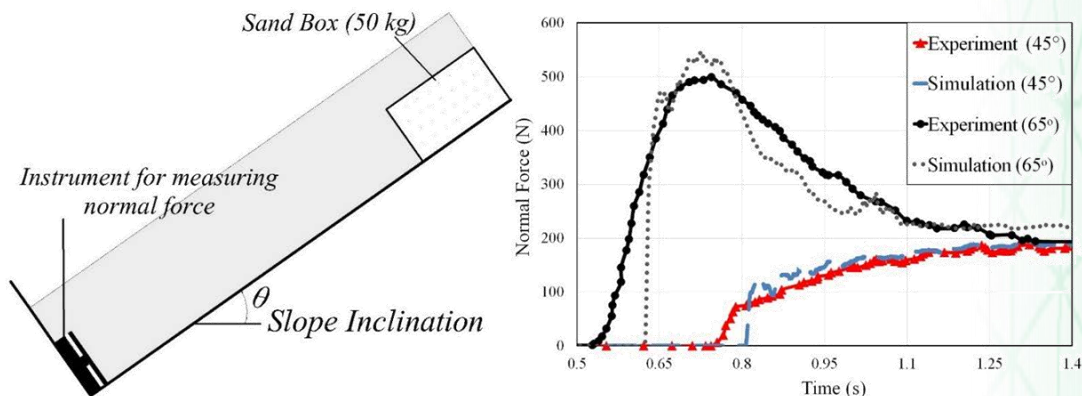
Figure 6. GIMP simulation replicating experiment where forces of sand avalanche on an obstacle were measured for different slope inclinations [20]

Int J Numer Meth Eng 2011; **86** (12):1435–56.

[5] Sadeghirad A, Brannon RM, Guilkey J. Second-order convected particle domain interpolation (CPDI2) with enrichment for weak discontinuities at material interfaces. *Int J Numer Meth Eng* 2013; **95**(11):928–52.

[6] Zhang DZ, Ma X, Giguere PT. Material point method enhanced by modified gradient of shape function. *J Comput Phys* 2011; **230** (16):6379–98.

[7] Cummins S, Brackbill J. An implicit particle-in-cell method for granular materials. *J Comput Phys* 2002;**180** (2):506–48.

[8] Beuth L, Benz T, Vermeer PA, Więckowski Z. Large deformation analysis using a quasi-static material point method. *J Theoret Appl Mech* 2008; **38**:45–60.

[9] Beuth L, Więckowski Z, Vermeer PA. Solution of quasi-static large-strain problems by the material point method. *Int J Numer Meth Eng* 2011; **35**:1451–1465.

[10] Wang B, Vardon PJ, Hicks MA, Chen Z. Development of an implicit material point method for geotechnical applications. *Comput Geotech* 2016;**71**:159–67.

[11] Charlton TJ, Coombs WM, Augarde CE. iGIMP: An implicit generalised interpolation material point method for large deformations. *Comp Struct* 2017; **190**:108-125.

[12] Al-Kafaji IKJ. Formulation of a dynamic material point method (MPM) for geomechanical problems. Stuttgart (Germany): Universität Stuttgart; 2013.

[13] Phuong NTV, van Tol AF, Elkadi ASK, Rohe A. Numerical investigation of pile installation effects in sand using material point method. *Comput Geotech* 2016; **73**:58–71.

[14] Gan Y,Sun Z, Chen Z, Zhang X, Liu Y. Enhancement of the material point method using B-spline basis functions. *Int J Numer Methods Eng* 2018; **113**:411–431.

[15] Chen ZP, Qiu XM, Zhang X, Lian YP. Improved coupling of finite element method with material point method based on a particle-to-surface contact algorithm. *Comp Meth App Mech Eng* 2015 **293**: 1-19.

[16] Bandara S, Soga K. Coupling of soil deformation and pore fluid flow using material point method. *Comp Geotech* 2015; **63**: 199-214.

[17] Tran QA, Sołowski WT, Cummings E. Hydro-mechanical coupled dual domain material point method stabilized with a null-space filter. *V International Conference on Particle-Based Methods. Fundamentals and Applications, Particles 2017*, pp. 659-669.

[18] Sołowski W, Sloan S. Evaluation of material point method for use in geotechnics. *Int J Numer Anal Meth Geomech* 2015; **39**(7):685–701.

[19] Stomakhin A, Schroeder C, Jiang C, Chai L, Teran J, Selle A. Augmented MPM for phase change and varied materials. *ACM Trans Graph* 2014, **33**(4): 138.

[20] Soga K, Alonso EE, Yerro A, Kumar K, Bandara S. Trends in large-deformation analysis of landslide mass movements with particular emphasis on the material point method. *Geotechnique* 2016, **66** (3): 248-273.

[21] Seyedan S, Sołowski WT. Estimation of Granular Flow Impact Force on Rigid Wall Using Material Point Method. *V International Conference on Particle-Based Methods. Fundamentals and Applications, Particles 2017*, pp. 648-658.

[22] Cortis M, Coombs WM, Augarde CE, Brown M, Brennan A, Robinson S. Imposition of essential boundary conditions in the material point method. *Int J Numer Meth Eng* 2018, **113**:130–152.

W.T. Sołowski

Q.A. Tran

S.M.J. Seyedan

Aalto University,

Finland

WOJCIECH.SOLOWSKI@AALTO.FI

COMPUTATIONAL AND DATA SCIENCES IN LUXEMBOURG

LUXEMBOURG, AN EMERGING KNOWLEDGE ECONOMY

Luxembourg is one of the wealthiest countries in the world in terms of gross domestic product (GDP) per capita. The country has successively and successfully transitioned from an agricultural to a service-driven economy, through the heavy industry characteristic of the industrial revolution. In spite of these undeniable successes, driven in the recent past by the financial sector, Luxembourg has still not achieved the status of world-leading marketplace.

In 2003, the University of Luxembourg was created, with the aim to diversify the country's economy and facilitate its transition to a Knowledge Economy. Yet, in 2012, Luxembourg spent only 1.51% of its GDP on Research and Development, complemented by as much as 1% of its GDP provided by large companies such as ArcelorMittal, GoodYear (who is today the second employer in the country) and Delphi. The University, along with most of the research, development and innovation actors, including start-up incubators are now collocated in the exciting Belval Campus in the south of the country Figure 1.

Luxembourg has developed a Smart Specialisation Strategy (S3), focusing on Information and Communication Technology (ICT), Ecotechnology and Biotechnology. The materials, space and ecotechnology sectors are already somewhat consolidated and host a number of competitive companies, from metallurgy to high-performance composites (ArcelorMittal, Eurocomposites, e-Xstream, GoodYear and many others).

The health/biomedical sector was created ex nihilo from a 140M euro government investment in 2008 and reinforced by the creation within the University of the Luxembourg (Interdisciplinary) Centre for Systems Biomedicine (LCSB), which led to the creation of various spin-offs supported by fundamental research in Systems Biology. The ICT sector is supported by the Interdisciplinary Centre for Security and Trust (SnT) at the University of Luxembourg, and benefits from world-class interconnect infrastructure, providing the country with a clear competitive edge which attracted the likes of Google, Paypal and Amazon to the Grand Duchy.

This research and innovation landscape includes recent initiatives ranging from additive layer manufacturing to space and asteroid mining and may, at first, appear disparate in focus. Over the last 5 years, Computational and Data Science has been emerging as a

Figure 1. Belval Campus in the South of Luxembourg where the government, the funding council (FNR), the national research institutes and the University of Luxembourg, along with incubators are collocated
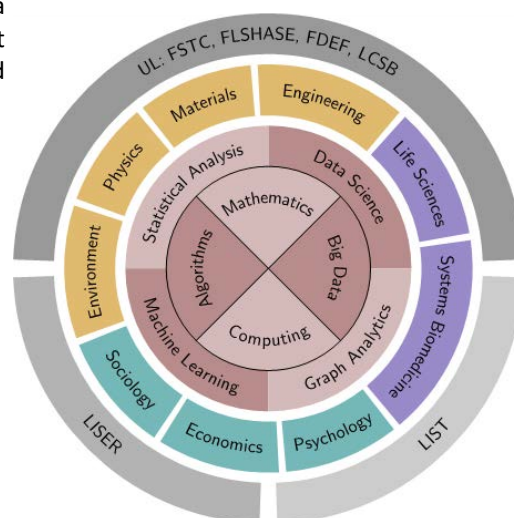

Figure 2. The methodological approach for computational and data sciences in Luxembourg. The methodological core relies on mathematical and computer science constructs which is used for a wide variety of applications, in collaboration with research centres and the industrial sector

unifying discipline. In 2013, the University of Luxembourg has made the field one of its core priorities. This unifying multi-disciplinary focus area relies on a strong mathematical, computational and methodological core (Figure 2) and has convinced policy makers, funding councils and the private sector through its ability to drive education, research and innovation across a wide range of sectors of central importance to Luxembourg.

We review in the following the key concepts underlying computational and data sciences in Luxembourg and focus on one particular application area: Computational Engineering Sciences, particularly relevant to ECCOMAS.

WHAT IS COMPUTATIONAL AND DATA SCIENCE (CODES) AND WHY IS IT IMPORTANT TO LUXEMBOURG?

Computational Sciences are fundamental to all fields: Translating complex real-world processes into mathematical models and simulations in the virtual world has been a key aspect of scientific advancement since the 1940's. The upcoming challenge is to build on the undeniable successes of Computational Sciences in Engineering and Technology to ethically and efficiently harness and exploit the soaring amounts of data and address open problems in medicine, social sciences and finance and build a smart, resilient, future-proof society (Bordas and Ley, 2018).

With powerful computers and robust algorithms, we are now able to simulate increasingly complex systems on the computer, and thus gain valuable insights without performing elaborate and costly experiments. Computations underpin disciplines as varied as biology, biomedicine, transportation, materials science, engineering, social sciences and even art.

Computations are pervading all disciplines. Modelling techniques are relevant to all technical and scientific areas. CoDeS aims to leverage this methodological commonality to increase the research and innovation productivity. Computational and Data Sciences researchers act as translators by using mathematical language as a common communication means to bridge gaps between disciplines and make research and innovation more effective.

At the University of Luxembourg, the CoDeS Community unites 10 core Faculty and 40 application Faculty members (including 5 ERC grants) who submitted third party projects for a total approximate cost of 240 million euros (20% of the total number of projects submitted at UL), produced half of the highly cited publications in Luxembourg at large.

- In years 2015-2016: 2,152 journal papers were published in Luxembourg. A third of those publications are in the field of Computational Sciences, including 8 highly cited articles, of which half were published by UL. The UL hosts a ISI Highly Cited Researcher in Computer Science (2015, 2016) and in Engineering (2017) [Link]
- A Doctoral Programme in Computational and Data Science was created.
- A Data Driven Computational Modelling Doctoral Training Centre application (DRIVEN - 22 PhD students) was funded by the Fonds National de la Recherche (FNR) funding council. The proposal bridges across all faculties and inter-disciplinary centres as well as two of the Luxembourg Public Research Institutes.

The Computational and Data DRIVEN Science Doctoral Training Unit (DTU) will train a cohort of Doctoral Candidates (DCs) who will develop data-driven modelling approaches common to a number of applications strategic to the Luxembourgish Research Area and Luxembourg's Smart Specialisation Strategies.

We propose to create this bridge between a methodological core and application domains by training each DC both in state-of-the-art data-driven approaches, and in the particular application domain in
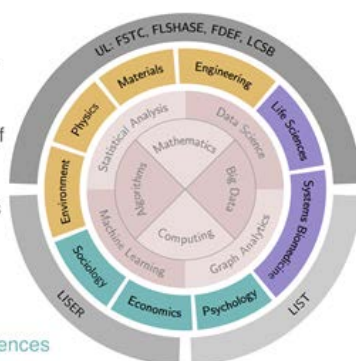

Figure 3. Concept behind the DRIVEN Data-Driven Modelling and Simulation Doctoral Training Unit (19 PhD students) funded by the FNR (2018-2023), led by Prof. Andreas Zilian (Computational Engineering) and supported by the University of Luxembourg Computational and Data Science Priority (CoDeS)

which these approaches are expected to lead to new discoveries: Computational Physics and Engineering Sciences, Computational Biology and Life Sciences, and Computational Behavioural and Social Sciences (Figure 3). In six years, DRIVEN will result in a group of scholars that enriches Luxembourg's socio-economic landscape not only with expertise in data-driven discovery and machine learning, but also with a fundamental understanding of how these approaches can be of most use to a wide range of focus areas.

We will strengthen the data-driven repertoire in areas already benefiting from these techniques, and will strive to establish similar techniques in areas where these approaches are only nascent. By embedding the DRIVEN DTU in the existing Doctoral School (DS) structure of the University of Luxembourg (UL), we will create its first transversal Doctoral Programme (DP), spanning all three Faculties and reaching out to the Interdisciplinary Centres, the LIST and LISER. DRIVEN will benefit from the already established doctoral education framework and best practices gleaned from previous DTUs, allowing our DTU to focus on innovative doctoral training strategies for its highly interdisciplinary research directions.

DRIVEN will contribute, in conjunction with strong national and European initiatives such as Digital Lëtzebuerg and the Important Project of Common European Interest on HPC and Big Data Enabled Applications, to boosting Luxembourg's competitiveness thanks to an increased ability to make use of the vast amount of data generated worldwide on a daily basis.

COMPUTATIONAL ENGINEERING

The Department of Computational Engineering Sciences (DCES) will provide a means to link and rationalise research and education efforts across a wide range of disciplines by tackling common fundamental methodological hurdles involved in modelling, simulating, controlling and understanding the physical world. Built around an open-source, open-data and collaborative approach, DCES will inspire and foster innovation and collaborative opportunities to ensure Luxembourg's international competitiveness and economic growth.

The aim of DCES is to become an internationally renowned institute, dealing with methodological research in Computational Engineering Sciences. By focusing on fundamental research while keeping a link to different applied science domains, we will continue to foster a nimble and adaptive economy and provide general methodologies on which to strengthen existing and build future priority application areas of National Importance.

The Department aims at building intuitive and interactive platforms for computational engineering problems that allow the users not only to understand and predict the behaviour of real systems but also to better capture the interaction between models and data and hence gain insights into unconventional and counter-intuitive phenomena.

We target the data-driven modelling, simulation, control and quality assurance of complex (dynamical) systems governed by partial differential equations applied among others to glacier, energy harvesting, medicine and surgery research, through the multi-scale design of lighter, stronger tunable,

adaptive functional and reconfigurable matter (with Marie Curie Fellow Jakub Lengiewicz, IPPT Poland) as well as the modelling of organisms and diseases progression. As a second research strand, we target complex networks and their interaction with human behaviour, such as those arising in logistics, traffic, communication, energy, biological and social systems.

To achieve this goal, several challenges must be overcome, which are the core research directions of the Department.

- **Data** Acquire, process and fuse data sets for phenomena and systems of interest;
- **Model** Select the proper mathematical models capturing the problem dynamics and identify the most relevant parameters, given experimental evidence. This includes adopting multi-scale and single-scale approaches, multi- or single-field problems and solving large-scale instances;
- **Simulate and Control** Discretise and control the computational complexity of the models and of the predictive simulations. This will require working hand-in-hand with HPC developers, through co-design to optimise hardware for given computational needs, e.g. for (machine) learning algorithms and neural networks;
- **Assure quality** Quantify, measure and control the effects of uncertainties and errors on quantities of interest to the modeller;
- **Visualize** Provide tools for interpreting and visualising phenomena in order to develop decision support systems for different application domains.

The Department focuses on general methodological developments which are as application independent as possible in order to streamline

research and optimise open innovation and productivity.

The research done at DCES is primarily data-driven modelling. We work in close synergy with (applied) mathematicians to ensure the mathematical rigour of the numerical methods we develop. We collaborate with computer scientists to create robust computational techniques required for reliable analysis and control of complex systems. Finally, we include in the Department an engineering flavour to guarantee that the theories and models developed are proven to provide societal and economic impacts.

DCES is instrumental in building powerful and impactful interdisciplinary connections between engineering, computer science, mathematics, physics and other priority application areas in Luxembourg. Areas where we have already had impact include in particular: Space Science, Advanced Manufacturing and Materials, Robotics, Automotive, Transport and Logistics as well as Neuro-degenerative Diseases.

The Department is organised within three subgroups:
- Data acquisition and analysis;
- Computational Modelling and Simulation for Networks and PDEs;
- Control.

In the following, we provide a few ongoing research directions of the Computational Modelling and Simulation subgroup as it is most relevant to ECCOMAS. The subgroup is led by three professors (Bordas, Peters, Zilian) working alongside three experienced postdoctoral researchers (Beex, Besseron, Hale). The team deals with advanced discretisation techniques for partial differential equations and particulate systems aiming at understanding the effects of

variability, ambiguity, uncertainty in the selection of the most adequate models and their discretisations. Another key research direction deals with simulation quality control and acceleration, through model order reduction, error estimation and adaptivity. The team deals with problems ranging from real-time simulations (for image-based surgical guidance) to large multi-scale scale simulations. Through specific research examples, we provide below an overview of the work done in this subgroup.

MULTI-SCALE ANALYSIS OF MECHANICAL IMPACT OF GRANULAR MATERIAL ON STRUCTURES THROUGH EXTENDED DISCRETE ELEMENT METHOD (XDEM)

Handling of granular media e.g. transport and storage generates severe mechanical loads on walls or structures in contact. The latter may be static or moving in an arbitrary mode. In particular devices such as conveyors, chutes, truck bodies, grain elevators, hoppers or tyres are important examples of structures that experience a strong mechanical impact from moving granular material. Forces exerted may be predominantly static as during storage or may have a highly dynamic character as observed during discharge operations. It is essential for both design and operation to assess these evolving loads and to avoid major failure.

In order to estimate these forces acting on structures a coupling between the Finite Element Method (FEM) and the Discrete Element Method (DEM) is applied in the LuXDEM team. Contrary to approaches involving overlapping domains, the current concept employs non-overlapping computational domains. Thus, deformable structures and their stresses are represented by the Finite Element Method (FEM) while the granular material is described by the Discrete Element Method (DEM). The coupling technique identifies contact between discrete elements and the FEM mesh i.e. its surface elements. Contacts between the surface elements of the mesh and discrete elements generate forces due to impact that determine motion of individual particles
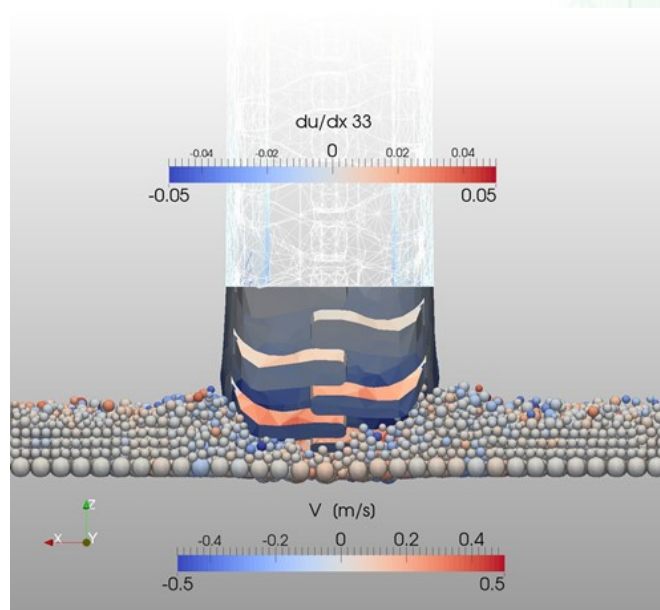

Figure 4. Deformation of a tyre and displacement of granular underground during rolling motion
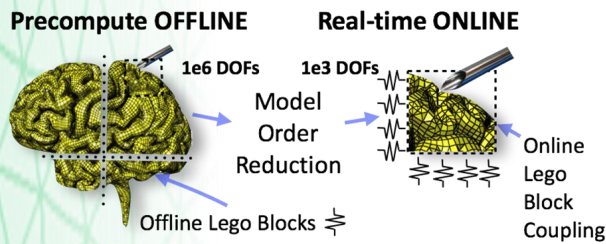
Figure 5. The principle of our domain-based model order reduction approach. Only the reducible subdomains are reduced (precomputed), whilst the subdomain where the needle is inserted or the tissue is cut cannot be reduced and is fully assembled into the system matrix. This work was done in collaboration with Pierre Kerfriden (Cardiff) and published in a series of papers
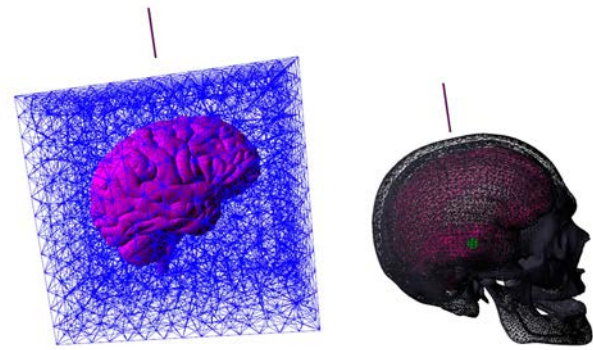

Figure 6. Implicit boundary definition and adaptive XFEM (CutFEM) approach to needle insertion for deep-brain stimulation. This work by Bui Huu Phuoc and Satyendra Tomar was submitted for publication in March 2018 (CMAME)

according to Newton´s second law for translation and rotation.

Similarly, forces generated exert a mechanical load on structures that consequently deform and respond with an internal stress distribution as shown in the following fig. X. The tyre supports the weight of the vehicle and thus, generates forces between the tread and the loose underground. It responds with a compaction and a displacement of individual particles. Integrating these individual contacts yields the total traction forces of the tyre that has a strong influence on load-carrying ability, steering stability and driveability.

REAL-TIME ERROR-CONTROLLED SIMULATIONS FOR SURGICAL TRAINING AND GUIDANCE

The team of S. Bordas has been working since 2012 (ERC RealTCut) on the development of real-time simulation tools for surgical training and guidance. This work has been done in collaboration with Dr. Pierre Kerfriden (Cardiff), Dr. Jack Hale and Dr. Lars Beex as well as strong collaborations with colleagues in computer science (Stéphane Cotin and Christian Duriez) and mathematics (Profs. Franz Chouly and Alexei Lozinski) as well as with neurosurgeons (Dr. Pierre Robe and Dr. Frank Hertel).

The work has focused mainly on the acceleration of non-linear computational mechanics of soft tissue deformation undergoing severe strains, cutting or topological changes. The main difficulty lies in the fact that model order reduction such as the proper orthogonal decomposition fails in regions where localisation takes place (Figure 5). To circumvent such problems, we developed adaptive reduced order modelling based on domain decomposition techniques. To further control the computational cost, we investigated the use of a posteriori error estimates, which we employed successfully for needle insertion problems with applications to deep brain stimulation.

To address the difficulties associated with dealing with complex geometries and topological changes, we developed enriched finite element methods (CutFEM approaches) where the boundary of the domain and that of the cuts or material interfaces (tumour/tissue) are not meshed conformally.

Finally, we realised that some of the most difficult questions in surgical simulation arise because of the difficulties associated with identifying the optimal material model, and associated parameters for a given patient. These requirements for patient-specific simulations led us to investigate model selection and model parameter identification using

Bayesian inference, which is the focus of the team of Dr. Jack Hale and of part of the endeavours of Dr. Lars Beex, presented next.

EFFICIENT SCALABLE METHODS FOR UNDERSTANDING UNCERTAINTY AND IDENTIFYING OPTIMAL MODELS IN PHYSICAL SYSTEMS

The work described within this section is carried out by experienced researcher Dr Jack Hale whose team deals with large scale stochastic inverse problems and uncertainty quantification alongside advanced discretisation techniques for problems involving small parameters (e.g. locking).

Uncertainty quantification is an area of recognised importance in the computational sciences, and is receiving an ever-increasing amount of attention from the ECCOMAS community. In Luxembourg, we are developing new techniques and methodologies to tackle the next generation of uncertainty quantification problems.

We have recently looked at the question of how to calculate derivatives of systems with respect to their underlying stochastic parameters [Hauseux et al. 2017a]. We apply the Malliavin Calculus, a

powerful tool of mathematical analysis, which extends the more classical notions of a derivative (e.g. Fréchet, Gâteaux) to stochastic processes. We have developed a computational method based on Monte-Carlo sampling to efficiently and accurately calculate this Malliavin derivative. In a hyperelastic beam buckling problem (Figure 7) we have shown that the classical notion of a derivative taken about the mean parameter is insufficient to quantify the sensitivity of the system. The Malliavin derivative gives a far more complete picture, taking rigorously into account the stochastic nature of buckling processes. Other interesting examples in fluid mechanics, viscoelasticity and elasticity are shown in the paper.

In another paper we looked at using classical (Fréchet) derivatives as a control variate method to reduce the sampling error of a classical Monte-Carlo estimator (Figure 8). In low to moderate-variance regimes, the proposed estimator is orders of magnitude more efficient than a standard Monte Carlo approach. We automatically compute derivatives of high-level finite element models using the FEniCS Project, making the approach broadly applicable to many different numerical models.

Ongoing work in the group includes

the extension of the estimator in [Hauseux et al. 2017b] to random field problems [Hale et al. 2018].

MULTISCALE MECHANICS OF FIBROUS AND DISCRETE MATERIALS

The research conducted and supervised by experienced researcher Dr Lars Beex, whose team deals with the computational modeling of materials with some form of small-scale discreteness. Examples are paper materials, fabrics, foams and printed lattices. His efforts focus on

(i) the development of appropriate discrete models at the small-scale
(ii) the development of multiscale and model order reduction techniques to allow their use at the engineering scale.

For some time, Beex' group also targets (iii) the identification and propagation of the small-scale randomness of fibrous materials.

i) The development of discrete models for metal printed lattices and fabrics currently takes place thanks to the financial support of the Luxembourg National Research Fund and the University of Luxembourg, respectively. Issues of special interest are model-order-reduction with hyperreduction and volume-to-

volume contact approaches for beams.

ii) Beex is mostly experienced with the quasicontinuum (QC) method as the multiscale method to allow discrete micromodels in engineering-scale computations. Advantages of the QC method compared to other nested multiscale approaches are its intrinsic concurrent character and the lack of scale separation (top in Figure 9). Originally developed for atomistic lattices, Beex et al. have widened its application domain towards elastoplastic, damageable spring and beam lattices [Beex et al., 2011, 2014a,b,c]. He has also advised in the efforts of Dr Ondrej Rokos and Dr Jan Zeman to include adaptivity in the QC method [Rokos et al, 2016, 2017]. His own efforts currently focus on the enhancement to treat random networks instead of lattices (top in Figure 9).

iii) The randomness in discrete materials such as random fiber networks is assumed to originate from two issues. First, each fiber has its own set of material parameters. This set is assumed to be a realisation from a probability distribution [Rappel et al., 2017]. Second, geometrical randomness is present. Current efforts focus on identifying the
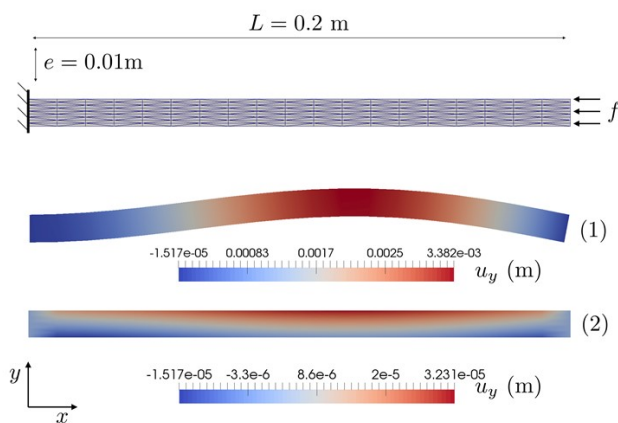
Figure 7. Two realisations of the solution of a geometrically non-linear hyperelastic beam problem with stochastic Young's modulus. Source: https://doi.org/10.1371/journal.pone.0189994.g006 Creative Commons Attribution License
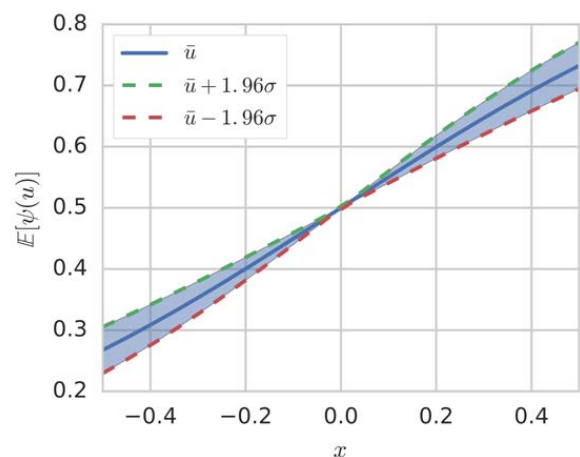
Figure 8. Solution of a stochastic non-linear Burgers equation using the proposed sensitivity control variate method. Mean and 95% predictive envelope shown. Source: https://dx.doi.org/10.6084/m9.figshare.3561306.v2. License: GNU LGPLv3 or later.
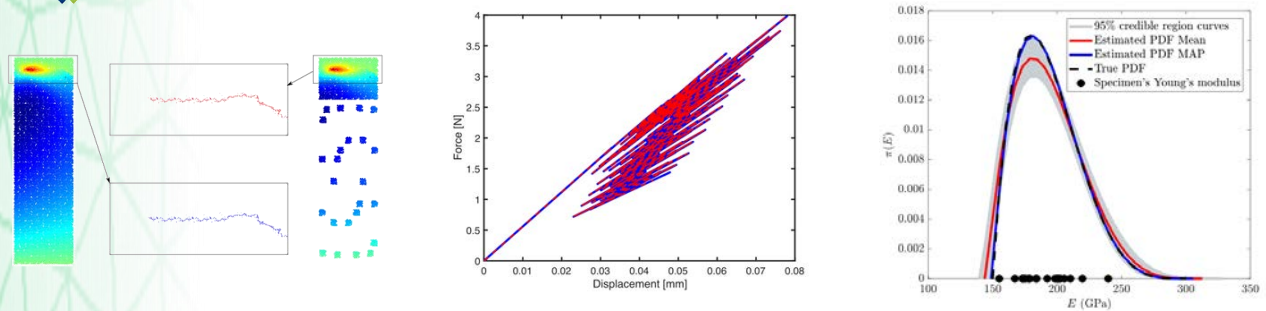
Figure 9. LEFT: Results of the DNS (blue) and a QC simulation for a model of 35x10 unit cells. Each unit cell consists of 100 fibers, discretized by 2001 linear elastic-perfectly brittle beams. Shown are broken beams and force-displacement responses. RIGHT: 15 Young's moduli (black dots) are generated from a beta-distribution ('True PDF'). Based on these 15 'measurements', the parameters of the beta-distribution are to be identified. These identified parameters are distributions themselves, and some realisations are shown in grey, whilst the mean is shown in red (a result of the PhD of Mr. Hussein Rappel)

parameters of the material parameter distribution, if only a small number of fibers are tested (bottom in Figure 9). Bayes' theorem is used to incorporate additional assumptions and to regularise the identification problem. The question currently being investigated is how precise we need to know the material parameter distribution, if geometrical randomness of the network itself will also be of influence.

SELECTION OF RECENTLY ACQUIRED PROJECTS BY THE COMPUTATIONAL AND DATA SCIENCE TEAM AT THE UNIVERSITY OF LUXEMBOURG

4 million euros for a doctoral training centre funded by the FNR for 20 PhD students

ERA chair funded by H2020 in Data Science and Mathematical Statistics for 2.5 million euros

Several grants funded by the FNR including

- a proof of concept grant to create a start-up from our research in CAD analysis transition for 250k
- a private public partnership with GOODYEAR for 700k euros
- a fundamental OPEN FNR grant for 350k from FNR on quantum continuum coupling using many body approaches

REFERENCES

[1] Hauseux P, Hale JS, Bordas SPA, *Calculating the Malliavin derivative of some stochastic mechanics problems*. PLoS ONE 12 (12): 2017, e0189994. https://doi.org/10.1371/journal.pone.0189994

[2] Hauseux P, Hale JS, Bordas SPA, *Accelerating Monte Carlo estimation with derivatives of high-level finite element models*, Computer Methods in Applied Mechanics and Engineering. 1 May 2017. 318, pp. 917-936. http://dx.doi.org/10.1016/j.cma.2017.01.041

[3] Hale JS, Hauseux P, Bordas SPA, *Using higher-order adjoints to accelerate the solution of UQ problems with random fields*, Isaac Newton Institute Workshop UNQ01. http://hdl.handle.net/10993/34385

[4] Beex LAA, Peerlings RHJ, Geers MGD, *A quasicontinuum methodology for multiscale analyses of discrete microstructural models*, International Journal for Numerical Methods in Engineering 87(7), 2011, 701-718.

[5] Beex LAA, Peerlings RHJ, Geers MGD, *A multiscale quasicontinuum method for dissipative lattice models and discrete networks*, Journal of the Mechanics and Physics of Solids 64, 2014a, 154-169.

[6] Beex LAA, Peerlings RHJ, Geers MGD, *A multiscale quasicontinuum method for lattice models with bond failure and fiber sliding*, Computer Methods in Applied Mechanics and Engineering 269, 2014b, 108-122.

[7] Beex LAA, Kerfriden P, Rabczuk T, Bordas SPA, *Quasicontinuum-based multiscale approaches for plate-like beam lattices experiencing in-plane and out-of-plane deformation*, Computer Methods in Applied Mechanics and Engineering 279, 2014c, 348-378.

[8] Rokos O, Beex LAA, Zeman J, Peerlings RHJ, *A variational formulation of dissipative quasicontinuum methods*, International Journal of Solids and Structures 102, 2016, 214-229.

[9] Rokos O, Peerlings RHJ, Zeman J, Beex LAA, *An adaptive variational quasicontinuum methodology for lattice networks with localized damage*, International Journal for Numerical Methods in Engineering 112(2), 2017, 174-200.

[10] Rappel H, Beex LAA, Bordas SPA, *Bayesian inference to identify parameters in viscoelasticity*, Mechanics of Time-Dependent Materials, 2017, In Press

[11] Ley C., & Bordas SPA What makes Data Science different? A discussion involving Statistics2. 0 and Computational Sciences. *International Journal of Data Science and Analytics*, 1-9, 2017.

STEPHANE BORDAS

UNIVERSITY OF LUXEMBOURG, LUXEMBOURG

STEPHANE.BORDAS@GMAIL.COM

ON THE PROSPECTS OF USING MACHINE LEARNING FOR THE NUMERICAL SIMULATION OF PDEs: TRAINING NEURAL NETWORKS TO ASSEMBLE APPROXIMATE INVERSES

ABSTRACT

In an unconventional approach to combining the very successful Finite Element Methods (FEM) for PDE-based simulation with techniques evolved from the domain of Machine Learning (ML) we employ approximate inverses of the system matrices generated by neural networks in the linear solver. We demonstrate the success of this solver technique on the basis of the Poisson equation which can be seen as a fundamental PDE for many practically relevant simulations [Turek 1999]. We use a basic Richardson iteration applying the approximate inverses generated by fully connected feed-forward multilayer perceptrons as preconditioners.

Keywords: machine learning, FEM, preconditioning, SPAI

1 INTRODUCTION

There is conclusive evidence that we are on the edge of a technical revolution driven by artificial intelligence. To be more precise Machine Learning is a class of methods that can solve a multitude of problems by storing knowledge to and inferring it from a knowledge base that had previously been created via a training process. These techniques can be seen as a black box framework since they are strong in providing classification or even regression when exploring and altering large (unstructured) datasets for example for pattern recognition in text-, image-, video- or – in general – signal processing [Goodfellow et al. 2016]. Due to its success the hardware industry and chip vendors adapt their roadmaps to satisfy an ever larger demand to computing hardware that is especially tailored for ML. For example, due to the fact that the underlying computations in many cases don't need high precision, low (e.g. half-) precision accelerators are hitting the hardware ecosystem like Intel Knights Mill and NVIDIA Pascal and Volta or new microarchitectures are developed like Google's TPUs.

However at the moment it is unclear in what way and in how far these comparatively new methods and – alongside with them the modern and future compute hardware – can be exploited to assist solving PDEs in technical simulations: In the course of discretizing multidimensional PDEs at a certain point we have to deal with a high number of degrees of freedom leading to the global system matrix being large and sparse. Hence, iterative methods have to be chosen over direct ones. In the former everything breaks down to how clever the linear solver can adapt to the system to be solved and here using specially tailored solvers that are implemented in a target hardware-oriented way can be orders of magnitude faster than simple ones.

The idea of this paper is based on the observations, that (1) besides pattern recognition ML can also be used for function regression and (2) that preconditioners in linear solvers can be kind of underdetermined and yet yield a good preconditioner: In previous studies we were able to show, that Sparse Approximate Inverses (SPAI) are a good representative of such a

preconditioner [Geveler et al. 2013]. The application of an approximate inverse can be broken down to sparse matrix vector multiply (SpMV) and with sophisticated storage formats SpMV kernels map decently to for example GPUs. In contrast to that usual implementations of SPAI algorithms to assemble the approximate inverse are (in spite of their good parallelization properties) quite expensive. Hence the idea is to compute a rough draft of an explicitly stored preconditioner in a different way and therefore provide an alternative to SPAI: Use the system matrix as input to a trained neural network and render the result into another (sparse) matrix that is used as an approximation to its inverse. This way the output of the function regression process in the machine learning pipeline is a matrix like in many image processing cases the output of this process would be another (enhanced) image.

In order to pioneer into the fusing of FEM and ML in this paper we provide insight into how such a system could work and concentrate on providing evidence that the resulting inverses can numerically compete with other precondition-ers.

2 A CONCISE APPLICATION OF NEURAL NETWORKS IN A LINEAR SOLVER

2.1 MODEL PROBLEM AND FEM DISCRETISATION

As a starting point we define the Poisson equation to be our model problem, which is posed as:
Find $u : \Omega \to \mathbb{R}$ such that

$$-\Delta u = f \text{ in } \Omega, \quad u = 0 \text{ on } \partial \Omega. \quad (1)$$

Following the guidelines of [Braess 2013] we can convert this problem by using the variational formulation of (1) and the well-known Galerkin method into a discrete problem: Find $u_h \in V_h$ such that

$$a_h(u_h, v_h) = b_h(v_h) \quad \forall v_h \in V_h \quad (2)$$

In our case V_h is the finite element space of linear polynomials, which are zero on the boundary. The domain Ω is the unit square $(0,1)^2$ discretized with regular triangles T_h and a conforming refinement at the midpoints of the edges.
The global system matrix can be written as

$$(A_h)_{ij} = \sum_{m=1}^{N} \int_{K_m} \nabla \phi_j \cdot \nabla \phi_i dx = \sum_{m=1}^{N} A_{ij}^{(m)} \cdot (3)$$

with a nodal basis $\{\phi_l, ..., \phi_M\}$ and the local element matrices $A_{ij}^{(m)}$ on the element K_m. Analogously we can proceed with the right hand side as $(b_h)_i = \int_\Omega f \phi_i dx$.

2.2 TRAINING TENSOR AND BASIC ITERATION

To solve the corresponding system of equations $A_h u_h = b_h$, with a sparse matrix $A_h \in \mathbb{R}^{n \times n}$ which satisfies the M-matrix property [Saad 2003], we want to use a neural network. Hence a mechanism is needed to bring up a sufficiently large training dataset (called a training tensor). For this purpose we construct instances of A_h by randomly shifting the inner nodes on the finest level by maximum half the grid step size.

As the solver we use the Richardson iteration, which reads in its fixpoint formulation as:

$$x^{(k+1)} = x^{(k)} + \omega M(b_h - A_h x^{(k)}) \quad (4)$$

Here M is an approximate inverse we generate with the neural network.

3 CONSTRUCTING A MACHINE LEARNING FRAMEWORK FOR SOLVING LINEAR SYSTEMS OF EQUATIONS

3.1 NEURAL NETWORK DESIGN AND PRECONDITIONER CONSTRUCTION

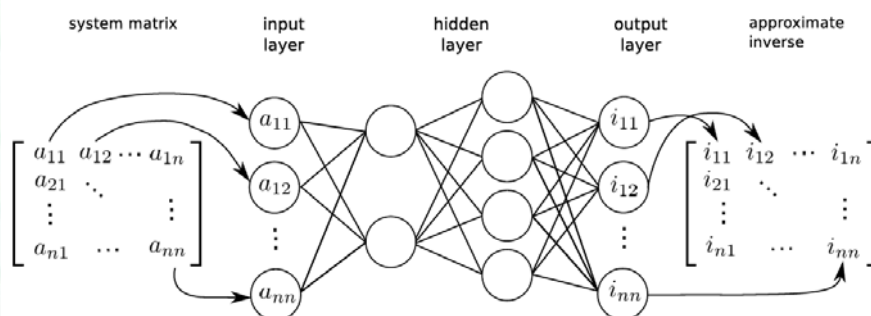The design space for Neural Networks is very large. Since this

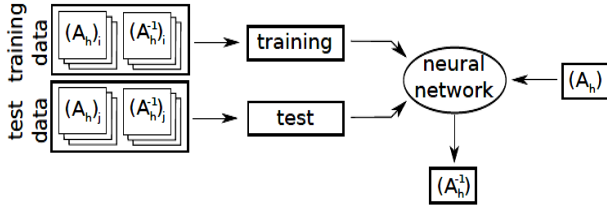*Figure 1. Model of a neural network for matrix inversion*

Figure 2. Model of a neural network to generate an approximate inverse

Algorithm 1 test and training phase

input: $n_{hl}, n_i, n_{epoch}, n_{batch}, n_{train}, l, n_{test}, n_{testbatch}$
· define the neural network (n_{hl}, n_i)
· initialize weights
· initialize bias neurons b
· define error function and optimizer
start training:
for i in n_{epoch} do
    A = load_training_matrices (n_{train})
    A_inv = load_training_inverses (n_{train})
    for j in n_{batch} do
        x = A_batch$_j$
        y = A_inv_batch$_j$
        apply optimizer: (W, b) = opt(x, y, l)
test phase:
for i in $n_{testbatch}$ do
    A = load_test_data (n_{test})
    evaluate the neural network
    apply error function or test scenario
output: W, b

paper is meant as a starting point for the exploration of fusing FEM and ML we keep it as simple as possible and employ straightforward choices where possible. Therefore we use fully connected feed-forward multilayer perceptrons. Fully connected means that every neuron in the network is connected to each neuron of the next layer. Moreover there are no backward connections between the different layers (feed-forward). The evaluation of such neural networks is a sequence of chained-up matrix vector products. The entries of the system matrix are represented in the input layer vector-wisely (cf. Figure 1). In the same way, our output layer contains the entries of the approximate inverse. Between these layers we can add a number of hidden layers consisting of a bunch of hidden neurons. How many hidden neurons we need to create strong approximate inverses is a key design decision and we discuss this below.

3.2 TRAINING AND TESTING PHASE

In figure 2 we can see how we want to handle the neural network. First of all we use a pile of matrix pairs $(A_h)_i$ and its corresponding inverse $(A_h^{-1})_i$ to train the neural network via supervised learning. With some test data we can identify whether the neural network is able to generalise. This way we can determine how good the neural network works for approximating inverses of general matrices that are somehow similar but not identical to those used in training. Whether we are able to produce a suitable approximate inverse mainly depends on the structure of the neural network and the training algorithm.

In general our supervised training algorithm is called backward propagation with random initialisation. Alongside a linear propagation function

$$i_{total} = W \cdot o_{total} + b$$

with the total (layer) net input i_{total}, the weight matrix W, the vector for the bias weights b and the total output of the previous layer o_{total}, we use the rectified linear unit (ReLu) function as activation function $\alpha(x)$ [Goodfellow et al. 2016] and thus we can calculate the output y of each neuron as:

$$y := \alpha\left(\sum_j o_j \cdot w_{ij}\right)$$

Here o_j is the output of the preceding sending units and ω_{ij} the corresponding weights between the neurons.

For the optimization we use the L2-error-function and employ for the update for the weights:

$$w_{ij}^{(t+1)} = w_{ij}^{(t)} + \gamma \cdot o_i \cdot \delta_j$$

with the output o_i of the sending unit, γ learning rate and δj symbolises the gradient decent method:

$$\delta_j = \begin{cases} f'(i_j) \cdot (\hat{o}_j - o_j), \\ f'(i_j) \cdot \sum_{k \in S}(\delta_k \cdot w_{kj}), \end{cases}$$

if neuron j is an output neuron
if neuron j is a hidden neuron.

With these definitions we can describe the training and testing phases with the pseudocode presented in Algorithm 1.

			# it		it down	κ	
lvl	n	$J_{\omega=0.7}$	GS	NN		before	after
2	9	49	17	8	2.13	5.9	1.6
3	49	273	95	21	4.52	29.8	2.9
4	225	1 323	463	66	7.02	127.3	7.8
5	961	5 879	2 057	39	52.74	516.0	23.4

Table 1. Iteration and condition number κ, tol = 1.0 e—05, 3 layer neural networks

4 NUMERICAL EXPERIMENTS

4.1 PRECONDITIONER QUALITY

In order to get an impression on whether it is possible to gain suitable approximate inverses with neural networks we eliminate for any complicated tweaks and start with networks for a fixed problem size (i.e. degrees of freedom) n and train it with pairs of (dense) system matrices and their inverses.

In Table 1 we deploy the results for using the approximate inverse of the system matrices with problem size-specific neural networks in Richardson iterations (labelled NN) in comparison to the damped Jacobi (J) and Gauss-Seidel (GS) defect correction methods. In addition to the iteration number the reduction of the condition number κ is shown for the neural networks. For the problem size levels 2, 3 and 4 the number of neurons in the 3 hidden layers equals the corresponding matrix dimension. The number of training epochs is set to 1 000.

As we can see from the data for every test configuration the neural network is able to generate a matrix that serves well as a preconditioner. The corresponding Richardson method needs less iterations than the damped Jacobi or the Gauss-Seidel method. Moreover the condition number is strongly reduced by the neural networks-generated preconditioner.

With neural networks it is a priori not possible to determine which number of hidden neurons and how many training epochs would work out best. Even other parameters like the learning rate and the matrix dimensions between the neurons have a large impact on the iteration numbers: The level 5 configuration needs even less iterations to converge than the previous level 4 configuration, because the parameters - fewer neurons with the same amount of training epochs and the online learning - fit better to that configuration. With error functions like the L2-loss function we can get a training accuracy and a rough idea of how good a neural network will be functional in the test and application phase, but a good enough accuracy for one network can be much too low for another case.

4.2 TIME TO SOLUTION AND MEMORY CONTROL

Initialisation and application The timings and the speedup between two different large neural networks and the Jacobi as well as the Gauss-Seidel method are shown for refinement level 4 in Figure 3. The underlying hardware is a Intel Xeon E5-2670 with 8 cores and a frequency of 2.60 GHz.

The noticeable differences between the methods are resulting from the initialisation time on the one hand and from the numbers of iterations on the other hand. While the Jacobi method needs only 3.59e-05 s to initialize the neural network with 50 neurons needs 3.44e-03 s and the network with 225 neurons needs 5.80e-03 s for the assembly. However the Gauss-Seidel defect correction needs 1.50e-02 s. The neural networks and the Gauss-Seidel are able to catch up with a lower number of iterations. For instance we get it_J = 990, it_{GS} = 346, it_{NN50} = 32 and it_{NN225} = 23 for a tolerance of 10e-03 and it_J= 2323, it_{GS} = 812, it_{NN50} = 106 and it_{NN225} = 72 for a tolerance of 10e-10. Here it is noticeable that we do not need that many neurons even if the iteration number might decrease a bit.

Memory footprint Due to storage problems for larger matrices we use the online learning method in which we train our network with only one pair of system matrix and associated inverse in each training step instead of the batch learning with 100 pairs for the lower level. Moreover we reduce the number of the hidden neurons to 100 in each hidden layer for the level 5 configuration.
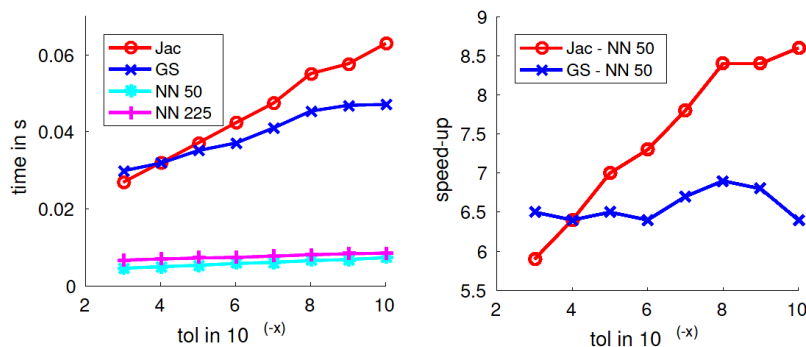

Figure 3. Time and speed-up between Jacobi, Gauss-Seidel and the neural network preconditioned Richardson iteration

In addition we found that we do not need as many neurons in the hidden layer as in the input layer. This leads to a reduction of the weight matrices and therefore to decreased assembly and application times.

Since we use fully connected neural networks the structure of the matrix which depends on the node numbering is irrelevant. Hence for further simplification we can assume a banded system matrix and instead of using every matrix entry as input data, we save the matrix bands sequentially. By utilizing the matrix symmetry we can reduce the input data even more. Like for the unit square we have to store only 4 bands instead of 7. The resulting benefits are shown in table 2.

Reducing time to solution and memory footprint We now employ a sparsity pattern which leads to less storage requirements and a faster application owing to smaller weight matrices. Due to the large matrix size the first matrix vector multiplication corresponding to the input layer and the last one to assemble the output matrix are the most expensive operations. By reducing the number of input values the first matrix vector multiplication can be reduced as well. Again we take a look at a matrix resulting from refinement level 4. By utilizing

the sparsity pattern the dimension of the weight matrix is changed from 50.625 x 225 to 868 x 225 which equates to a factor of 58. For a new test matrix the assemble time is lowered from 4,378e -03 s to 2,474e -03 s. Since one of the two expensive operations is decreased massively the initialisation time is nearly halved.

Training Another benefit we generate from a reduced amount of input values is that we simplify the training in general. Table 3 displays the iteration number of a Richardson iteration scheme with the approximate inverse of three different neural networks with the same setting as above. The first one uses the sparse storage format and is trained with 10 000 pairs of input matrices and inverses in 1 000 training cycles. The other are trained on a dense storage format with a greater amount of 25 000 input data and 1 500 respectively 2 000 training epochs.

With the dense storage the neural network got a greater weight matrix between the input and the first hidden layer. To adjust the greater amount of weights we need much more training data and epochs. Moreover we see the behaviour of the damped Richardson method with different damping parameters

which is again difficult to optimise a priori.

On the other hand we lose the flexibility of the dense format and are bounded to a 'fixed' matrix structure. In most PDE-based simulations only sparse matrices with a predefined matrix structure due to the coupling of degrees of freedom and their numbering are used which neutralize this disadvantage. Moreover we can get more flexibility by adding zeros in those matrix locations where they are needed and take the benefits described above.

4.3 DESIGNING SPARSE APPROXIMATE INVERSES

To be competitive to SPAI and ILU preconditioners we have to speed up the second large matrix vector multiplication and produce sparse output matrices. In general the inverse of a sparse matrix is not a sparse matrix. That is the reason why we use a filter method to reduce the approximate inverse of the matrix afterwards.

Table 4 contains the iteration number of the damped Richardson iteration method (ω = 0.8) with an approximate inverse out of a neural network compared to the exact inverse after setting all entries

n	49	225	961	3 969	16 129
full	2 401	50 625	923.521	15 752 961	260 144 641
$\bar{n}$	289	1 457	6 481	27 281	111 889
diag	180	868	3 780	15 748	64 260
%	7.497	1.715	0.409	0.100	0.025

Table 2. Storage of a n x n matrix with a dense (full) storage, the number of non-zeros ($\bar{n}$) and by utilizing the symmetry (diag), unit square

	NN_{sparse} (1 000)			NN_{full}(1 500)			NN_{full} (2 000)		
ω	0.6	0.7	0.8	0.6	0.7	0.8	0.6	0.7	0.8
1	33	27	23	118	110	88	29	24	37
2	37	31	26	110	94	82	31	25	20
3	35	29	25	109	93	81	29	24	22

Table 3. Number of damped Richardson iterations with a sparse and a full storage for neural networks trained with different problem sizes

ϵ	# it (NN)	$\bar{n}$(NN)	%	# it (exact)	$\bar{n}$ (exact)
0.00	23	50 625	100.0	1	50 625
0.01	24	35 469	70.1	9	35 319
0.02	29	26 755	52.8	12	26 663
0.03	48	21 029	41.5	21	21 095
0.04	58	17 133	33.8	38	17 173
0.05	279	14 171	28.0	620	14 233

Table 4. Number of iterations with the Richardson solver (ω = 0.8) and different filtered approximate inverses in comparison to the filtered accurate inverse

smaller than ϵ to zero. With this filter method the matrix can be reduced to a sparse matrix. The underlying neural network is the same as above.

As we can see it is possible to reduce the approximate inverse by approximately 2/3 and still get a converging method. In comparison to that the Gauss-Seidel method, which operates on nearly 50% of the matrix entries, needs 462 iterations to reach the same tolerance of 10^{-5}.

5 CONCLUSION AND FUTURE WORK

We were able to demonstrate that it is at least possible to bring up simple learning systems that extrapolate strong approximate inverses for FEM matrices. Many of the descibed techniques are presented in detail in [Ruelmann 2017] and we are also preparing a follow-up publication that dives into many other aspects we abstained from presenting in this short introduction [Ruelmann et al. 2018]. The current state of our research triggers a lot of questions that have to be answered by future work, including

• Is it possible to bring up an optimised performance model describing the complete process from training a specific network for a problem over initialisation (aka assembly of the approximate inverse) up to the application?

• What is an optimal (or at least better) design for the neural network – since there are many screws to adjust e. g. the number of hidden layers and neurons as well as the size of the training data, the learning rate or the functions like activation, propagation and loss function in addition to the choice of the optimizer?

• Since our results indicate that the potential of the resulting approximate inverses is really big – how competitive is it with SPAI? A simple SPAI-1 method for example theoretically should speed up convergence in the order of magnitude of Gauss-Seidel. Note that in our results, the preconditioner is (much) better than GS.

• How beneficial will neural networks be as smoother or preconditioner in stronger solvers especially multigrid?

• How well will the neural network cope with larger alteration of the problem than modelled in the training tensor?

• What is the shape of a ML system for arbitrary matrices with arbitrary sizes, sparsity patterns, coefficients?

REFERENCES

BRAESS, D. 2013. *Finite Elemente: Theorie, schnelle Löser und Anwendungen in der Elastizitätstheorie*. Springer-Verlag.

GEVELER, M., RIBBROCK, D., GÖDDEKE, D., ZAJAC, P., AND TUREK, S. 2013. Towards a complete FEM–based simulation toolkit on GPUS: Unstructured Grid Finite Element Geometric Multigrid solvers with strong smoothers based on Sparse Approximate Inverses. *Computers and Fluids 80* (July), 327–332. doi: 10.1016/j.compfluid.2012.01.025.

GOODFELLOW, I., BENGIO, Y., AND COURVILLE, A. 2016. Deep *Learning*. MIT Press. http://www.deeplearningbook. org.

RUELMANN, H., GEVELER, M., AND TUREK, S. 2018. Machine Learning-generated Sparse Approximate Inverses. under preparation.

RUELMANN, H. 2017. *Approximation von Matrixinversen mit Hilfe von Machine Learning*. Master's thesis, TU Dortmund, Dortmund, Germany.

SAAD, Y. 2003. *Iterative methods for sparse linear systems*. SIAM.

TUREK, S. 1999. *Efficient Solvers for Incompressible Flow Problems: An Algorithmic and Computational Approach*, vol. 6. Springer, Jan. 3-540-65433-X.

HANNES RUELMANN
MARKUS GEVELER
STEFAN TUREK

TU DORTMUND UNIVERSITY, GERMANY

TURE@FEATFLOW.DE

THE CUT FINITE ELEMENT METHOD: DISCRETIZATION OF GEOMETRY AND PDE

1 INTRODUCTION

CutFEM. Efficient simulation of physical phenomena modeled by partial differential equations require discretization of the *geometry* of the computational domain as well as discretization of the governing partial differential *equations*. In many cases of interest the geometry is complex and/or changes throughout the computation, for instance in large deformation fluid structure interaction problems or in shape optimization problems, and thus a flexible, accurate, and stable discretization method is required.

The Cut Finite Element Method (CutFEM) is a novel approach, adressing both discretization of geometry and partial differential equations, which is based on the following key ideas:

- Representation of the geometry of the domain on a fixed mesh where the geometry is allowed to cut through the elments in an arbitrary way leading to so called cut elements in the vicinity of the boundary.

- Weak enforcement of all boundary and interface conditions.

- A stabilization procedure which provides control over possible instabilities caused by the cut elements.

Properly designed, *CutFEM rests on a solid mathematical foundation which completely mirror the properties of standard meshed finite element methods*. More precisely, CutFEM has the following properties:

- Stable independent of the position of the domain in the fixed grid.

- Optimal order accuracy, also for higher order approximations.

- Well conditioned in the sense that the condition number of the stiffness matrix is the same as for standard meshed methods.

Short Literature Review. CutFEM was originally developed in the context of interface problem in [12] and overlapping meshes[13]. Face-based so-called ghost penalties were then employed to solve the Poisson boundary problem [5], the Stokes boundary problem [6, 18] and Stokes interface problems [14, 23]. Alternative CutFEM schemes for the Stokes interface problem can be found in [11] where the pressure space was enriched in the vicinity of the interface, and in [15, 21] which are based on unfitted discontinuous Galerkin methods using cell-merging techniques problems to obtain stable and well-conditioned numerical schemes. Higher order discontinuous Galerkin with extended element stabilization for an elliptic problem were investigated by [16]. CutFEM was applied to surface PDEs in [20, 8], and oupled surface-bulk problems, see [7, 10]. See [17] for implementation issues. We finally refer to the overview article [3] on cut finite element methods and the recent conference proceedings [2].

CutFEM is related to the XFEM method of Belytschko and co-workers, e.g., [19, 22, 9], but with the important distinction that, whereas XFEM is based on a partition of unity method [1], CutFEM relies only on the standard basis functions of classical FEM. This
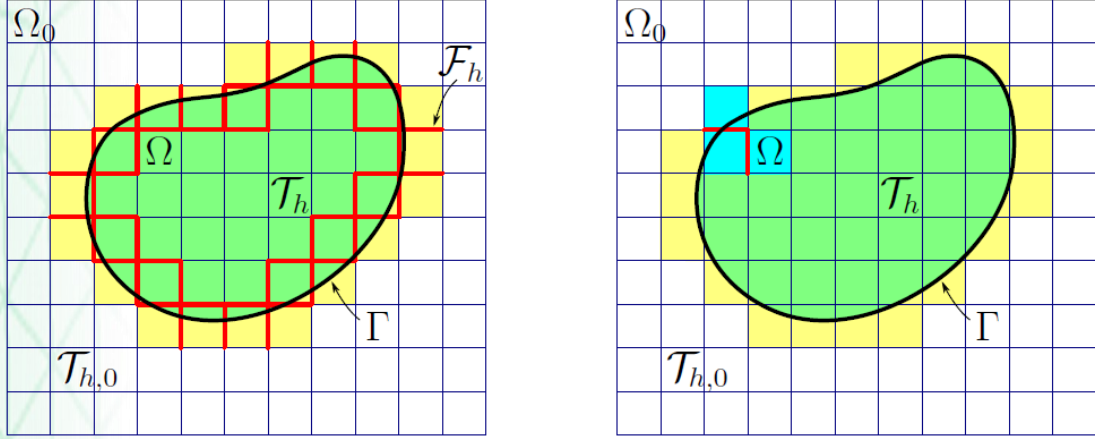
Figure 1. Left. The background mesh $\mathcal{T}_{h,0}$, the active mesh $\mathcal{T}_h$, the domain Ω, and the stabilized faces $\mathcal{F}_h$. Right. Stabilization of a cut element using a path of face neighbors.

is key to its simplicity in dealing with weak internal discontinuities and fictitious domain type simulations.

Outline. In this short communication we review the formulation and theoretical results for the CutFEM applied to a second order elliptic boundary value problem and then we present an application to shape optimization where the geometry is described using a levelset function.

2 CUTFEM FOR A BOUNDARY VALUE PROBLEM

2.1 MODEL PROBLEM

Let Ω be a domain in $\mathbb{R}^d$ with smooth boundary $\partial\Omega$ and exterior unit normal n. We consider the problem: find $u : \Omega \to \mathbb{R}$ such that

$$-\Delta u = f \qquad \text{in } \Omega \qquad (1)$$
$$u = g_D \qquad \text{on } \partial\Omega_D \qquad (2)$$
$$n \cdot \nabla u = g_N \qquad \text{on } \partial\Omega_N \qquad (3)$$

where f, g_D, g_N, are given functions and $\partial\Omega = \partial\Omega_D \cup \partial\Omega_N$ is a partition of the boundary into the parts with Dirichlet and Neumann conditions.

2.2 THE MESH AND FINITE ELEMENT SPACES

Let Ω_0 be polygonal domain such that $\Omega \subset \Omega_0 \subset \mathbb{R}^d$ and let $\mathcal{K}_{0,h}$, $0 < h \leq h_0$ be a family of quasi uniform partitions, with mesh parameter h, of Ω_0 into shape regular triangles or tetrahedra T. We refer to Ω_0 as the background domain and $\mathcal{T}_{h,0}$ as the background mesh.

Let $\mathcal{T}_h = \{T \in \mathcal{T}_{0,h} : \overline{T} \cap \overline{\Omega} \neq \emptyset\}$ (4)

be the submesh of $\mathcal{T}_{h,0}$ consisting of elements that intersect $\overline{\Omega}_i$, see Fig. 1. We refer to $\mathcal{T}_h$ as the active mesh. Dene $V_{h,0}$ as the space of piecewise linear continuous polynomials on $\mathcal{T}_{h,0}$ and $V_h = V_{h,0|\mathcal{T}_h}$ as the restriction of $V_{h,0}$ to the active mesh $\mathcal{T}_h$.

2.3 THE METHOD

To construct a finite element method we will employ weak enforcement of the Dirichlet boundary condition based on Nitsche's method.

Method: find $u_h \in V_h$ such that

$$A_h(u_h, v) = l_h(v) \qquad v \in V_h. \quad (5)$$

where the forms are defined by

$$A_h(v, w) = a_h(v, w) + \tau_{s_h} s_h(v, w) \quad (6)$$

$$a_h(v, w) = (\nabla v, \nabla w)_\Omega - (n \cdot \nabla v, w)_{\partial\Omega_D} - (v, n \cdot \nabla w)_{\partial\Omega_D} + \tau_{a_h} h^{-1}(v, w)_{\partial\Omega_D} \quad (7)$$

$$s_h(v, w) = h([n \cdot \nabla v], [n \cdot \nabla w])_{\mathcal{F}_h} \quad (8)$$

$$l_h(v) = (f, v)_\Omega + (g_N, v)_{\partial\Omega_N} - (g_D, n \cdot \nabla w)_{\partial\Omega_D} + (g_D, w)_{\partial\Omega_D} \quad (9)$$

Here $\mathcal{F}_h$ is the set of interior faces belonging to an element that intersect the boundary $\partial\Omega$, the jump of the normal gradient across face F is defined by

$$[n \cdot \nabla v] = n_1 \cdot \nabla v_1 + n_2 \cdot \nabla v_2 \quad (10)$$

where F is shared by elements T_1 and T_2 with exterior unit normals n_1 and n_2, and τ_{sh}, τ_{ah} are positive parameters.

Remarks: The forms a_h and l_h are associated with the standard Nitsche method; note, however, that we integrate over cut elements of the form $\Omega \cap T$ and $\partial\Omega_D \cap T$ for $T \in \mathcal{T}_h$.

The additional form s_h is a stabilization term providing additional control of the variation

of the finite element functions on the elements in the vicinity of the boundary.

3 OVERVIEW OF THEORETICAL RESULTS

- Using the control provided by the stabilization term s_h we can show that

$$\|\nabla v\|_{\mathcal{T}_h}^2 \lesssim \|\nabla v\|_\Omega^2 + \|v\|_{s_h}^2 \quad (11)$$

where $\|w\|_{\mathcal{T}_h}^2 = \sum_{T\in\mathcal{T}_h}\|w\|_T^2$ is the L^2 norm on $\Omega_h = \cup_{T\in\mathcal{T}_h}T$, and

$\|v\|^2 = s_h(v,v)$ is the seminorm associated with s_h. To prove (11) we make repeated use of the following estimate

$$\|\nabla v\|_{T_2}^2 \lesssim \|\nabla v\|_{T_1}^2 + h\|[\nabla v]\|_F^2 \quad (12)$$

which holds for each pair of elements T_1 and T_2 sharing a face F. See Figure 1 for a path of elements connecting a cut element at the boundary to en element in the interior.

- Defining the energy norm

$$\||v\||_h^2 = \|\nabla v\|_\Omega^2 + \|v\|_{s_h}^2 + $$
$$h\|n\cdot\nabla v\|_{\partial\Omega_D}^2 + h^{-1}\|v\|_{\partial\Omega_d}^2 \quad (13)$$

and using (11) together with standard arguments we can prove coercivity

$$\||v\||_h^2 \lesssim A_h(v,v) \qquad v \in V_h \quad (14)$$

We also have the standard continuity

$$A_h(v,w) \lesssim \||v\||_h\||w\||_h$$
$$v, w \in V_h + V \quad (15)$$

- To construct an interpolation operator we recall that there is a continuous extension operator $E : H^s(\Omega) \to H^s(\mathbb{R}^d)$ and we define

$$\pi_h v = \pi_{h,Cl}Ev \quad (16)$$

where $\pi_{h,Cl} : L^2(\mathcal{T}_h) \to V_h$ is the standard Clement interpolation operator. We may then prove the interpolation error estimate

$$\||v - \pi_h v\||_h \lesssim h\|v\|_{H^2(\Omega)} \quad (17)$$

- Using coercivity and continuity together with the approximation property (17) we obtain the energy norm error estimate

$$\||u - u_h\||_h \lesssim h\|u\|_{H^2(\Omega)} \quad (18)$$

and using duality we can also derive estimates in the L_2 norm.

- Using the control provided by the stabilization s_h we can derive the Poincaré estimate

$$\|v\|_{\mathcal{T}_h}^2 \lesssim A_h(v,v) \qquad v \in V_h \quad (19)$$

and using an inverse estimate we have

$$A_h(v,v) \lesssim h^{-2}\|v\|_{\mathcal{T}_h}^2 \quad v \in V_h (20)$$

which together imply the following bound on the condition number $\operatorname{cond}(\widehat{A})$ of the stiffness matrix $\widehat{A}$ associated with A_h,

$$\operatorname{cond}(\widehat{A}) \lesssim h^{-2} \quad (21)$$

We note that this is the estimate that also holds for standard mesh based finite elements.

4 APPLICATION TO SHAPE OPTIMIZATION

CutFEM is developed with evolving geometries in mind and thus a natural application is in shape and topology optimization, which is an area that attracts significant interest both in the research community and in industrial applications. One driving factor is the rapid development of new flexible additive manufacturing techniques. In shape optimization the boundary of the domain is typically described by a level-set function or a parametrization.

Given the boundary representation we need to generate a discretization of the domain. This can be done using a standard meshing body fitted approach which may lead to distorted elements or expensive re-meshing steps when the boundary is updated. Alternatively using a fictitious domain method no mesh motion and/or re-meshing are required. CutFEM is an excellent choice since it is stable and provides optimal order approximation.

The optimization problem takes the form: find

$$\min_\Omega J(\Omega) \quad (22)$$

where $J(\Omega) = J(\Omega, u(\Omega))$ is an objective functional subject to the constraints

$$a_\Omega(u, v) = l_\Omega(v) \ \forall v \in V \quad (23)$$

and the volume constraint

$$|\Omega| = \alpha |\Omega_0| \quad (24)$$

for some $\alpha \in (0,1)$. In gradient based optimization we compute sensitivities of the objective function with respect to the design parameters. This information is used to update the boundary. For example, let β be a velocity field such that

$$\Omega_t = (\operatorname{Id} + t\beta) \ \Omega$$

is a perturbation of the domain. We denote the shape derivative with respect to the pseudo time t in direction β as

$$D_{\Omega,\beta} J(\Omega) \quad (25)$$

The steepest decent direction

$$\beta \in [H^1(\Omega)]^d$$

given some smoothness is determined by

$$\epsilon(\beta\otimes\nabla, \theta\otimes\nabla)_\Omega + (\beta,\theta)_\Omega = -D_{\Omega,\theta}J(\Omega)$$
$$\forall\theta \in [H^1(\Omega]^d \quad (26)$$

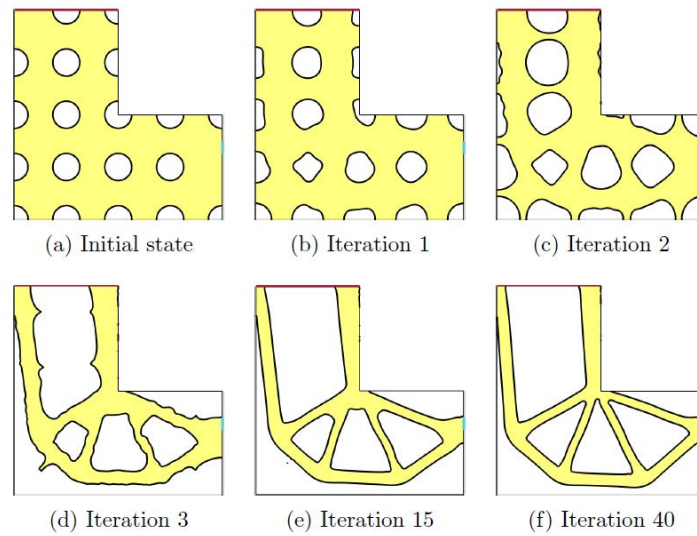The level-set $\phi(x)$ is then moved in the direction of the velocity field by solving the transport equation

(a) Initial state   (b) Iteration 1   (c) Iteration 2

(d) Iteration 3   (e) Iteration 15   (f) Iteration 40

Figure 2. Sample iteration states in a L-shape beam problem using quadratic elements. Note that the topology changes when void separations breaks

$$\phi(t) + \beta \cdot \nabla \phi = 0 \qquad (27)$$

See [4] for further details.

In Figure 2 we give an example of an elastic optimization problem with respect to the compliance $J(\Omega) = \alpha_\Omega(u, u) = l_\Omega(u)$, where u is the solution to the weak problem (23) corresponding to linear elasticity. We used no-displacement boundary condition on the top and a traction boundary condition on part of the left boundary.

ACKNOWLEDGEMENTS

REFERENCES

[1] I. Babuska and J. M. Melenk. The partition of unity method. *Internat. J. Numer. Methods Engrg.*, 40(4):727{758, 1997.

[2] S. Bordas, E. Burman, M. G. Larson, and M. Olshanskii, editors. *Geometrically Unifitted Finite Element Methods and Applications. Proceedings of the UCL Work-shop 2016*, volume 121 of *Lecture Notes in Computational Science and Engineering*. Springer Verlag, 2017.

[3] E. Burman, S. Claus, P. Hansbo, M. Larson, and A. Massing. CutFEM: discretizing geometry and partial differential equations. *Internat. J. Numer. Meth. Engng*, 104(7):472{501, 2015.

[4] E. Burman, D. Elfverson, P. Hansbo, M. G. Larson, and K. Larsson. Shape optimization using the cut finite element method. *Comput. Methods Appl. Mech. Engrg.*, 328:242{261, 2018.

[5] E. Burman and P. Hansbo. Fictitious domain finite element methods using cut elements: II. A stabilized Nitsche method. *Appl. Numer. Math.*, 62(4):328{341, 2012.

[6] E. Burman and P. Hansbo. Fictitious domain methods using cut elements: III. A stabilized Nitsche method for Stokes' problem. *ESAIM, Math. Model. Num. Anal.*, 48(3):859{874, 2013.

[7] E. Burman, P. Hansbo, M. Larson, and S. Zahedi. Cut finite element methods for coupled bulk-surface problems. *Numer. Math.*, 133(2):203{231, 2016.

[8] E. Burman, P. Hansbo, and M. G. Larson. A stabilized cut finite element method for partial differential equations on surfaces: The Laplace-Beltrami operator. *Comput. Methods Appl. Mech. Engrg.*, 285:188{207, 2015.

[9] J. Chessa, P. Smolinski, and T. Belytschko. The extended finite element method (XFEM) for solidification problems. *Internat.*

J. Numer. Methods Engrg., 53 (8):1959{ 1977, 2002.

[10] S. Gross, M. A. Olshanskii, and A. Reusken. A trace finite element method for a class of coupled bulk-interface transport problems. *ESAIM Math. Model. Numer. Anal*., 49(5):1303{1330, 2015.

[11] S. Gross and A. Reusken. An extended pressure finite element space for two-phase incompressible flows with surface tension. J. *Comput. Phys.*, 224(1):40{58, 2007.

[12] A. Hansbo and P. Hansbo. An unfitted finite element method, based on Nitsche's method, for elliptic interface problems. *Comput. Methods Appl. Mech. Engrg*., 191(47-48):5537{5552, 2002.7

[13] A. Hansbo, P. Hansbo, and M. G. Larson. A finite element method on composite grids based on Nitsche's method. ESAIM: *Math. Model. Num. Anal*., 37(3):495 {514, 2003.

[14] P. Hansbo, M. G. Larson, and S. Zahedi. A cut finite element method for a Stokes interface problem. *Appl. Numer. Math*., 85:90{114, 2014.

[15] F. Heimann, C. Engwer, O. Ippisch, and P. Bastian. An unfitted interior penalty discontinuous Galerkin method for incompressible Navier-Stokes two-phase flow. *Internat. J. Numer. Methods Fluids*, 71

(3):269{293, 2013.

[16] A. Johansson and M. G. Larson. A high order discontinuous Galerkin Nitsche method for elliptic problems with fictitious boundary. *Numer. Math*., 123 (4):607{628, 2013.

[17] A. Massing, M. Larson, and A. Logg. Efficient implementation of finite element methods on non-matching and overlapping meshes in 3D. *SIAM J. Sci. Comput.*, 35(1):C23{C47, 2013.

[18] A. Massing, M. Larson, A. Logg, and M. Rognes. A stabilized Nitsche fictitious domain method for the Stokes problem. *J. Sci. Comput*., 61(3):604{628, 2014.

[19] N. Moës, J. Dolbow, and T. Belytschko. A finite element method for crack growth without remeshing. *Internat. J. Numer. Methods Engrg*., 46 (1):131{150, 1999.

[20] M. A. Olshanskii, A. Reusken, and J. Grande. A finite element method for elliptic equations on surfaces. *SIAM J. Numer. Anal*., 47(5):3339{3358, 2009.

[21] W. E. H. Sollie, O. Bokhove, and J. J. W. van der Vegt. Space-time discontinuous Galerkin finite element method for two-fluid flows. *J. Comput. Phys*., 230 (3):789{817,2011.

[22] N. Sukumar, D. L. Chopp, N. Moës, and T. Belytschko. Modeling holes and inclusions by level sets in the extended finite-

element method. *Comput. Methods Appl. Mech. Engrg*., 190 (46-47):6183{6200, 2001.

[23] Q. Wang and J. Chen. A new unfitted stabilized Nitsche's finite element method for Stokes interface problems. *Comput. Math. Appl*., 70(5):820{834, 2015.

ERIK BURMAN
UNIVERSITY COLLEGE LONDON,
UNITED KINGDOM

PETER HANSBO
JÖNKÖPING UNIVERSITY,
SWEDEN

DANIEL ELFVERSON
MATS G. LARSON
KARL LARSSON
UMEÅ UNIVERSITY,
SWEDEN

MATS.LARSON@UMU.SE

COMPUTATIONAL DESIGN OF 2D NANOSTRUCTURES BASED ON CARBON

1 INTRODUCTION

Carbon atoms form various types of bondings and spatial configurations. This ability is determined by the atoms' hybridization states, which depend on their particular electronic configuration. This phenomenon is responsible for the existence of many different allotropes of the carbon. This is due to unique electronic, thermal and mechanical properties of such structures. Additionally, 2D graphene-like materials can be used to create another, more complex class of nanostructures, such as nanotubes. Graphene-like materials can be classified as periodic, flat atomic networks, made of stable configurations of carbon atoms in certain hybridization states. Since the stable configurations of atoms correspond to the global minima on the Potential Energy Surface (PES), such a task can be considered as a special optimization problem in which optimal material layout is searched on the nano-scale. However, the number of local minima increases almost exponentially with the number of atoms in the considered structure, thus searching for the global
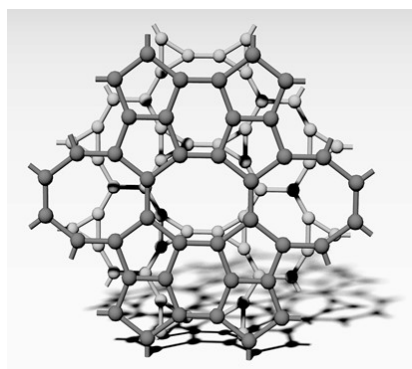
New carbon network - X graphene

minimum on a PES became a non-trivial, NP-hard problem.

The paper contains description of the two-stage computational design searching strategy to generate new graphene-like materials X and Y. In the first stage new graphene-like materials are generated by means of the memetic algorithm for the molecular model. The second stage consists in a thorough examination obtained in the previous stage new potentially materials using ab-initio computation.

2 THE FIRST STAGE – MOLECULAR AND MEMETIC COMPUTATION

The memetic algorithms [1,2] combine evolutionary, global, population based algorithm with local improvements methods for some individuals or chromosomes. The memetic algorithms are sometimes named hybrid algorithms or hybrid evolutionary algorithms because they are a kind of a hybrid of global and local optimization techniques.

The memetic algorithm, proposed and presented in this work, combines the parallel **E**volutionary **A**lgorithm (EA), prepared by the authors, and the classical **C**onjugated - **G**radient (CG) minimization of the total potential energy of the optimized atomic system. Since the processed structure is considered as a discrete atomic model, the behavior and the potential energy of carbon atoms are determined using the **A**daptive **I**ntermolecular **R**eactive **E**mpirical **B**ond **O**rder (AIREBO) [3] potential developed for molecular dynamics simulations of hydrocarbons.
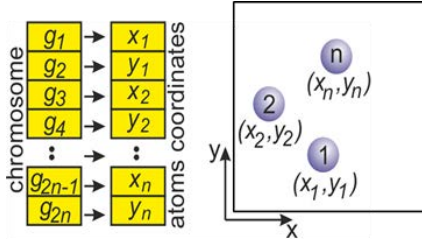
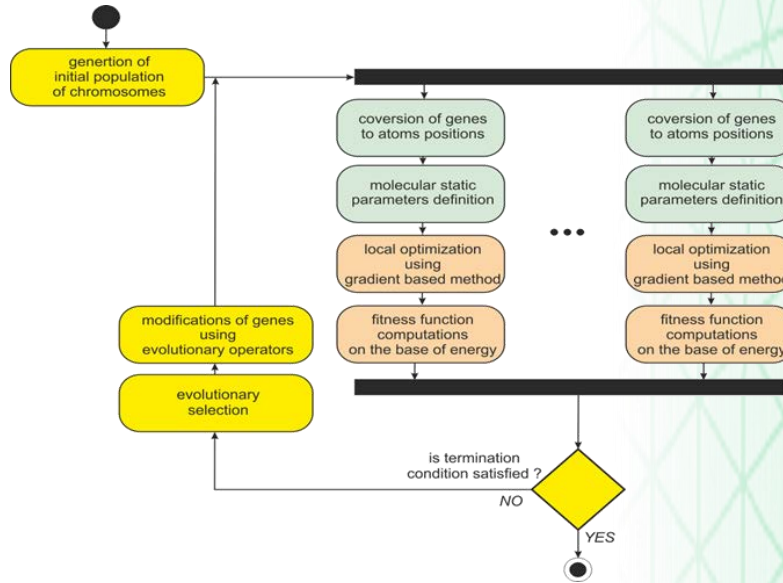Figure 1. The example of chromosome and corresponding atomic structure

Figure 2. Bock diagram of the memetic parallel algorithm

A chromosome represents design variables in the form of real-valued Cartesian coordinates of each atom in the considered unit cell of the newly created atomic lattice (Figure1).

Each chromosome represents a certain spatial arrangement of atoms. In the initial population, atoms have randomly generated coordinates and are placed in the area of the unit cell with periodic boundaries. Dimensions, the rectangular or triclinic type of the unit cell, as well as the number of atoms, are part of a set of parameters of the simulation. Such an approach allows to control the value of atomic density of the newly-created structure. The periodicity of the atomic structure significantly reduces the number of design variables.

The fitness function is formulated as the total potential energy of the considered atomic system, i.e., the total sum of all potential energies of particular atomic interactions. The AIREBO potential in the following form is used in computation:

$$FF = \sum_i \sum_{j \neq i} \left(E_{ij}^{REBO} + E_{ij}^{LJ} + \sum_{k \neq i, j} \sum_{l \neq i, j, k} E_{kjl}^{TORSION} \right)$$

where: E^{REBO} corresponds to the short range interactions between covalently bonded pair of atoms, E^{LJ} is responsible for the long range interactions and is computed in a simplified way, using the Lennard-Jones-like function with additional distance-dependent switching functions and $E^{TORSIONAL}$ is torsional potential which depends on the neighboring atom's dihedral angles.

In order to avoid the situation when distances between atoms are very small, the initial and offspring populations have to be equilibrated, i.e., the potential energy has to be minimized by correction of the positions of atoms. The CG algorithm is used for this purpose. This routine is invoked in each iteration of EA for all individuals in the processed population and temporarily pushes solutions into the local minima.

Such an approach assists in forming of the new, real carbon-based molecular structure, i.e., during the conjugate gradient minimization, each individual – a certain spatial configuration of atoms, starts to form a unique, hybridization-dependent, geometry of flat carbon networks.

This step ensures that EA does not process the sets of randomly placed atoms, but operates on fragments of properly bonded carbon structures. Additionally, this method ensures that the optimized structure of atoms is properly equilibrated. The coordinates of atoms are exchanged between two blocks: EA and CG and the equilibration process is performed using the minimization method based on the Polak-Ribiere algorithm. The periodicity of the newly-created structure is also achieved in this step by proper boundary conditions, imposed on the unit cell. After the CG minimization of the potential energy, the objective function is computed for each individual in the population. The CG optimization is the most time-consuming part of the algorithm. To overcome this problem, the authors decided to
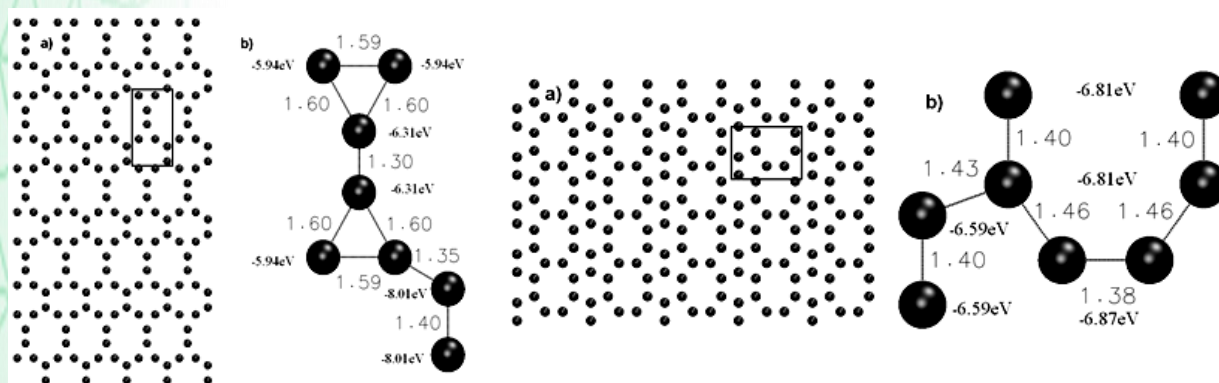
Figure 3. Layout of new stable carbon networks X (A) and Y (B) found by the hybrid algorithm

parallelize the proposed algorithm and make it suitable for running on multiprocessor computers. Thus, the population is scattered into certain number of parts using the MPI library. In the next step, each part is further processed in the parallel way running on a separate core or node of the computer (Figure 2).

In order to validate the accuracy of the presented methodology, certain arrangements of carbon atoms already known from literature were examined, e.g. the supergraphene (triclinic unit cell containing 8 carbon atoms) and the graphyne (triclinic unit cell containing 12 carbon atoms) [4]. Since all the tests yield promising results, the proposed optimization algorithm was applied to search for new stable configurations of a given number of carbon atoms in a unit cell of given size and periodic boundaries [4]. For eight carbon atoms placed in the 4 Å×7 Å rectangular unit cell obtained a stable flat network named X (Figure 3A) and for the same number of carbon atoms placed in the rectangular unit cell 4 Å×6 Å obtained a stable flat network named Y (Figure 3B).

The mechanical properties of the newly-obtained flat carbon networks X and Y were also computed [3].

3 THE SECOND STAGE – AB-INITION COMPUTATION

Two potentially new, 2D-graphene-like materials X and Y generated in the previous stage searching strategy were thoroughly analysed within the framework of the first principles Density Functional Theory (DFT) from the structural, mechanical, phonon and electronic properties point of view.

First-principles calculations based on Density Functional Theory (DFT) [5, 6] within the PseudoPotential, Plane-Wave approximation (PP-PW) implemented in the Cambridge Serial Total Energy Package (CASTEP) [7] were performed in this work.

The extensive analysis of two potentially new polymorphs of graphene within the framework of DFT from the structural, mechanical, electronic and phonon properties point of view was performed in the paper. All calculations were performed with Ultra-Fine Quality settings, the modified Perdew-Burke-Ernzerhof Generalized Gradient Approximation for solids exchange-correlation functional and additionally for band structure calculations nonlocal exchange-correlation functional HSE06. Numerical results of the examination are presented in [8].

The following conclusions can be stated:

- both proposed polymorphs of graphene X and Y are mechanically and dynamically stable,

- X-graphene and Y-graphene can be metallic-like.

Some results in this paper, especially referring to the X-graphene, are the first to be reported and we hope will be confirmed by other studies. The examination of new carbon-based 2D materials with predefined mechanical properties are presented in [9].

4 CONCLUSIONS

The main purpose of this paper was to present the parallel memetic algorithm, applied to searching for new 2D graphene-like materials in the first stage and the thorough examination and authentication of them by ab-initio computation in the second stage. The proposed approach is able to find already-known structures like supergraphene and graphyne as well as new stable ones, named X and Y. The semi-empirical potential (AIREBO) seems to be surprisingly reliable for carbon structures.

Examples performed for new carbon networks clearly show that the final form and properties of optimized structures depend on the assumed size, type and atomic density of the unit cell.

Ab-initio computation shows that both proposed polymorphs of graphene X and Y are mechanically and dynamically stable.

ACKNOWLEDGEMENTS

REFERENCES

[1] Moscato, P., On genetic crossover operators for relative order preservation. C3P Report 778, California Institute of Technology, Pasadena, USA 1989.

[2] Moscato, P., Cotta, C., Mendes, A., Memetic algorithms. In: Onwubolu, G.C., Babu, B.V. (eds.) New Optimization Techniques in Engineering. Studies in Fuzziness and Soft Computing, vol. 141, pp. 53–85. Springer, Heidelberg 2004.

[3] Stuart SJ, Tutein JA, Harsison A., A reactive potential for hydracarbons with intermolecular interactions. *J. Chemical Physics* **112**, 2000, 6472-6486.

[4] Mrozek A, Kuś W, Burczyński T., Nano level optimization of graphene allotropes by means of hybrid parallel evolutionary algorithm, *Computational Material Science* 106, 2015 161-1.

[5] Hohenberg P., Kohn W., Inhomogeneous electron gas, Phys. Rev. 136365, 1964, B864–B871.

[6] Kohn W., Sham L. J., Self-consistent equations including exchange and correlation efects, Phys. Rev. 140, 1965, A1133–A1138.

[7] Clark S. J., Segall M. D., Pickard C. J., Hasnip P. J., Probert M. J., Refson K., Payne M., First principles methods using CASTEP, Z. Kristall. 220, 2005, 567–570.

[8] Maździarz M. , Mrozek A., Kuś W., Burczyński T., First-principles study of new X-graphene and Y-graphene polymorphs generated by the two stage strategy. *Materials Chemistry and Physics*, 2017, 202, 7-14.

[9] Mrozek A. , Kuś W. , Burczyński T., Method for determining structures of new carbon-based 2D materials with predefined mechanical properties. *International Journal for Multiscale Computational Engineering*, 2017, 15(5), 379-394.

TADEUSZ BURCZYŃSKI
POLISH ACADEMY OF SCIENCES, POLAND

WACŁAW KUŚ
SILESIAN UNIVERSITY OF TECHNOLOGY, POLAND

MARCIN MAŹDZIARZ
POLISH ACADEMY OF SCIENCES, POLAND

ADAM MROZEK
AGH UNIVERSITY OF SCIENCES AND TECHNOLOGY, POLAND

TBURCZYNSKI@IPPT.PAN.PL

ECCOMAS YOUNG INVESTIGATORS CORNER

TOWARDS NEW ACTIVITES AND INCREASED VISIBILITY OF THE ECCOMAS YOUNG INVESTIGATORS COMMITTEE

The past year has seen a series of new activities being launched by the ECCOMAS Young Investigators Committee (EYIC) in order to increase its visibility within ECCOMAS and beyond. The EYIC has been created in order to promote the main goals of ECCOMAS among young researchers and to encourage activities of young ECCOMAS members. In pursuit of this goal, the first ever two-day EYIC workshop was organized in Aachen (Germany) with 14 participants from among our group, who represent the different national and regional associations within ECCOMAS. The main results of this workshop were then presented at the ECCOMAS Board Meetings in Vienna in May 2017. Among the most important novelties is the official ECCOMAS Facebook group, which was launched in March 2017 and at present counts almost 100 members. As you are reading this, please consider joining the group!

Other current activities of the committee include the testing of new scientific formats at current and future ECCOMAS events (such as Science Slams and the so-called Young Investigators Minisymposia), as well as the preparation of an ECCOMAS Job Database for young researchers. One of the highlights of this year has definitely been the 4th ECCOMAS Young Investigators Conference, which took place at Politecnico di Milano (Milan, Italy), September 13-15, 2017. The conference chairman, Massimiliano Cremonesi and his team, attracted more than 150 participants from all over the world with their very comprehensive scientific program in combination with a dash of Italian "la dolce vita" during the social program. We are all very much looking forward to the next edition of the ECCOMAS Young Investigators Conference series, which will be organized in Krakow, Poland on September 1-6, 2019.

EYIC website: http://www.eccomas.org/vpage/1/0/Committees/YIC-General

Alexander Popp – alexander.popp@unibw.de
Stefanie Elgeti – elgeti@cats.rwth-aachen.de
ECCOMAS Young Investigators Committee

The ECCOMAS Young Investigators Committee at work during the ECCOMAS Young Investigators Conference 2017 in Milan

BEYOND FEM: MESHFREE SIMULATIONS OF MANUFACTURING PROCESSES ON GPU

1 INTRODUCTION

The improvement potentials of manufacturing processes and structural technologies can be markedly leveraged with the help of simulations. Understanding the physics involved on one hand, and improving the associated numerics on the other, could in one way or another expand the limitation borders of the analysis. This explains why the design of a robust numerical tool for simulating such engineering phenomena sees an evergrowing share of interest in literature. In 1989, it was claimed that the future research strongly hinges on numerical methods and (high-performance) computational techniques [1]. Aligned with this insightful statement, the Institutes of Machine Tools & Manufacturing (IWF), and Structural Mechanics Engineering (IBK), at ETH Zürich, have been developing novel and advanced numerical techniques to solve real-world engineering applications. This report offers a brief review of some recent achievements in this regard.

Heat and mass transfer problems comprise the dominant physics for a vast spectrum of applications. Specifically, for a number of manufacturing processes, the thermal behavior governs the entire process. This is for instance elaborated upon in the work of Haitao et al. [2] on thermal deformations of a CNC machine tool spindle, as well as in the extensive overview of thermal issues in machine tools by Mayr et al. [3]. While a number of numerical tools have been adopted to such an end, e.g., [4,5,28], a meshfree discretization of the heat equation remains relatively unexploited. This article aims to motivate adoption of a meshfree approach, opening new pathways for further and more detailed investigations.

Most manufacturing processes are associated with challenging simulation tasks including large deformations, high strain rates, fracture, and contact problems. For appropriately incorporating such effects, it is necessary to conduct thermo-mechanical coupling simulations, where the modeling of metal cutting remains a primary challenge, yet one carrying substantial weight in terms of practical implementation. Indeed, the cutting operation is one of the most widely used processes in the manufacturing and machine tool industries accounting for 20% of the overall production cost according to [6]. In 2007, Limido et al. applied the Smoothed Particle Hydrodynamics (SPH) method to high speed cutting models [7]. Their work further extended the SPH models of both single grain [8] and hexa-octahedral diamond grain [9] cutting tests, which were carried out in IWF, ETH Zürich. Yet, the number of conducted works adopting the Finite Element Method (FEM) in this area is significantly larger than its meshfree counterpart.

Meshfree methods have lately been seeded into a completely new field of application. In 2008, the first SPH simulation of a laser cutting process was reported by Gross [10]. Through this inceptive exploitation, it was understood that tremendous potential lies in the adoption of meshfree methods for laser manufacturing processes. The original SPH formulation was then developed by investigating the thermal modeling of the direct laser interference patterning [11]. This original work has since then been refined to include both dry and wet laser cutting cases up to 3D multi-pulse applications with SPH [12], the improved SPH formulation for approximating higher derivatives in heat transfer of laser ablation in Aluminum [13], as well as development of a Radial Point Interpolation Method (RPIM) for heat conduction in laser drilling [14]. This latter work relies on adoption of Radial Basis Function (RBF) methods for solving the heat conduction problem. Meshfree

algorithms offer an efficient means for discretizing the heat equation with mixed and/or complex boundary conditions, thereby serving as a valuable candidate for solution of a variety of laser machining problems, wherein thermal issues dominate the simulation. This work thus aims at offering an overview of the state of the art as well as recent advances in meshfree simulation of laser manufacturing processes up to 3D.

The main methodological as well as computational advances offered herein can be summarized as: i) alleviation of the cumbersome remeshing procedure in FEM cutting simulations, by employing Lagrangian particle-based techniques, ii) incorporation of highly accurate meshfree schemes associated with several manufacturing processes featuring complex boundary conditions, iii) enhancement of the computational efficiency through implementation on Graphics Processing Unit (GPU).

2 RESEARCH GAP AND CHALLENGES

Meshfree methods have been successfully implemented in various problems of solid [15] and fluid [16, 17,29] mechanics. Nonetheless, a recurring question lies in whether the use of such techniques proves more advantageous than mesh–based methods. In the domain of heat transfer analysis two axiomatic reasons limit the applicability of meshfree methods, particularly in 3D, when compared against its long-time competitor, i.e., the Finite Element Method. The first lies in the adeptness of the conventional FEM solution in thermal problems; while the second is the very high cost of meshfree computations in higher dimensions. The first issue has been tackled in recent advances by introducing extra mathematical

manipulations in order to achieve higher order schemes for approximating the higher order spatial derivatives. The second issue has been addressed in recent endeavors, thanks to the growth of parallel computations and the notable increase in computing power. Strictly speaking, a three dimensional application of the contemporary meshfree techniques for real-world manufacturing processes cannot be found in literature. This work aims to fill this gap by demonstrating the suitability of a meshfree solver proposed for thermal simulations in complex structural and manufacturing applications.

A multiplicity of algorithms has been devised to increase the proficiency of meshfree methods across different applications. These algorithms fall into the categories of boundary treatments [18], partition of unity by smoothing kernel reconstruction [19, 20], and approximation of higher order spatial derivatives [21, 22, 23], to name a few. In spite of few accomplished efforts on meshfree cutting simulations, an open source software incorporating these recent improvements in meshfree methods is still lacking. Towards this end, an orthogonal cutting operation in 2D is also studied to accentuate the functionality of the proposed meshfree toolkit. The present solution implements the most recent numerical developments in computational continuum mechanics and computer graphics and recombines them for simulation of metal cutting processes. As such, higher order renormalization tensors are utilized in the strong form meshfree methods for

resolving the boundary deficiency, i.e., re-approximation of the smoothing kernel, especially near the boundaries where the kernel's supporting domain is truncated by the boundary. Furthermore, and in order to enhance the throughput, the proposed solution employs general purpose computations on the graphics processor (GPGPU) to increase the simulation resolution and/or calculation speed.

In view of the above the present investigation aims at developing a robust yet efficient tool to handle thermal simulations. The fundamental differences (and similarities) in the structure and implementation of two advanced meshfree schemes are elaborated upon in this work, namely the Particle Strength Exchange [21,30], and the Improved Corrective Smoothed Particle Method [23], hereinafter referred to as PSE and ICSPM, for the sake of brevity.

In this report, the following three different processes in machine tools and manufacturing technology are
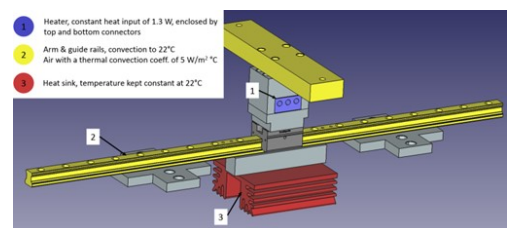

Figure 1. CAD model and boundary conditions in the linear positioning system examined.
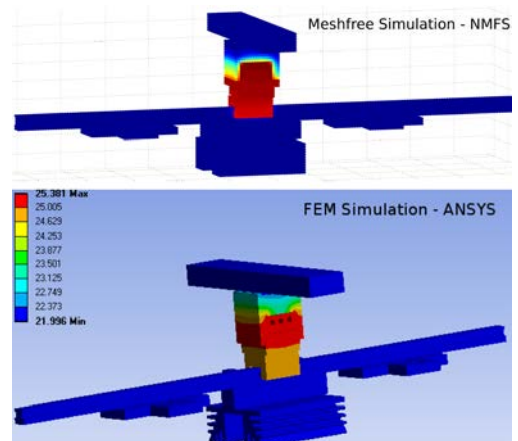

Figure 2. Temperatures at steady state: NMFS vs. FEM.

accordingly presented.

- *Model 1*: 3D heat transfer modeling in ultra-precision machining.
- *Model 2*: 2D orthogonal metal cutting simulation.
- *Model 3*: Material removal in laser drilling with both 2D and 3D simulations.

3 ULTRA-PRECISION MACHINING

As a real-world engineering application, the selected meshfree methods are applied to simulate heat transfer in ultra-precision machining. This benchmark features a combination of complex geometries and mixed boundary conditions in three dimensions. The system to be analyzed is a positioning system for wafer inspection. For this purpose, the wafer to be investigated is to be positioned with nano–scale accurate positioning stability. Thermally induced displacements, or rather the reduction thereof, becomes of utmost importance in this problem setting. This implies that the heat generated by the linear motors needs to be rapidly extracted from the system, resulting in a uniform and nominal temperature distribution. This is no trivial task since the structuring process must be performed in a vacuum setup. If no liquid cooling cycles are run through the motors, the heat leaves the structure via the bearings and the guide rail to the granite table, forming a large heat sink. In this case it is crucial to know the temperature distribution, for which the calculation of the thermal resistance of the bearing assembly is necessary.

Instead of the whole positioning system a sub-model of interest was identified. Only one linear axis was considered. The linear motor was replaced by a heating element to be able to introduce heat into the structure without actually running the linear motors. The granite table, as the heat sink, was replaced by a set of cooling fins. An arm was attached atop for weighing the structure down. This is because the weight of the orthogonal axis, or the payload, respectively, would press the bearings against the rail (thus, potentially affecting the thermal resistance).

Fig. 1 illustrates the CAD model including boundary conditions of that reduced model. In the experimental setup, thermal sensors were introduced at two points: at the guide rails and at the carriage, respectively. The structure was then heated by a heater placed on top. Measurements were taken until steady state is reached. For the meshfree simulations, the CAD model at hand was voxelized using `binvox`, which implements the method described in [24]. Drilling holes and fillets were omitted to provide a clean voxelization, since existence of geometric complexities would hinder the tensorial computations required for the meshfree approximations.

The simulation results are verified against both FEM–ANSYS® results and the experimental measurements performed at IWF laboratory. Illustrated in Fig. 2, the steady state thermal distribution in this positioning system for wafer inspection is modeled using a New MeshFree Scheme (NMFS) originally introduced in [22], demonstrating the functionality of this meshfree scheme for handling thermal problems in the application at hand. The computational efficiency of the performed meshfree simulation is not discussed here, since the fixed-in-space particles cannot appropriately reflect the privilege of meshfree vs. mesh-dependent techniques. Moreover, the FEM solver considers the steady state, whereas the meshfree simulation takes the transient state into account until a certain small threshold is obtained.
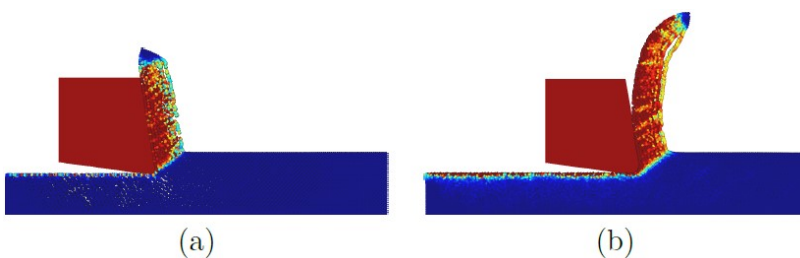
Figure 3. (a) `mfree_iwf` *simulation providing the similar result as the LS-DYNA commercial package, (b) chip curling using* `mfree_iwf`*.*
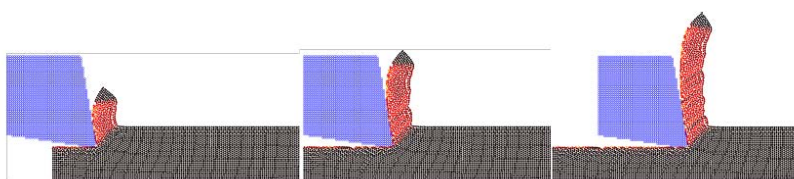
Figure 4. Snapshots of thermal distribution in the workpiece using 5640 particles computed on GPU. Concentrated shear zones nearly adiabatic can be detected. The temperature is color coded in the workpiece, scaling from 0 to 1.

Figure 5. High resolution SPH simulation results of 2D orthogonal cutting with 500'000 particles computed on GPU.

4 METAL CUTTING OPERATION

The computational software used for the thermal aspect, named `thermal_iwf`, is further coupled with the mechanical solver, named `mfree_iwf`. Through this joint framework, the metal cutting operations are eventually simulated, thereby addressing the complicated issues in SPH models, such as contact, thermal loads, friction, and plasticity. Orthogonal cutting may now be performed using in-house software. As a preliminary study, the results of the algorithms used in LS-DYNA are reproduced via the `mfree_iwf` solver for validation purpose, where the Johnson- Cook material model with thermal softening is implemented. Fig. 3-(a) represents the simulation results for the orthogonal cutting geometry at hand, comparable to the LS-DYNA, both qualitatively and quantitatively. By incorporating some improvements suggested by Gray et al. in [25], certain advancement over LS-DYNA can be achieved, like the correct resolution of chip curling, shown in Fig. 3-(b). This effect cannot be resolved in in-house studies using LS-DYNA. The color code in Fig. 3 is the plastic strain, ranging from 0 to 1. In the following cutting simulations, a workpiece with a length of 2 [mm] is considered.

Successful implementation of this software on GPU allows for even more sophisticated modeling. One can, for instance, consider the generation of heat due to the plastic work and perform the respective simulation using higher resolutions, yet for a longer cutting length. The simulation performed for the cutting geometry at hand takes 966.35 GPU seconds on **NVIDIA GeForce GTX 760** graphics card. The corresponding throughput of this parallel programming offers a speed –up factor of 15, although the

algorithms have not yet been optimized.

Illustrated in Fig. 5 is the temperature distribution in the workpiece, in which the colder zones are shown with darker colors. Next, the available meshfree algorithms on the CPU are further parallelized on the GPU. Some first results obtained via GPU parallelization are illustrated in Fig. 5, where 500, 000 particles have been used to simulate a 2D orthogonal metal cutting.

In Fig. 5, the higher temperature zones are represented with brighter colors. To the best of the authors' knowledge, the illustration presented in Fig. 5 delivers the highest resolution results available in the current state of the art for metal cutting simulation with meshfree methods. It should be pointed out, that the concentrated shear bands can be recognized and the high temperature in these shear bands demonstrates that they are nearly adiabatic.

5 LASER DRILLING PROCESS

A second-order PSE method [21] is adopted for simulating the heat transfer in laser drilling processes motivated by the trade-off of accuracy vs. computational cost. In fact, the heat transfer modeling followed by the phase change in the materials can mimic the metal removal in a simplified laser drilling problem. To this end, the problem of transient state heat transfer is solved by exerting a static laser beam with a Gaussian intensity distribution, as the external heat source. The employed PSE scheme is a fully Lagrangian approach, which is straightforward to implement as compared to alternative meshless methods currently used in the state of the art. The performance of the PSE method in solving the heat transfer problem at hand is assessed
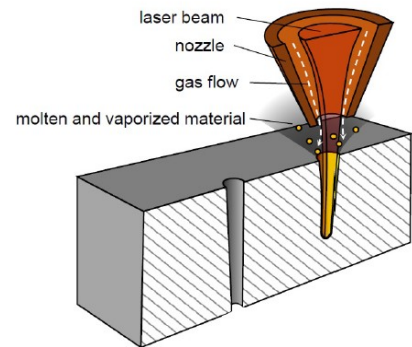

Figure 6. Schematic laser drilling of a metallic workpiece [31].

through a case-study on single-pulse laser heating of a metal workpiece. The simulation results are validated against numerical as well as experimental data available in literature, demonstrating the suitability of the proposed approach in addressing the thermal issues of such complex manufacturing processes.

In essence, the laser machining of metallic materials centers around a thermal process. Therefore, the focus in the associated numerical analyses lies in discretization of the heat transfer equation. With the exception of femtosecond-pulse range lasers, material removal is mostly caused by melting, vaporization plus the auxiliary action of assist gas [26]. Succinctly, assist gas aids cutting via an exothermic reaction (usually with oxygen) and/ or evacuates molten material from the drilled hole. Not only is the assist gas a crucial component to remove the molten material from the processed workpiece through the cut kerf, but further alleviates the unfavorable recast and dross in laser machining. This pressurized gas may also serve as a protector shield for the processing area against its surrounding. A schematic depiction of a classical laser drilling process is therefore illustrated in Fig. (6), where the workpiece is subjected to phase changes from
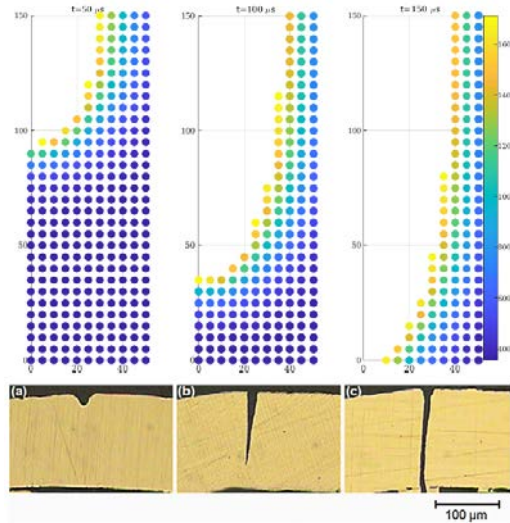
Figure 7. Temperature distribution and penetration depth using PSE (top) & experimental penetration depth at the respective pulse durations [12] (bottom).

solid to liquid and eventually to vapor with the laser beam indicated in red. As demonstrated in what follows, this very involved multi-phase procedure leads to remarkable changes in material characteristics.

The key in treating the boundary conditions in this case lies in effectively identifying the surface particles. Problems of moving interfaces and the representation of the geometry are often referred to as one of the most challenging issues in numerical simulations (see [27]). In this work, nevertheless, a simple approach is adopted for detecting the surface particles during the simulation: termed as "neighboring–flag". That is, the simulation initiates via consideration of the four prescribed walls as the initial well–defined surfaces. The particles located in these four walls are known as surface particles, tagged with a "*surface*" flag. The heat source is applied only if the particle bears a "*surface*" label and further belongs to the top wall or the cut hole. A particle is termed "*active*" if its temperature lies under the melting limit, and the diffusion PDE is solved only on "*active*" particles. The dynamic boundary conditions in this problem are enforced only on particles bearing

the "*surface*" flag in staggered positions. Later, once a particle reaches its melting temperature (here 1723 [K]), its first-level neighbors are redefined as "*surface*" particles. This particle is then deleted from the simulation, which is equivalent to material removal, hence the moving boundary of the cutting surface. The term "first-level -neighbor" indicates any neighboring particle with distance smaller or equal to the initial spacing in uniformly spaced particle ensembles. For more sophisticated models, one should also extract the melting enthalpy for the mass represented by the particle out of the system.

The PSE method is first applied to a 2D laser drilling problem. The case study pertains to a workpiece made of stainless steel (SS 316L) with a width of 100 [μm], length of 200

[μm], and a thickness of 150 [μm]. The domain is uniformly discretized by 11×31 and 25×45×35 particles, for 2D and 3D simulations, respectively. A laser beam source with "μs" to "ms" pulse duration is considered, while the assist gas is not included in the simulation. For further details on the simplifying assumptions, the summary of the parameters used throughout this simulation plus the thermo-physical properties of SS 316L, readers are encouraged to refer to [14].

The comparison presented in Fig. 7 yields a good agreement between numerical and experimental approaches in predicting the penetration depth of the laser beam inside the metallic workpiece. From left to right, Fig. 7 provides the three sequences of the 2D axisymmetric laser drilling process until full penetration is reached. It is worth noting that the empirical values of the temperatures are lacking in the corresponding reference.

The generated heat propagates throughout the material until the full-depth penetration is achieved. In terms of computational cost, the measured CPU runtime of this PSE simulation implemented in **C99** is almost 5 [s], taken on an **Intel® Core™ i5-4690**. Compared to the CPU calculation times given in [14], the aforementioned runtime of PSE simulation results are approximately two orders of magnitude less than the previous meshfree simulations available in the state of the art. This efficient computer implementation
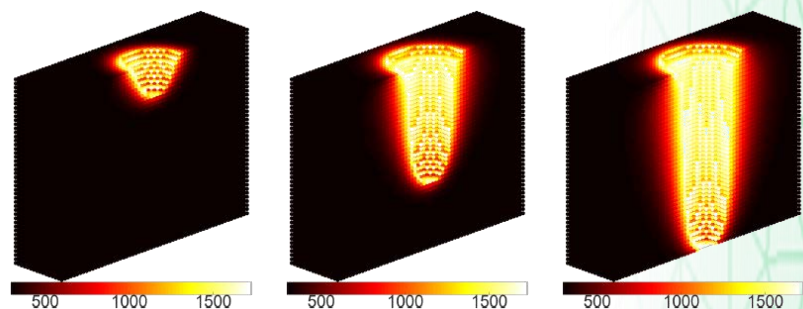

Figure 8. ICSPM 3D simulation: drilled hole and temperature distribution in the workpiece.

allows for extending to full three dimensional model. Thus, the same pulsed laser dry machining is modeled with thermal simulation in 3D using another advanced meshfree scheme, namely ICSPM.

The snapshots associated with the same time instants as in the 2D case are chosen where only half of the workpiece is shown for the sake of better visualization. As can be observed in Fig. 8, the drilled hole is formed upon the exertion of the static laser beam. The molten particles (invisible in this figure) are ejected from the kerf, and the laser beam is applied to the newly generated surface. As such, ill–defined boundaries are evolved during this evolutionary procedure which necessitates a robust strategy for handling the surface detection. Among few conventional techniques, the same "neighboring–flags" approach is exploited here again, offering a remarkable saving of the computation together with a reasonable accuracy.

6 Conclusion

The contribution of this work lies in the tailoring of state-of-the-art meshfree techniques in a unified methodological framework. Through this contribution, this study is intended to shed some light into the salient potential of meshfree methods in modeling various manufacturing problems (in both academic and real-world scale per se) with different levels of complexity. The highly promising performance of these techniques together with the unique simplicity of meshfree methods in treating complex geometries brings them in practical use for complicated physical phenomena. The workability of the proposed numerical tool is demonstrated in not only the fixed-in-space discretization particles (e.g., the

thermal simulation in an ultra-precision machining and a laser drilling case), but also in a metal cutting operation where the Lagrangian discretization points are free to move. Plus, the offered three dimensional benchmark illustrates the computational credibility and efficiency of our implementation, even for a single threaded execution. The principal computational burden in the corrective schemes, e.g., ICSPM, stems from incorporation of higher-order tensors (i.e., correction terms) to reconstruct the mollifying kernel and to amend boundary deficiencies of meshfree methods, especially when these terms have to be calculated for each single particle at each time increment, as is the case in advection–diffusion problems. This very expensive computational labor of moving particle simulations in 3D demands high-performance computing which is acquired by both parallel programming on GPU or OpenMP/MPI accelerated codes. The numerical results presented in Fig. 4 and Fig. 5, illustrate the effectiveness of this fulfillment via GPU–parallelization. An outlook to future research and upcoming achievements will be centered around the design and implementation of more efficient algorithms in order to obtain the maximum speed-up in 3D manufacturing and structural applications for the developing software.

Acknowledgement

References

[1] D. P. Bertsekas and J. N. Tsitsiklis, *Parallel and distributed computation: numerical methods*, vol. 23. Prentice hall Englewood Cliffs, NJ, 1989.

[2] Z. Haitao, Y. Jianguo, and S. Jinhua, "Simulation of thermal behavior of a cnc machine tool spindle," *International Journal of Machine Tools and Manufacture*, vol. 47, no. 6, pp. 1003–1010, 2007.

[3] J. Mayr, J. Jedrzejewski, E. Uhlmann, M. A. Donmez, W. Knapp, F. Härtig, K. Wendt, T. Moriwaki, P. Shore, R. Schmitt, et al., "Thermal issues in machine tools," *CIRP Annals-Manufacturing Technology*, vol. 61, no. 2, pp. 771–791, 2012.

[4] S. V. A. Laakso, "Heat matters when matter heats–the effect of temperature-dependent material properties on metal cutting simulations," *Journal of Manufacturing Processes*, vol. 27, pp. 261– 275, 2017.

[5] E. Segebade, M. Gerstenmeyer, F. Zanger, and V. Schulze, "Cutting simulations using a commercially available 2d/3d fem software for forming," *Procedia CIRP*, vol. 58, pp. 73–78, 2017.

[6] N. Rüttimann, *Simulation of metal cutting processes using meshfree methods*. PhD thesis, Diss., Eidgenössische Technische Hochschule ETH Zürich, Nr. 20646, 2012.

[7] J. Limido, C. Espinosa, M. Salaün, and J.-L. Lacome, "Sph method applied to high speed cutting modelling," *International journal of mechanical sciences*, vol. 49, no. 7, pp. 898–908, 2007.

[8] N. Ruttimann, S. Buhl, and K. Wegener, "Simulation of single grain cutting using sph method," *Journal of Machine Engineering*, vol. 10, 2010.

[9] N. Rüttimann, M. Roethlin, S. Buhl, and K. Wegener, "Simulation of hexa-octahedral diamond grain cutting tests using the sph method," *Procedia CIRP*, vol. 8, pp. 322–327, 2013.

[10] M. Gross, "Smooth particle hydrodynamics (sph) modelling of laser cutting," in *Int. Congress on Aplications of Lasers & Electro Optics*, pp. 637–44, 2008.

[11] C. Demuth, M. Bieda, A. F. Lasagni, A. Mahrle, A. Wetzig, and E. Beyer, "Thermal simulation of pulsed direct laser interference patterning of metallic substrates using the smoothed particle hydrodynamics approach," *Journal of Materials Processing Technology*, vol. 212, no. 3, pp. 689–699, 2012.

[12] N. Muhammad, B. Rogers, and L. Li, "Understanding the behavior of pulsed laser dry and wet micromachining processes by multi-phase smoothed particle hydrodynamics (sph) modelling," *Journal of Physics D: Applied Physics*, vol. 46, no. 9, p. 095101, 2013.

[13] A. Alshaer, B. Rogers, and L. Li, "Smoothed particle hydrodynamics (sph) modelling of transient heat transfer in pulsed laser ablation of al and associated free-surface problems," *Computational Materials Science*, vol. 127, pp. 161–179, 2017.

[14] D. Abidou, N. Yusoff, N. Nazri, M. O. Awang, M. A. Hassan, and A. A. Sarhan, "Numerical simulation of metal removal in laser drilling using radial point interpolation method," *Engineering Analysis with Boundary Elements*, vol. 77, pp. 89–96, 2017.

[15] T. Rabczuk, S. Bordas, and G. Zi, "On three-dimensional modeling of crack growth using partition of unity methods," *Computers & structures*, vol. 88, no. 23, pp. 1391–1411, 2010.

[16] M. Afrasiabi and S. Mohammadi, "Analysis of bubble pulsations of underwater explosions by the smoothed particle hydrodynamics method," in *ECCOMAS International Conference on Particle Based Methods*, *Spain, 2009.*

[17] M. Liu and G. Liu, "Smoothed particle hydrodynamics (sph): an overview and recent developments," *Archives of computational methods in engineering*, vol. 17, no. 1, pp. 25–76, 2010.

[18] P. Randles and L. Libersky, "Smoothed particle hydrodynamics: some recent improvements and applications," *Computer methods in applied mechanics and engineering*, vol. 139, no. 1, pp. 375– 408, 1996.

[19] W. K. Liu, S. Jun, and Y. F. Zhang, "Reproducing kernel particle methods," *International journal for numerical methods in fluids*, vol. 20, no. 8-9, pp. 1081–1106, 1995.

[20] G. R. Johnson and S. R. Beissel, "Normalized smoothing functions for sph impact computations," *International Journal for Numerical Methods in Engineering*, vol. 39, no. 16, pp. 2725–2741, 1996.

[21] J. D. Eldredge, A. Leonard, and T. Colonius, "A general deterministic treatment of derivatives in particle methods," *Journal of Computational Physics*, vol. 180, no. 2, pp. 686–709, 2002.

[22] R. Fatehi and M. Manzari, "Error estimation in smoothed particle hydrodynamics and a new scheme for second derivatives," *Computers & Mathematics with Applications*, vol. 61, no. 2, pp. 482–498, 2011.

[23] S. Korzilius, W. Schilders, and M. Anthonissen, "An improved cspm approach for accurate second-derivative approximations with sph," *Journal of Applied Mathematics and Physics*, vol. 5, no. 01, p. 168, 2016.

[24] F. S. Nooruddin and G. Turk, "Simplification and repair of polygonal models using volumetric techniques," *Visualization and Computer Graphics*, IEEE Transactions on, vol. 9, no. 2, pp. 191–205, 2003.

[25] R. J.P. Gray, J.J. Monaghan, "Sph elastic dynamics," *Computer methods in applied mechanics and engineering*, 2001.

[26] G. Ng, P. Crouse, and L. Li, "An analytical model for laser drilling incorporating effects of exothermic reaction, pulse width and hole geometry," *International Journal of Heat and Mass Transfer*, vol. 49, no. 7, pp. 1358–1374, 2006.

[27] J. A. Sethian, *Level set methods and fast marching methods: evolving interfaces in computational geometry, fluid mechanics, computer vision, and materials science*, vol. 3. Cambridge university press, 1999.

[28] Afrasiabi, Mohamadreza, et al. "A Particle Strength Exchange Method for Metal Removal in Laser Drilling", Procedia CIRP, ISSN 2212-8271.

[29] Afrasiabi, M., M. Roethlin, and K. Wegener. "Thermal simulation in multiphase incompressible flows using coupled meshfree and particle level set methods." Computer Methods in Applied Mechanics and Engineering 336 (2018): 667-694.

[30] S. Mas-Gallic and P. A. Raviart, Particle Approximation of Convection Diffusion Problems, Technical Report R86013 (Laboratoire d'Analyse Numerique ´ d I'Universite´ Pierre et Marie Curie, 1986).

[31] http://www.ionix.fi/en/ technologies/laser-processing

M. AFRASIABI
M. ROETHLIN
H. KLIPPEL
E. CHATZI
K. WEGENER

ETH ZÜRICH, SWITZERLAND

AFRASIABI@IBK.BAUG.ETHZ.CH
CHATZI@IBK.BAUG.ETHZ.CH

COMMUNICATED BY ALEXANDER POPP AND STEFANIE ELGETI, CO-CHAIR PERSONS OF THE ECCOMAS YOUNG INVESTIGATORS COMMITTEE

MODELING AND SIMULATION OF ADDITIVE MANUFACTURING PROCESSES

INTRODUCTION

Additive manufacturing (AM) technology is defined by the American Society for Testing and Materials (ASTM) as the "process *of joining materials to make objects from 3D model data, usually layer upon layer, as opposed to subtractive manufacturing methodologies, such as traditional machining*" [1]. The main differences between the various AM processes are the employed material, the deposition methodology, and the hardening process.

ASTM classifies Additive Manufacturing processes into seven categories [2], among which the most frequently adopted are Powder Bed Fusion (PBF) and Fused Deposition Modeling (FDM) [3]. In PBF, firstly a layer of powder (mostly metal) is deposited on the building tray and then the powder is melted. The most commonly used PBF technologies are Selective Laser Melting (SLM) and Electron Beam Melting (EBM). The difference between SLM and EBM lies in the heat source used to melt the powder: a laser beam for SLM and an electron beam for EBM [4]. In FDM, a thermoplastic polymer wire is heated into a semi-molten state,

and subsequently it is extruded through a nozzle in a very thin filament. The material is deposited while the nozzle moves following a predefined printing path calculated by a so-called *slicing software*; the first layer is usually deposited on the building plate, while the following layers are deposited on top of the previous ones [5].

Both PBF and FDM are very complex processes as they entail several physical aspects. Figure 1 shows the primary physical phenomena (highlighted in blue) and the secondary ones (in black) rising during the two mentioned AM processes.

Due to the complexity of the phenomena, it is not currently possible to consider each physical aspect into a single simulation model. Some effects, like powder wetting (in PBF) [6] or filament

bonding (in FDM) [7], show up at a microscopic scale, compared to the component size. To simulate these effects, microscopic simulations are necessary to investigate the printing process at the scale of micrometers. As such models are in general very expensive in terms of computational costs, they are used to study only small portions of the domain (millimeters). On the contrary, to study a complete 3D printed component, macroscopic simulations [8] are usually adopted, to describe the process at a scale ranging from hundreds of micrometers to centimeters. As a consequence, macroscopic simulations often neglect phenomena rising at lower scales. The main purpose of macroscopic simulations is to evaluate both temperature gradients and residual stress fields during the printing process. Non-uniform thermal
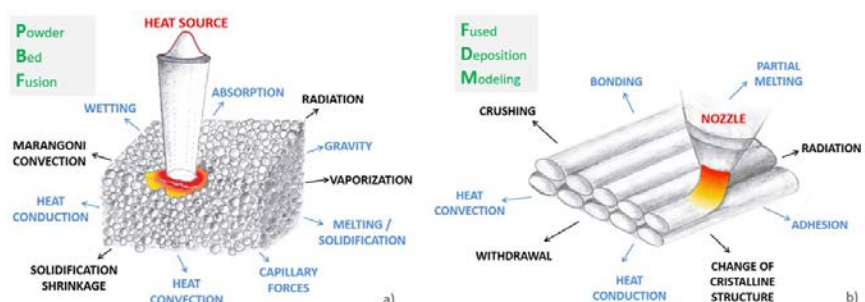

Figure 1. Physical phenomena involved in Additive Manufacturing processes: (a) Powder Bed Fusion (PBF) process, (b) Fused Deposition Modeling (FDM) process. In blue the principal physical effects, in black the secondary physical effects .
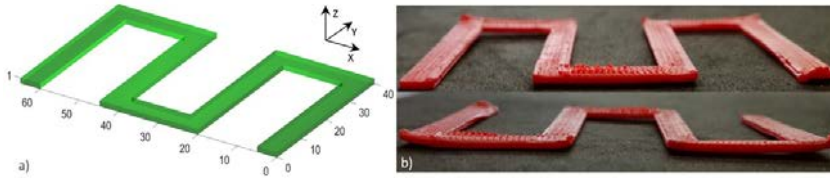
Figure 2. 3D printed planar spring. (a): Geometry of the model (mm); (b) Model after the detachment from the building plate. Deformations are especially located at the corners.
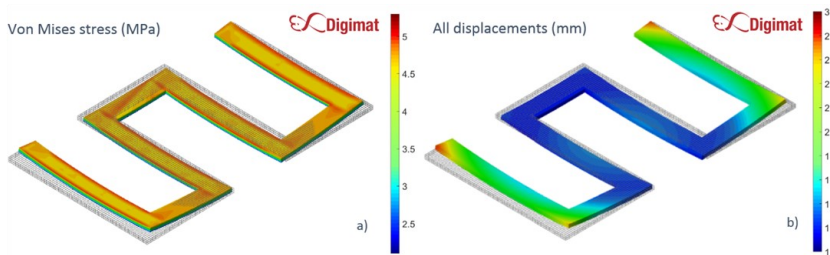

Figure 3. Results of the FDM printing simulation: (a) Von Mises stress distribution: higher stresses are in the upper surface of the planar spring; (b) Displacements distribution: higher displacements are found at the corners of the model. Simulations carried out using Digimat (e-Xstream engineering).

gradients lead, as a matter of fact, to the formation of residual stresses [9], that can produce part deformation affecting the component mechanical performance.

Many numerical approaches to reproduce the complex microscopic phenomena are available, as well as to simulate the component production adopting a macroscopic point of view.

In this article, we opted to present briefly the Lattice Boltzmann Method (LBM) for microscopic simulations and the Finite Element Method (FEM) for macroscopic ones. With respect to this latter simulation framework, many commercial codes are already available on the market: Abaqus (Simulia, Dassault Systemès) and Digimat (e-Xstream engineering), just to name a few. Herein, we have tested the performance of one of these tools (Digimat [10]), comparing the obtained numerical results with experimental measures.

MACROSCOPIC SIMULATIONS FOR FUSED DEPOSITION MODELING

Currently, macroscopic simulations are, by far, the most used approach for AM processes. As mentioned, the main purpose is to evaluate temperature gradients and residual stress distributions on the component, as well as to predict part distortions [10]. To this end, finite element analyses are performed in most cases. In FDM, the printing process instructions are defined in a GCODE file containing all the process parameters (e.g., nozzle velocity, extrusion path and temperature). The basic idea of macroscopic simulations is to reproduce a sequential activation of finite elements, following the data reported in the GCODE, and to solve step by step the equations governing the problem. Usually, the thermal problem is solved before the mechanical one [12] with an *uncoupled* approach: first, a heat-transfer analysis is performed to solve heat-conduction-convection

equations; then, the results of the thermal analysis are used as forcing term of the static one, whose output is stress distributions and component distortions.

Many software houses are now developing tools for simulation of 3D printing processes. However, we will present the results obtained using the dedicated software package developed by Digimat for additive manufacturing problems, based on the so-called *Inherent Strain Method* [13]. The inherent strain method relies on a multiscale modeling approach. First, a fully coupled thermomechanical Finite Element Analysis is performed at the Representative Volume Element (RVE) level, as a function of the thermal and mechanical properties of the material as well as the deposition conditions. Then, based on the identified inherent strains at the RVE level a layer-by-layer mechanical analysis is performed at the full structure level, which enables the prediction of warpage and residual stresses for the final application.

In particular, we have considered as validation benchmark a polymeric planar spring, whose geometry is shown in Figure 2(a). The spring has been printed with four layers of ABS filament and, at the end of the printing process, the planar spring has been removed from the building plate before cooling. Figure 2(b) shows the 3D printed planar spring after the detachment from the building plate.

It is interesting to observe that the most pronounced deformations occur at the corners of the model. Generally, corners are critical points of the printing process as they are subject to stress concentration and, consequently, to high deformation [14].

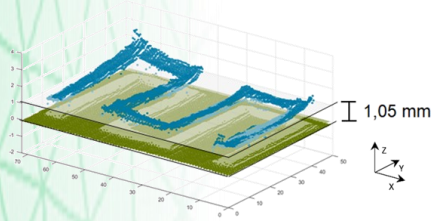The simulation was performed tacking into account the GCODE

Figure 4. Measurement results of the planar spring. The effective height is slightly greater (1,05 mm) than the design height (1,00 mm).

Figure 5. Comparison between the Z-axis displacements determined with (a) the experimental test and (b) the numerical simulation.

information and adopting a thermo-elastic constitutive model. Figure 3 (a) shows the distribution of Von Mises stresses. Higher stresses are present on the upper surface of the spring, while lower stresses are in the bottom part; moreover, the stress pattern justifies the observed bending of the structure. Figure 3(b) shows the Euclidean norm of the displacement vector. As expected, the higher deformation is located at the corners of the spring.

A comparison between experimental and numerical vertical displacements of the upper surface has validated the results. The 3D printed spring has been measured with a high precision laser scanner (Julight Srl, www.julight.it) and the experimental measurements are shown in Figure 4. The undeformed upper surface of the planar spring (z = 1.05 mm) has been assumed as reference plane for the evaluation of the experimental vertical displacements.

Figure 5 shows the comparison between the z-axis displacements measured from the experimental test (Figure 5(a)) and computed with the numerical simulation (Figure 5(b)).

Despite some printing imperfections of the real model (i.e., roughness of the upper surface and presence of a small amount of residual material in the corner G, the last spot printed), a qualitatively good agreement is observed.

Improved results may be obtained,

for example, considering more accurate models of the adhesion force between the component and the building plate.

MICROSCOPIC SIMULATIONS FOR POWDER BED FUSION

Some physical effects in PBF can be appreciated only at the scale of micrometers; therefore, microscopic simulations can be performed to predict phenomena such as local porosity, surface roughness, wetting, vaporization, and surface tension, that can affect the mechanical properties of the component [6].

In the literature, most of the works aiming at microscopic insights in metal additive manufacturing simulation are based on the *Lattice Boltzmann Method* (LBM) [15,16,17]. LBM rises from the discretization of Boltzmann's equation, used in place of the Navier-Stokes-Fourier equations, to solve thermo-fluid dynamic problems [18]. Coupling LBM with a free surface treatment and with a phase change modeling makes possible to simulate PBF processes [19].

We will focus on the wetting problem, one of the most relevant phenomena during PBF, to show, with a simple example, how LBM can be used for the simulation of free-surface problems. The proposed LBM scheme is based on

the multiphase multicomponent Shan-Chen model [20]. The equations governing the problem are the following:

- Boltzmann equation: describing the microscopic kinetic problem for particle distribution functions $f(x, \xi, t)$, where x is the position and ξ is the velocity of the particle at time t. The equation is obtained through the discretization of the continuous velocity ξ with a set of velocities ξ_i:

$$f_i(\boldsymbol{x} + \boldsymbol{\xi}_i \delta t, t + \delta t) =$$
$$f_i(\boldsymbol{x}, t) - \frac{1}{\tau}\Big(f_i(\boldsymbol{x}, t) - f_i^{eq}(\boldsymbol{x}, t)\Big) + F_i \quad (1.1)$$

where f_i is the particle distribution function on i-th velocity direction, τ is the relaxation time, f_i^{eq} is the equilibrium distribution function, and F_i represents the external force (e.g., gravity force);

- Young's equation: describing the wetting problem, expressed as follows:

$$\theta_C = \arccos\left(\frac{\gamma_{SG} - \gamma_{SL}}{\gamma_{SL}}\right) \quad (1.2)$$

where θ_c is the wetting angle, γ_{SG}, γ_{SL} and γ_{SL} are the surface tensions between different phases (solid, liquid and gas) [21]. Figure 6 shows the wetting problem as proposed by Young.
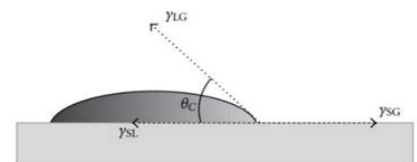

Figure 6. Equilibrium angle between a liquid droplet and a solid plane [23].
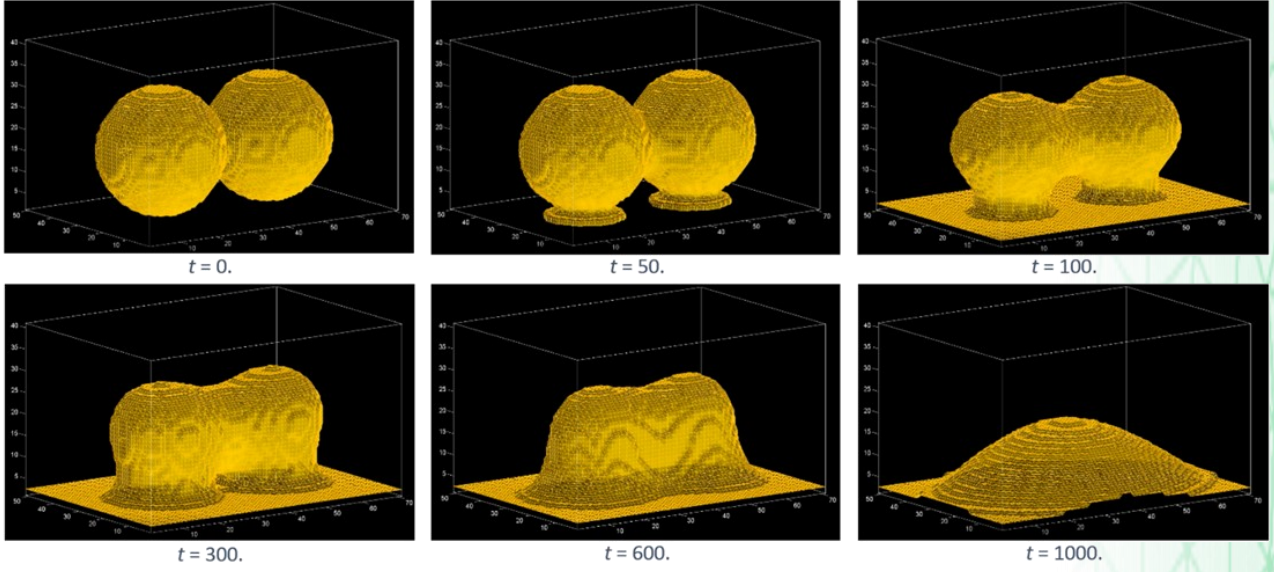
Figure 7. Example of droplets wetting on a smooth surface. The He&Doolen model has been used to include the forcing term.

- Interaction equation: describing the interaction forces between particles and solid surfaces:

$$F_{int}(\boldsymbol{x},t) = -G\, s(\boldsymbol{x},t) \sum_i w_i\ s(\boldsymbol{x}+\boldsymbol{\xi}_i\delta t,t)\boldsymbol{\xi}_i$$

where G is parameter that controls the strength of the interaction force and $s(x, t)$, is a main-field potential [23].

Furthermore, the model proposed by He & Doolen [24] has been used to include forcing terms, the Van der Walls equation of state has been adopted for the formulation of the main-field potential, and the LBM model to simulate the wetting of two droplets on a smooth solid surface. Figure 7 shows the simulation results for different time steps (in lattice units).

Finally, a thermal lattice Boltzmann model (TLBM) has been developed using the solution proposed by He & Doolen [25]. A second particle distribution function $h(x, \xi, t)$, is used to model the thermal problem. The TLBM is obtained coupling Equation (1.1) with the following equation:

$$h_i(\boldsymbol{x} + \boldsymbol{\xi}_i\delta t, t + \delta t) =$$
$$h_i(\boldsymbol{x},t) - \frac{1}{\tau}\Big(h_i(\boldsymbol{x},t) - h_i^{eq}(\boldsymbol{x},t)\Big) + \phi_i$$

where ϕ_i represents the forcing term (e.g., the heat flux).

The TLBM has been used to simulate the wetting of a single droplet on a smooth surface. On the domain bottom side, a high temperature is imposed. Figure 8 shows the simulation results for different time steps (in lattice units). Temperature distribution is represented within a domain cross-section.

The color scale ranges from blue (lower temperature) to red (higher temperature). Higher temperature is detected in the area with higher density and thermal capacity.

CONCLUSIONS

Macroscopic simulation approaches can predict temperature gradients and residual stresses on the whole component without reproducing effects at the microscopic scale (as porosity, wetting, surface tension…), that can be investigated only with dedicated tools. With respect to this, in this article, the LBM has been briefly described and adopted to solve a simple free-surface thermo-fluid-dynamic problem.
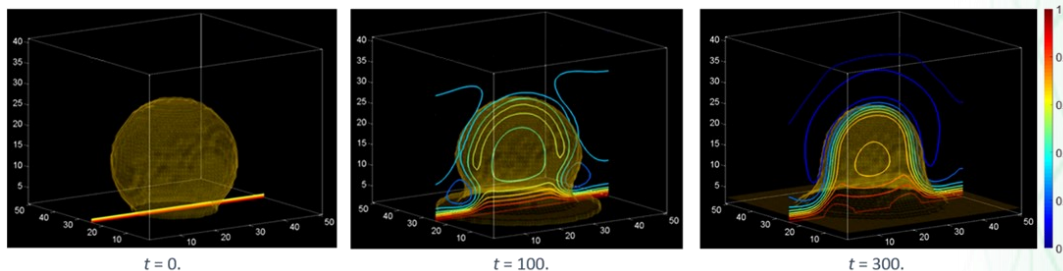
ACKNOWLEDGEMENT

Figure 8. Droplet wetting on a smooth surface. The colored iso-lines represent the temperature distribution rising form the temperature gradient imposed on the bottom side of the domain.

REFERENCES

[1] Standard, A. S. T. M. "F2792-12a. (2012*)."."Standard Terminology for Additive Manufacturing Technologies,"* ASTM International, West Conshohocken, Pa.

[2] Standard, A. S. T. M. "F2792-12a, 2012,"Standard Terminology for Additive Manufacturing Technologies" ASTM International. West Conshohocken, PA, 2012, DOI: 10.1520/F2792-12A." *Laser Enclosure Cooling Head Deposition Head Delivery Powder Ar Carrier Gas Cr 2.*

[3] Gibson, Ian, D. Rosen and B. Stucker. *Additive manufacturing technologies: 3D printing, rapid prototyping, and direct digital manufacturing*. Springer, 2014.

[4] Su, Xubin, et al. "Processability investigatation of non-assembly mechanisms for powder bed fusion process." *The International Journal of Advanced Manufacturing Technology* 64.5-8 (2013): 1193-1200.

[5] Zein, Iwan, et al. "Fused deposition modeling of novel scaffold architectures for tissue engineering applications." *Biomaterials* 23.4 (2002): 1169-1185.

[6] Matthias Markl and Carolin Körner. Multiscale modeling of powder bed –based additive manufacturing. Annual Review of Materials Research, 2016.

[7] Bellehumeur, Céline, et al. "Modeling of bond formation between polymer filaments in the fused deposition modeling process." *Journal of Manufacturing Processes* 6.2 (2004): 170-178.

[8] Michael F Zaeh and Gregor Branner. Investigations on residual stresses and deformations in selective laser melting. Production Engineering, 4 (1):35–45, 2010.

[9] Wu, Amanda S., et al. "An experimental investigation into additive manufacturing-induced residual stresses in 316L stainless steel." *Metallurgical and Materials Transactions* A 45.13 (2014): 6260-6270.

[10] DIGIMAT: www.e-xstream.com;

[11] Zhang, Y., and K. Chou. "A parametric study of part distortions in fused deposition modelling using three- dimensional finite element analysis." *Proceedings of the Institution of Mechanical Engineers: Journal of Engineering Manufacture* 222.8 (2008): 959-968.

[12] Zhang, Y., and K. Chou. "Three-dimensional finite element analysis simulations of the fused deposition modelling process." *Proceedings of the Institution of Mechanical Engineers, Part B: Journal of Engineering Manufacture* 220.10 (2006): 1663-1671.

[13] Hill, Michael R., and Drew V. Nelson. "The inherent strain method for residual stress determination and its application to a long welded joint." *ASME-PUBLICATIONS-PVP* 318 (1995): 343-352.

[14] Crump, S. Scott, et al. "Process of support removal for fused deposition modeling." U.S. Patent No. 5,503,785. 2 Apr. 1996.

[15] Körner, Carolin, Elham Attar, and Peter Heinl. "Mesoscopic simulation of selective beam melting processes." Journal of Materials Processing Technology 211.6 (2011): 978-987.

[16] Markl, Matthias, et al. "Electron beam absorption algorithms for electron beam melting processes simulated by a three-dimensional thermal free surface lattice Boltzmann method in a distributed and parallel environment." *Procedia Computer Science* 18 (2013): 2127-2136.

[17] Attar, Elham, and Carolin Körner. "Lattice Boltzmann model for thermal free surface flows with liquid–solid phase transition." *International Journal of Heat and Fluid Flow* 32.1 (2011): 156-163.

[18] Cercignani, Carlo. "The boltzmann equation." The Boltzmann Equation and Its Applications. Springer New York, 1988.

[19] Ammer, Regina, et al. "Simulating fast electron beam melting with a parallel thermal free surface lattice Boltzmann method." *Computers & Mathematics with Applications* 67.2 (2014): 318-330.

[20] Shan, Xiaowen, and Hudong Chen. "Lattice Boltzmann model for simulating flows with multiple phases and components." Physical Review E 47.3 (1993)

[21] Finn, Robert. "The contact angle in capillarity." Physics of Fluids 18.4 (2006): 047102.

[22] Abdulmajeed, Aous A., et al. "The effect of exposed glass fibers and particles of bioactive glass on the surface wettability of composite implants." *International journal of biomaterials 2011* (2011).

[23] Martys, Nicos S., and Hudong Chen. "Simulation of multicomponent fluids in complex three-dimensional geometries by the lattice Boltzmann method." *Physical review E* 53.1 (1996): 743.

[24] He, Xiaoyi, Xiaowen Shan, and Gary D. Doolen. "Discrete Boltzmann equation model for nonideal gases." *Physical Review E* 57.1 (1998): R13.

[25] He, Xiaoyi, Shiyi Chen, and Gary D. Doolen. "A novel thermal model for the lattice Boltzmann method in incompressible limit." *Journal of Computational Physics* 146.1 (1998): 282-300.

ALBERTO CATTENONE
GIANLUCA ALAIMO
SIMONE MORGANTI
FERDINANDO AURICCHIO

UNIVERSITY OF PAVIA,
ITALY

SIMONE.MORGANTI@UNIPV.IT

4ᵀᴴ ECCOMAS Young Investigators Conference 2017

ECCOMAS PhD Olympiad 2017

The 4th ECCOMAS Young Investigators Conference (YIC2017) took place from September 13th through 15th, 2017 at Politecnico di Milano in Milan, Italy. The conference was organized by the Department of Civil and Environmental Engineering and chaired by Massimiliano Cremonesi.

The conference was attended by 152 participants from many different European countries, but with some participants even coming from the US and Canada. Each day of the conference started with two invited plenary lectures given by distinguished young researchers: the first day, Santiago Badia and Alexander Popp presented their research, and the second day Gianluigi Rozza and Stefanie Elgeti followed. On the last day, the two winners of the ECCOMAS Best PhD Award 2016, Diane Guignard (nominated by SWICCOMAS, Switzerland) and Rogelio Ortigosa (nominated by UKACM, U.K.), presented their award-winning theses. During the final ceremony of the conference, an ECCOMAS representative officially conferred the ECCOMAS Best PhD Awards.

ECCOMAS Best PhD Awardee 2016 Diane Guignard (Switzerland) and Rogelio Ortigosa (U.K.) with Professor Umberto Perego (Politecnico di Milano)

As a part of YIC2017, also the seventh edition of the ECCOMAS PhD Olympiad was organized. The two winners, Tom de Geus (nominated by NMC, The Netherlands) and Nicola Nodargi (nominated by AIMETA, Italy), have been awarded with their prize during the final ceremony.

On Thursday night, a social dinner was organized in the city center. This was an excellent occasion to foster informal discussion between participants and to enjoy "la dolce vita". The three exciting days at YIC2017 have been a great success and further strengthened the very active young investigator community within ECCOMAS. We are all very much looking forward to YIC2019, which will be organized in Krakow, Poland in September 2019.

The finalists of the ECCOMAS PhD Olympiad together with YIC2017 chairman Massimiliano Cremonesi.

MASSIMILIANO CREMONESI
POLITECNICO DI MILANO,
ITALY

MASSIMILIANO.CREMONESI@POLIMI.IT

ECCOMAS 5TH YOUNG INVESTIGATORS CONFERENCE 2019
ECCOMAS PHD OLYMPIAD 2019

On behalf of the **ECCOMAS 5th Young Investigators Conference** organizers we would like to kindly invite you to participate in this prestigious event.

The main aim of the YIC conferences is to bringing together young researchers working in the fields of computational science and engineering in order to encourage fruitful discussions, collaborations, and interchange of ideas among the young generation. Participation of senior scientists sharing their knowledge and experience is also critical for this event.

The next YIC conference will be held in the historical city of **Krakow, Poland** on **September 1–6, 2019** and is being organized by the AGH University of Science and Technology.

AGH University of Science and Technology, is a leading Polish technical university and one of the biggest higher education institutions in Poland. Throughout almost 100 years the University has educated generations of engineers who have always been highly valued by the Polish industry. Collaboration with other Polish and foreign universities is also being dynamically developed.

Prospective authors are invited to submit, through the conference website www.yic2019.agh.edu.pl an extended abstract in English together with the pre-registration form by **February 10, 2019**. Abstracts have to be prepared according to the template and should outline the main features, results and conclusions of the work. The Scientific Committee will review the extended abstracts and all authors will be notified about the decision. Although the target group of the YIC 2019 are young researchers (under 35 years of age), senior scientists are welcome as well. The participation of early career scholars and postgraduate researchers is positively encouraged. Contributions are welcome on any aspect of **computational science and engineering**, including computational material science, solids and structural mechanics, scientific computing, multiscale modelling, computational fluid mechanics, computational biomechanics, computational fracture and damage mechanics as well as artificial intelligence, computational applied mathematics, industrial applications and challenges, computational geomechanics, artificial intelligence in modelling and simulations, advances in numerical methods and computational advances in composites.

The registration fee for delegates and authors is 200 EURO if paid before May 31, 2019 and 250 EURO if paid after this date. The fee includes optional accommodation at the AGH University Student Campus. Detailed information regarding fees and social program are available at the conference website.

The **PhD ECCOMAS Olympiad** will take place in conjunction with the **YIC2019.** The purpose of the ECCOMAS PhD Olympiad is to present the best PhD Theses approved by a University or Research Organization in Europe during the previous year. Every National or Regional Association affiliated to the ECCOMAS is represented by a number of selected PhDs submitted for consideration for the ECCOMAS PhD Awards. The Award ceremony will also take place at the Olympiad. Information regarding submissions will be announced at the conference website.

Hope to see you in Krakow in 2019!

Conference Chairman:
Konrad Perzynski
kperzyns@agh.edu.pl

Conference Co-Chairman:
Krzysztof Bzowski
kbzowski@agh.edu.pl

website: www.yic2019.agh.edu.pl
contact: yic2019@agh.edu.pl

1ST CSMA JUNIORS WORKSHOP !!!

The French Computational Structural Mechanics Association (CSMA) launched in 2016 its section of young researchers, called CSMA Juniors. The goals of this section are (i) to facilitate exchanges and collaborations among the young generation of the CSMA; (ii) to propose scientific activities which are useful and unique for young researchers and (iii) to help the CSMA in its activities. It is driven by a committee comprising 9 young researchers.

On the occasion of the 2017 National Congress on Computational Structural Mechanics, organized every 2 years by CSMA in the beautiful Giens peninsula (on the French Riviera), the *CSMA Juniors* committee organized its first two-day workshop (13-14 May 2017). This workshop, dedicated to the young generation (under 40) of CSMA researchers, was considered as an extension of the CSMA congress. It gathered about 80 people (PhD students, post-docs, junior researchers), including the CSMA PhD prize awardees who were invited.

The workshop consisted of a set of six one-hour short courses, given by and for young scientists, on the key topics of the plenary lectures and mini-symposia of the CSMA congress:

- Shape optimization (by F. de Gournay, IMT Toulouse),
- Test-simulation dialog (by J-D. Garaud, ONERA),
- Non-linear vibrations (by K. Soobborayen, INSA Lyon),
- Fatigue, damage, rupture (by S. Feld-Payet, ONERA),
- Impressive simulations & HPC (by P. Jolivet, ENSEEIHT Toulouse),
- Behavior of large civil engineering structures (by S. Capdevielle, ENS Paris-Saclay).

Each course presented state-of-the-art, basic concepts, research challenges, and was illustrated with simple numerical applications (in practical sessions). It thus gave a background to follow the congress talks more easily.

In the evening of May 13, several activities also took place:

- a hackathon (software competition) on a problem related to contact;
- classes and exchanges on Python (animated by D. André) and Paraview (animated by F. Bordeu), with practical sessions;
- a sharing session on numerical methods & software;
- exchange talks with academic and industrialist seniors (P. Le Tallec, P. Massin, F. Feyel) on various topics related to scientific careers, links between industry and academia, and future opportunities.

Judging by the number of participants and the quality of scientific exchanges, the workshop was a major success that highlights the dynamism of the CSMA. The 2nd edition of the *CSMA Juniors* workshop, which is intended to be an annual event, is scheduled for Spring 2018. It will again propose innovative formats and activities for the benefit and pleasure of young CSMA members.

LUDOVIC CHAMOIN
ON BEHALF OF THE CSMA JUNIORS COMMITTEE

LUDOVIC.CHAMOIN@ENS-PARIS-SACLAY.FR

ECCOMAS THEMATIC CONFERENCES 2019

Acronym	ECCOMAS Thematic Conference	Location	Date
KomPlas Tech	Conference on Computer Methods in Materials Technology	Zakopane, Poland	Jan 13 - 16
HONOM	European Workshop on High Order Nonlinear Numerical Methods for Evolutionnary PDEs: Theory and Applications	Madrid, Spain	Apr 1 - 5
SYMCOMP	International Conference on Numerical and Symbolic Computation: Developments and Applications	Porto, Portugal	Apr 11 - 12
MultiBioMe	Multiscale Problems in Biomechanics and Mechanobiology	Cargese, Corsica (France)	Apr 22 - 25
MARINE	VIII International Conference on Computational Methods in Marine Engineering	Gothenburg, Sweden	May 13 - 15
ADMOS	IX International Conference on Adaptive Modeling and Simulation	Campello (Alicante), Spain	May 25 - 27
IPM	5th International Conference on Inverse Problems in Mechanics of Structures and Materials	Rzeszow, Poland	May 22-24
COUPLED PROBLEMS	VIII International Conference on Coupled Problems in Science and Engineering	Barcelona, Spain	Jun 3 - 5
CFRAC	Sixth International Conference on Computational Modeling of Fracture and Failure of Materials and Structures	Brauschwei, Germany	Jun 12 - 14
CompWood	II Computational Methods in Wood Mechanics - from Material Properties to Timber Structures	Växjö, Sweden	Jun 17 - 19
COMPDYN	7th International Conference on Computational Methods in Structural Dynamics and Earthquake Engineering	Creta, Greece	June 24 - 26
UNCECOMP	International Conference on Uncertainty Quantification in Computational Sciences and Engineering	Creta, Greece	June 24 - 26
M-FET	2nd Modern Finite Element Technologies - Mathematical and Mechanical Aspects	Bad Honnef, Germany	Jul 1 - 3
ICCCM	International Conference on Computational Contact Mechanics	Hannover, Germany	Jul 2 - 4
X-DMS	eXtended Discretization MethodS	Lugano, Switzerland	Jul 3 - 5
SMART	8th Conference on Smart Structures and Materials	Paris, France	Jul 8 - 12
MULTIBODY	Multibody Dynamics	Duisburg, Germany	Jul 15-18

Acronym	ECCOMAS Thematic Conference	Location	Date
CMP4	Computational Modelling of Multi-Uncertainty and Multi-Scale Problems	Porto, Portugal	Jul 17-19
COMPLAS	XIV International Conference on Computational Plasticity	Barcelona, Spain	Sept 5 - 7
CompCancer	Computational Simulation of Cancer: Molecular and Cellular Dynamics	Porto, Portugal	Sept 9-13
Sim-AM	II International Conference on Simulation for Additive Manufacturing	Pavia, Italy	Sept 11 - 13
EUROGEN	International Conference on Evolutionary and Deterministic Methods for Design, Optimization and Control with Applications to Industrial and Societal Problems	Guimarães, Portugal	Sept 12 - 14
MSF	4th International Conference on Computational Methods for Solids and Fluids	Sarajevo, Bosnia and Herzegovina	Sept 18-20
IGA	VII International Conference on Isogeometric Analysis	Munich, Germany	Sept 18 - 20
COMPOSITES	VII Conference on Mechanical Response of Composites	Girona, Spain	Sept 18 - 20
CMCS	Computational Modeling of Complex Materials Across the Scales	Glasgow, Uk	Oct 1 - 4
FORM & FORCE	XI Internacional Conference on Textile Composites and Inflatable Structures and IASS SYMPOSIUM 2019	Barcelona, Spain	Oct 7 - 10
VipIMAGE	VII Conference on Computational Vision and Medical Image Processing	Porto, Portugal	Oct 16 - 18
CORASS	3rd International Conference on Rehabilitation and Sustainability of Structures – Advanced structural models, materials and applications	Coimbra, Portugal	Oct 16 - 17
PARTICLES	VI International Conference on Particle-based Methods	Barcelona, Spain	Oct 28 - 30
MORTech	5th International Workshop on Reduced Basis, POD and PGD Model Reduction Techniques	Paris, France	Nov 20 - 22
CM3	Digital Technologies in Transport	Barcelona, Spain	Nov 25 - 27
ICBT	III International Conference on Biomedical Technology	Hannover, Germany	Nov

OTHER ECCOMAS CONFERENCES 2019

YIC	ECCOMAS Young Investigators Conference 2019	Krakow, Poland	Sept 1 - 6